NASA TECHNICAL NOTE

NASA TN D-4045

THEORETICAL COMPUTATIONS OF THE OUTGOING INFRARED RADIANCE FROM A PLANETARY ATMOSPHERE

by Virgil G. Kunde

Goddard Space Flight Center
Greenbelt, Md.

NATIONAL AERONAUTICS AND SPACE ADMINISTRATION • WASHINGTON, D. C. • AUGUST 1967

NASA TN D-4045

THEORETICAL COMPUTATIONS OF THE OUTGOING INFRARED RADIANCE FROM A PLANETARY ATMOSPHERE

By Virgil G. Kunde

Goddard Space Flight Center
Greenbelt, Md.

NATIONAL AERONAUTICS AND SPACE ADMINISTRATION

For sale by the Clearinghouse for Federal Scientific and Technical Information
Springfield, Virginia 22151 – CFSTI price $3.00

ABSTRACT

The solution to the radiative transfer equation for a non-gray absorbing atmosphere in local thermodynamic equilibrium has been programmed for an IBM 7094 computer to calculate theoretically the outgoing infrared radiance in five wave number spectral intervals. The spectral range covered is from 5 to 20 microns. The theoretical outgoing radiances may be utilized in several ways: (1) to assist in selection of the desired spectral characteristics for infrared satellite experiments, (2) to test the validity of balloon and satellite observations, and (3) to aid in the analysis of planetary infrared radiation data.

Theoretical thermal emission spectra have been computed for several representative model atmospheres for Earth and Mars. These spectra illustrate that a considerable amount of information is available from radiation data of five wave number resolution. This information allows the recovery of the atmospheric and surface parameters from measured thermal emission spectra.

CONTENTS

THEORETICAL COMPUTATIONS OF THE OUTGOING INFRARED RADIANCE FROM A PLANETARY ATMOSPHERE

by
Virgil G. Kunde
Goddard Space Flight Center

I. INTRODUCTION

The increasing spectral resolution and accuracy of satellite measurements of the outgoing radiation from a planetary atmosphere require a corresponding improvement in the theoretical determination of the outgoing radiation in order to properly interpret the measurements. Examples of the improved instrumentation are the Satellite Infrared Spectrometer (SIRS) (Hilleary, et al., 1966) and the Michelson type Infrared Interferometer Spectrometer (IRIS) (Hanel and Chaney, 1964, 1965). The primary purpose of this investigation was to develop a program for theoretical calculation of the outgoing spectral radiance as an aid in interpretation of the IRIS measurements. The IRIS measures the thermal emission spectra in the spectral range of 500(20μ) to 2000(5μ) wave numbers with a spectral resolution of 5 wave numbers. Thus, the theoretically determined spectral radiances must be of equal or greater spectral resolution and cover the same spectral range. The thermal emission spectrum of a planet, measured at the top of its atmosphere, depends on many atmospheric and surface parameters. The most important atmospheric parameters are the types of optically active gases present, abundance and distribution of these gases and the temperature profile, while the most important surface parameters are temperature, pressure, composition and structure. These atmospheric and surface parameters are recovered from the measured thermal emission spectra by using a synthetic approach. A secondary purpose of the program is to assist in selecting the desired spectral characteristics for infrared satellite experiments and to test the validity of balloon and satellite observations.

II. SUMMARY OF SPECTRAL LINE SHAPES

A monochromatic absorption line may be broadened by one or more of many different line broadening mechanisms, both physical and geometrical. The types of mechanisms which are applicable at any given time depend on the physical and geometrical conditions under which the

absorption takes place. In the infrared, for conditions representative of planetary atmospheres, only two physical mechanisms are of importance:

1. Collisional or pressure broadening, due to collisions with neighboring atoms or molecules, which is characterized by an absorption coefficient with a deep, narrow core and broad wings.
2. Doppler broadening, due to random molecular thermal motions, which is characterized by a Gaussian shaped absorption coefficient.

Pressure broadening produces a line profile which may be symmetric or asymmetric with respect to the unbroadened line; the Doppler line profile is symmetric.

A. Collisional Broadening

The absorption or emission line of an atom or molecule under the influence of collisions by neighboring particles can be characterized by certain properties:

1. Line intensity,
2. Frequency profile or line shape,
3. Asymmetries in the line shape,
4. Line shift.

These properties relate to fundamental properties of the emitting or absorbing particle, and of the interaction between these particles and the perturbing particles. To determine the fundamental properties of the particle or of the interaction during collision from the above listed properties of the absorption or emission line knowledge is needed of the basic physical laws governing the absorption and emission of radiation in the presence of a perturbing force. An extensive literature on collisional line broadening exists as it represents an area of application for basic physics, primarily quantum mechanics, and also is a means of obtaining information on the energy levels and intermolecular forces of atomic or molecular systems undergoing collisions.

It seems worthwhile and appropriate to briefly review the theoretical background concerning molecular line broadening. It is to be emphasized that the only purpose of this review is to place the various line shapes and the physical assumptions on which they are based in the proper perspective, in a theoretical sense. The details of the mathematical treatment and experimental verification are found in more extensive reviews by Townes and Schawlow (1955), Ch'en and Takeo (1957), and Breene (1961). The work of Margenau and Watson (1936), Foley (1946), Bloom and Margenau (1953), Unsold (1955), Benedict, et al. (1956a), Breene (1957), and Traving (1960) has also been considered in this review.

(1) Introduction

Historically, the theory of collisional broadening has been approached from two viewpoints. These are the phase-shift approach, where the spectral lines of the emitting and absorbing particle

are broadened by collisions with other particles, and the statistical or static approach, where the line broadening is due to the electric field of the surrounding particles. These approaches are limiting cases of a more general theory. The phase shift theory is considered valid for low pressures and for frequencies near the line center (1-3 cm^{-1} - Spitzer (1940), Goody (1964a)) while the statistical theory has its application for high pressures and for frequencies in the wing of the line. As the pressure increases, the line broadening changes from collisional broadening to statistical broadening. Holstein (1950) has shown that the statistical theory is a limiting case of the collisional theory.

The general theory of collisional broadening considers the intensity distribution of dipole radiation from a time-dependent charge distribution. The following development has been given by Woolley and Stibbs (1953). A convenient starting point is the classical expression for the instantaneous power radiated by an accelerating electron (non-relativistic)

$$G = \frac{2e^2}{3c^3} \ddot{x}\, \ddot{x}^* \,, \tag{1}$$

with the displacement x being considered complex. The total radiated power G_T is the time integral

$$G_T = \int_0^\infty G\, dt \,. \tag{2}$$

Equivalently, G_T can be considered as the integral over frequency of the emitted spectral intensity distribution

$$G_T = \int_0^\infty I^e(\omega)\, d\omega \,. \tag{3}$$

Equating Equations 2 and 3 and substituting in Equation 1

$$\int_0^\infty I^e(\omega)\, d\omega = \int_0^\infty \frac{2e^2}{3c^2}\, \ddot{x}\, \ddot{x}^*\, dt \,, \tag{4}$$

where ω is angular frequency.

The acceleration $\ddot{x}$ of the radiating electron may be determined by solving the equation of motion for $x(t)$. For an undamped oscillator, corresponding to monochromatic radiation from a

sharp line, the wave train is infinite and of constant amplitude. The wave train of a damped oscillator produces a broadened line and consists of radiation of different frequencies and amplitudes.

The amplitude of the wave train can be represented by the Fourier integral

$$x(t) = \frac{1}{\sqrt{2\pi}} \int_{-\infty}^{\infty} a(\omega)\, e^{i\omega t}\, d\omega \ , \tag{5}$$

where $a(\omega)$ is the spectral amplitude of the emitted radiation. The corresponding Fourier integral for $a(\omega)$is

$$a(\omega) = \frac{1}{\sqrt{2\pi}} \int_{-\infty}^{\infty} x(t)\, e^{-i\omega t}\, dt \ . \tag{6}$$

Substituting Equation 5 in Equation 4, we can write

$$\int_0^{\infty} I^e(\omega)\, d\omega = \frac{2e^2}{3c^3 2\pi} \int_{-\infty}^{\infty} \int_{-\infty}^{\infty} \int_0^{\infty} \omega'^2 \omega^2\, a(\omega)\, a^*(\omega')\, e^{i(\omega-\omega')t}\, d\omega\, d\omega'\, dt \ , \tag{7}$$

$$\int_0^{\infty} I^e(\omega)\, d\omega = \frac{4e^2}{3c^3} \int_0^{\infty} \omega^4\, a(\omega)\, a^*(\omega)\, d\omega \ .$$

Equating the integrands of Equation 7, we can define $I^e(\omega)$ as

$$I^e(\omega) = \frac{4e^2\omega^4}{3c^3}\, a(\omega)\, a^*(\omega) \ . \tag{8}$$

Using Equation 6 for $a(\omega)$, the above equation for the intensity distribution can also be written as

$$I^e(\omega) = \frac{2e^2\omega^4}{3\pi c^3} \left| \int_0^{\infty} x(t)\, e^{-i\omega t}\, dt \right|^2 \ . \tag{9}$$

With the definition of the dipole moment for the radiating system as

$$\mu(t) = e\, x(t) \ , \tag{10}$$

Equation 9 can be rewritten as

$$I^e(\omega) = \frac{2\omega^4}{3\pi c^3} \left| \int_0^{\infty} \mu(t)\, e^{-i\omega t}\, dt \right|^2 \ . \tag{11}$$

Either Equation 8, 9 or 11 represents the general formulation for the intensity distribution of a radiating system under the influence of collisional broadening. An equation analogous to

Equation 11 can be derived from quantum mechanics, using time dependent perturbation theory. Terms in the Hamiltonian due to collisions with neighboring particles and to incident electromagnetic radiation on the particle are considered perturbations. References to the literature on the quantum mechanical derivation of line broadening are found in Böhm (1960). The general case, too complex to be of practical use, is solved only for special limiting cases. A summary of the reduction of the general formulation to its limiting cases of phase-shift and statistical broadening can be found in Böhm (1960).

For very low pressures, damping by collisions is negligible and natural broadening occurs due to radiation damping. The spectral intensity distribution, corresponding to radiation damping, can be derived classically by solving the equation of motion for a radiation damped oscillator and substituting this expression into Equation 9. For conditions representative of planetary atmospheres, the natural line width is negligibly small compared to the Doppler and collision line half-widths.

Two basic assumptions concerning the particle interaction are necessary to reduce Equation 11 to either the phase shift or static approximation. They are (1) adiabatic collisions — no transitions are induced by the collision interaction, and (2) the classical path approximation. The adiabatic collision assumption requires that there be no energy loss from the emitted wave train due to the collision; the amplitude of the radiated wave must remain constant. Thus, the collision is considered to affect only the phase of the radiated wave. Quantum mechanically, with the exclusion of effects of the radiation process, adiabaticity requires the state of the system to remain the same during the collision, i.e., the collisions cannot cause a shift in the energy levels.

Criteria for determining if a collision is adiabatic or diabatic have been discussed by Breene (1961), Margenau and Lewis (1959), Spitzer (1940) and Townes and Schawlow (1955). In general, the adiabatic approximation starts breaking down in the infrared and microwave region as the transition energies become about equal to the interaction energy.

The classical path approximation consists of two assumptions: (1) the path of the perturbing particle can be described classically; (2) the path of the perturbing particle can be described by a straight line

$$r'(t) = (b'^2 + v_r^2 t^2)^{1/2} , \tag{12}$$

where $r'(t)$ is the distance between the radiating particle and perturbing particle as a function of time, b' is the impact parameter and v_r is the velocity of the perturbing particle relative to the emitting particle. This approximation is considered valid for encounters where the uncertainty in the velocity and position of the perturbing particle is small compared to the velocity and position of the perturber. From the uncertainty principle, Margenau and Lewis (1959) have shown that the classical path approximation is satisfied for large values of the angular momentum of the perturbing particle.

(2) Phase-Shift Theory

The intensity distribution in the phase shift approximation can be obtained by considering the instantaneous frequency change $\Delta\bar{\nu}$ in the emitted wave train, due to one collision, as

$$\Delta\bar{\nu}\,(t) = C/(r'(t))^{n'''} \quad , \tag{13}$$

where C and n''' are constants depending on the properties of the radiating and perturbing particle (Ch'en and Takeo, 1957) and $r'(t)$ is given by Equation 12. Values of n''' for different interaction forces can be found in Townes and Schawlow (1955). The total phase change $\eta'(\tau)$ due to all collisions during the time interval 0-τ is given by the integral

$$\eta'(\tau) = \int_0^{\tau} \Delta\omega'(t)\,dt \quad , \tag{14}$$

where $\Delta\omega'(t)$ is the instantaneous phase shift due to all perturbing particles undergoing a collision at time t. If the duration of collision is considered to be short, only binary collisions are of importance and the integrand of Equation 14 can be considered as a summation of the phase shifts of each individual collision,

$$\Delta\omega'(t) = \sum_i \Delta\bar{\nu}_i\,(t) = \sum_i C_i/(r_i'(t))^{n'''} \quad , \tag{15}$$

the subscript i denoting different values of the impact parameter. The exclusion of multiple collisions restricts the application to low pressures. The frequency of the emitted wave train can now be considered as

$$\omega_0' = \omega_0 + \eta'(\tau) \quad , \tag{16}$$

where ω_0 is the natural angular frequency and the corresponding amplitude equation is

$$x(t) = x_0\, e^{i(\omega_0 + \eta'(t))t} \quad . \tag{17}$$

With the radiating system described by Equation 17, the intensity distribution (Equation 9) for the phase shift approximation, as given by Weisskopf (1933), is

$$I^e(\omega) = \frac{2e^2\omega^4}{3\pi c^3} \left| \int_0^{\infty} x_0\, e^{i(\omega_0 + \eta'(t) - \omega)t}\, dt \right|^2 \quad . \tag{18}$$

(2a) Impact theory:

A limiting case of Equation 18 occurs for a type of interaction classified as a strong encounter. In a strong encounter, it is assumed that the emitted wave train is completely terminated by the collision and that no correlation exists between the phase of the wave train before and after the collision. Between collisions, radiation of the natural frequency of the oscillator is emitted. The main assumption which denotes an impact theory is that the time during collision can be neglected. This is equivalent to neglecting the phase-shifted radiation ($\eta' = 0$) emitted during the collision. With the above assumptions, Equation 18 becomes

$$I^e(\omega) = \frac{2e^2\omega^4}{3\pi c^3} \left| \int_{-T_B/2}^{T_B/2} x_0 e^{i(\omega_0 - \omega)t} dt \right|^2 , \tag{19}$$

where T_B is the time between collisions. The impact treatment involves a Fourier analysis of only the unperturbed radiation emitted between collisions. Equation 19 integrates to

$$I^e(\omega) = \frac{2e^2}{3\pi c^3} \omega^4 x_0^2 \left[\frac{\sin\left(\frac{\omega_0 - \omega}{2}\right) T_B}{\left(\frac{\omega_0 - \omega}{2}\right)} \right]^2 , \tag{20}$$

a line shape first obtained by Michelson (1895). The line broadening denoted by Equation 20 is due only to the finite extent of the wave train which is limited by the time between collisions.

For random collisions, kinetic theory gives the probability distribution for the time between collisions as

$$\Phi(v) = 1/T_{B_0}(v)\, e^{-T_B(v)/T_{B_0}(v)} , \tag{21}$$

where $T_{B_0}(v)$ is the mean time between collisions for a given molecular velocity v. Averaging the line shape of Equation 20 over the distribution function of Equation 21 yields the emission intensity per oscillator as

$$I^e(\bar{\nu}) = \frac{2e^2(2\pi\bar{\nu})^4}{3\pi c^3} x_0^2 \frac{1}{2\pi^2 T_{B_0}} \left[\frac{1}{(\bar{\nu}_0 - \bar{\nu})^2 + (1/2\pi T_{B_0})^2} \right] . \tag{22}$$

The volume emission intensity is

$$I_\nu^e(\nu) = N' f' I^e(\bar{\nu}) , \tag{23}$$

where N' is the number of absorbing particles per unit volume and f' is the oscillator strength, which represents the number of oscillators per absorbing particle. Equation 23 is normalized by

$$\int_{-\infty}^{\infty} I_{\nu}^{e}(\bar{\nu})\, d\bar{\nu} = I_{T}^{e} , \tag{24}$$

and the volume emission intensity can now be written as

$$I_{\nu}^{e}(\bar{\nu}) = \frac{I_{T}^{e}}{\pi} \frac{1/2\pi T_{0}(v)}{(\bar{\nu}_{0} - \bar{\nu})^{2} + \left(1/2\pi T_{B_{0}}(v)\right)^{2}} , \tag{25}$$

For local thermodynamic equilibrium, Van Vleck and Margenau (1949) have shown that the absorption and emission line shapes are identical, thus we can write the mass absorption coefficient as

$$k^{m}(\bar{\nu}) = S^{m}/\pi \frac{1/2\pi T_{0}(v)}{(\bar{\nu} - \bar{\nu}_{0})^{2} + \left(1/2\pi T_{B_{0}}(v)\right)^{2}} , \tag{26}$$

where S^{m} is the integrated absorption coefficient with dimensions $cm^{2}\ gm^{-1}\ sec^{-1}$. The above equation has been derived in the framework of the Weisskopf phase shift theory for impact collisions. However, Equation 26 is known as the Lorentz line shape as it was originally derived in a similar form by Lorentz (1906) by consideration of absorption of radiation by particles. The half-width of the spectral line $\alpha_{L}(v)$, defined by $k(\bar{\nu})$ equals half its maximum value, is given by

$$\alpha_{L}(v) = 1/2\pi T_{B_{0}}(v) . \tag{27}$$

Goody (1964a) has pointed out that the absorption coefficient should be averaged over all molecular velocities, but that usually it is assumed that a mean half-width α_{L} can be associated with the mean time between collisions. The expression from kinetic theory for the mean time between collisions is

$$\alpha_{L} = 1/2\pi T_{B_{0}} = N \bar{v}_{r} \Lambda_{e} , \tag{28}$$

where $\bar{v}_{r}$ is the mean relative velocity of the colliding particles, N the number of colliding particles per unit volume, and Λ_{e} is the effective collision cross-section.

The mean relative velocity $\bar{v}_{r}$ is

$$\bar{v}_{r} = \left[2k_{b}T\left(\frac{1}{M} + \frac{1}{M_{i}}\right)\right]^{1/2} . \tag{29}$$

The line half-width can now be written as

$$\alpha_L = \frac{1}{2} \sum_i N_i \, (D + D_i)^2 \left[2 k_b T \left(\frac{1}{M} + \frac{1}{M_i} \right) \right]^{1/2} , \tag{30}$$

where D is the optical collision diameter and M is the molecular mass. The i subscript represents the type of perturbing particle. If the optical collision diameter is known, the line half-width can be calculated from Equation 30. In general, it is found that the optical collision diameter is larger than the gas kinetic collision diameter by a factor ranging from two to a hundred [Ch'en and Takeo (1957), White (1934)]. For a binary mixture of absorbing gas and nonabsorbing broadening gas, α_L takes the form (Burch, et al., 1962)

$$\alpha_L = \alpha_0 \frac{P_e}{P_0} \left(\frac{T_0}{T} \right)^{1/2} , \tag{31}$$

where the equivalent pressure P_e is given by

$$P_e = P + (B - 1) \, p_a \, . \tag{32}$$

The constant B is the self-broadening coefficient, α_0 is the half-width at reference pressure P_0, P is the total pressure, and p_a is the partial pressure of the absorbing gases.

Weisskopf (1932) has arbitrarily defined an impact collision to have occurred when the phase shift η' of the emitted wave is greater than unity. The emitted wave train is thus terminated at $\eta' = 1$. This approximation neglects two types of collisions: (1) close collisions with $\eta' > 1$, and (2) distance collisions with $\eta' < 1$. An optical collision diameter can be determined from Equation 14 by equating $\eta' = 1$ and solving for the corresponding impact parameter b_0'; the line half-width is then formulated in terms of b_0' as

$$\alpha_W = \frac{1}{2} \sum_i N_i \, b_{0,i}'^2 \left[2 k_b T \left(\frac{1}{M} + \frac{1}{M_i} \right) \right]^{1/2} . \tag{33}$$

Characteristic of the impact theory is the linear dependence of the half-width on the number of perturbers. As the phase-shifted portion of the emitted wave train is neglected during the time of collision, the impact theory does not directly predict a value for the line half-width in terms of the interaction forces. Only indirectly is this accomplished in the Weisskopf theory through the definition of a collision by $\eta' = 1$.

The derivation of the Lorentz line shape using phase shift theory implicitly involves an assumption that α_L and $\bar{\nu} - \bar{\nu}_0$ are smaller than $\bar{\nu}_0$ (Goody, 1964a). Correcting for this assumption, the line shape is

$$k^m(\bar{\nu}) = \frac{S^m}{\pi} \frac{\bar{\nu}}{\bar{\nu}_0} \left[\frac{\alpha_L}{(\bar{\nu} - \bar{\nu}_0)^2 + \alpha_L^2} - \frac{\alpha_L}{(\bar{\nu} + \bar{\nu}_0)^2 + \alpha_L^2} \right] . \tag{34}$$

Further modification of the above theory is necessary to avoid contradicting a theory of nonresonant absorption by Debye (1929). If the orientation of the displacement and velocity vector of the oscillator after the collision is assumed to follow a Maxwell-Boltzmann distribution, the line shape becomes (Van Vleck and Weisskopf, 1945)

$$k^m(\bar{\nu}) = \frac{S^m}{\pi} \left(\frac{\bar{\nu}}{\bar{\nu}_0} \right)^2 \left[\frac{\alpha_L}{(\bar{\nu} - \bar{\nu}_0)^2 + \alpha_L^2} + \frac{\alpha_L}{(\bar{\nu} + \bar{\nu}_0)^2 + \alpha_L^2} \right] . \tag{35}$$

For $\bar{\alpha}_L << \nu_0$, which is satisfied in the infrared, the Van Vleck-Weisskopf line shape reduces to the Lorentz line shape.

(2b) Line shift:

Two of the assumptions involved in the impact theory were: (1) collisions due to distant perturbers are neglected as only collisions which cause quenching are considered, and (2) the time of collision is small compared to the time between collisions, which is the same as neglecting close collisions which give phase changes greater than unity. Consideration of these assumptions has indicated that the first is connected with line shifts and the second with line asymmetries. Lindholm (1941) considered the problem, including phase shifts due to distant collisions, and obtained the Lorentz type line profile

$$k^m(\bar{\nu}) = \frac{S^m}{\pi} \frac{\alpha_L}{(\bar{\nu} - \bar{\nu}_0 + \beta)^2 + \alpha_L^2} , \tag{36}$$

which is symmetric with respect to $\bar{\nu}_0$ but with the line center shifted to the red of $\bar{\nu}_0$ by the distance β. The line half-width is the same as the Weisskopf half-width (Equation 33) with the exception of a numerical constant. For van der Waals broadening, the relationship

$$\beta = \frac{\alpha_L}{2.75} \tag{37}$$

may be derived. The inclusion of the time during collision is in the realm of statistical broadening, which is discussed in the next section.

(3) Statistical Theory

The statistical theory considers both the absorbing or emitting particles and the perturbing particles to be at rest. Through distortion of the energy levels, each spatial configuration produces a shift in frequency of the emitted radiation with respect to the frequency of the radiation which would be emitted if no perturbers were present. The line intensity in the angular frequency range $d\omega$ is taken to be proportional to the probability of occurrence of the spatial configuration which yields a frequency shift in the range of $d\omega$.

Considering van der Waals forces and several perturbing molecules, Margenau (1935) finds the intensity distribution to be

$$I(\bar{\nu}) = \begin{cases} 0 & \Delta\omega < 0 \\ \frac{2\pi}{3}\,\gamma^{1/2}\;\; N\;\; \Delta\omega^{-3/2}\;\; e^{-\frac{4\pi}{9}\,\gamma\frac{N^2}{\Delta\omega}} & \Delta\omega > 0 \end{cases} , \tag{38}$$

where the half-width is given by

$$\alpha = 0.822\,\pi^3\,\gamma\,N^2 \tag{39}$$

and the line shift (to the red) is

$$\Delta\bar{\nu} = \left(\frac{2\pi}{3}\right)^3 \gamma\;\; N^2 \,. \tag{40}$$

In the above equations γ is a force constant, N the number of perturbers per unit volume, and $\Delta\omega = \omega - \omega_0$. For large $\Delta\omega$, the red wing intensity approaches

$$I(\omega) \sim \Delta\omega^{-3/2} \,. \tag{41}$$

The "statistical" theory in considering the time during collision yields an asymmetrical line shape.

Work by Spitzer (1939a, 1939b, 1940) and Holstein (1950) has indicated the regions of applicability for the phase-shift theory and the statistical theory. Spitzer has shown that the phase-shift theory is valid near the center of the line for frequencies satisfying

$$\Delta\omega << \frac{v_r^{n'''/n'''-1}}{(2\pi C)^{1/n'''-1}} \,. \tag{42}$$

Correspondingly, Holstein has shown the statistical theory is valid for frequencies satisfying

$$\Delta\omega >> \frac{v_r^{n'''/n'''-1}}{(2\pi C)^{1/n'''-1}} \quad , \tag{43}$$

which occurs in the wings of the line.

(4) Lindholm's General Theory - Line Shift and Asymmetry

Lindholm's general theory (Lindholm, 1945) takes into account the large phase shifts which occur during collision. Because the collision time is included, the theory is no longer considered an impact theory. Lindholm also included the small phase shifts, due to distant collisions, which lead to a line shift. The interaction force was assumed to be van der Waals (n = 6). The general formulation reduces to the statistical theory for high pressures and for the line wings and to the impact theory for low pressures and near the line center. As an approximation, Lindholm has determined the following expressions for the red and violet wings

$$k^m(\bar{\nu}) = .933 \frac{M'^2 S^m \alpha_L}{\pi} \left[M'(\bar{\nu}_0 - \bar{\nu})\right]^{-3/2} \quad (\text{red}) \quad , \tag{44}$$

$$k^m(\bar{\nu}) = .638 \frac{M'^2 S^m \alpha_L}{\pi} \left[M'(\bar{\nu} - \bar{\nu}_0)\right]^{-7/2} \quad (\text{violet}) \quad , \tag{45}$$

where the notation of Plass and Warner (1952a, 1952b) has been used. The above equations are valid for $|\bar{\nu} - \bar{\nu}_0| > 3M'^{-1}$. A value of M' of approximately 3 cm is typical for the earth's atmosphere (Plass and Warner, (1952a). From Lindholm's general theory, Curtis and Goody (1954a) have derived wing equations similar to those of Equations 44 and 45 plus an equation representing the center of the line by assuming only that the line half-width is smaller than the frequency representing the transition frequency between the impact and statistical theory. The effect of the Lindholm line shape on atmospheric transmission has been considered by Plass and Warner (1952) and Curtis and Goody (1954a; 1954b). The Lindholm theory has been experimentally verified for sodium lines broadened by argon (Kleman and Lindholm, 1945). The Lindholm theory is not considered to be applicable for molecular lines in the infrared in general because adiabaticity is assumed, and in the particular case of n = 6, because close collisions cannot be described by a van der Waals force (Plass, 1954).

(5) Anderson's Diabatic Theory for Molecular Lines

Anderson (1949) has generalized the theory of collisional broadening by including the effect of transitions between quantum states due to collisions. The starting point for Anderson is the

quantum-mechanical analog of the Fourier integral intensity expression given by Equation 11, with the subsequent treatment involving the assumptions of the classical path and of binary collisions. Anderson further assumes that the duration of the collision is small compared to the time between collisions, thus restricting the treatment to an impact type treatment. With the exception of a shift of the center frequency δ_A, a line shape similar to the Lorentz shape is obtained:

$$k^m(\bar{\nu}) = \frac{S^m}{\pi} \frac{\alpha}{(\bar{\nu} - \bar{\nu}_0 - \delta_A)^2 + \alpha^2} \quad , \tag{46}$$

where

$$\alpha = \frac{1}{2} \sum_j N_j(T)\, \Lambda(T) \left[2 k_b T \left(\frac{1}{M} + \frac{1}{M_j}\right)\right]^{1/2} \quad . \tag{47}$$

The collision cross-section $\Lambda(T)$ is given by

$$\Lambda(T) = \sum_{J_2} \rho_{J_2}(T)\, \Lambda_{J_2}(T) \quad , \tag{48}$$

with ρ_{J_2} being the Boltzmann distribution for the perturbing particle of quantum state J_2, and Λ_{J_2} being a partial collision cross-section for the transition between states i and f of the absorber, with the perturber in state J_2. The partial collision cross-section is

$$\Lambda_{J_2}(T) = \int_0^\infty 2\pi b' S(b, J_2)\, db' \quad , \tag{49}$$

with $S(b', J_2)$ representing the probability that the perturber in state J_2 at impact parameter distance b' will induce a transition from state i or f of the absorber. Following Ch'en and Takeo (1957):

$$S(b', J_2) = \frac{1}{2} \left[\sum_{m_f M_2} \frac{\langle f, m_f, J_2, M_2 | P^2 | f, m_f, J_2, M_2 \rangle}{(2J_f + 1)(2J_2 + 1)} + \sum_{m_i M_2} \frac{\langle i, m_i, J_2, M_i | P^2 | i, m_i, J_2, M_2 \rangle}{(2J_i + 1)(2J_2 + 1)} \right], \tag{50}$$

where J is the rotational quantum number, $2J_f + 1$ is the number of degenerate states, m_f is the degenerate index for the state f, and M_2 is the magnetic quantum number of the perturbing particle. A typical matrix element is given by

$$\langle m' | P | n' \rangle = \frac{1}{\hbar} \int_{-\infty}^{\infty} \langle m' | V_1(t) | n' \rangle \exp(i \omega_{m'n'} t)\, dt \quad , \tag{51}$$

with $V_i(t)$ being the perturbing potential due to collisions, and $\omega_{m'n'}$ the transition frequency between states m' and n'. Formulation of α for several types of molecular interactions is given by Townes and Schawlow (1955) and Tsao and Curnutte (1962). An important result of Anderson's theory is the prediction of the line half-width and its dependence on the rotational quantum number and temperature.

Benedict and Kaplan (1959) have applied the Anderson theory to calculate the half-widths of H_2O lines broadened by N_2 collisions. The main limitations of their calculations are: (1) the molecular interaction is due only to the dipole of H_2O and the quadrupole of N_2 and (2) all the half-widths depend on the calibration of one observed H_2O microwave line. Half-widths for the pure rotational H_2O spectrum were computed for several temperatures. In the Anderson theory the collision cross-section $\Lambda(T)$ depends on temperature through the Boltzman distribution for the perturbing molecule and the temperature dependence of the partial collision cross-sections (Smith, Lackner, and Volkov, 1955). The partial collision cross-section temperature effect is due to the dependence of Λ_{J_2} on the relative velocity between the absorbing and perturbing particles. In the range 220°-300°K, Benedict and Kaplan found the temperature variation of the half-width could be described for a constant pressure as

$$\alpha(T) = \alpha(T_0)\left(\frac{T_0}{T}\right)^{n''} \tag{52}$$

where n'' varied from 0.756 to -0.045. For 300°K, the line half-widths ranged from .111 to .032 cm^{-1} atm^{-1}. For collisions where Λ_{J_2} does not depend on temperature, n'' is equal to 0.5. In addition, half-widths for lines in the ν_2 and $2\nu_2$ vibration-rotation band were computed. The results showed a change in half-width ranging from +2% to -18% with respect to the pure rotational half-widths. Later calculations by Benedict and Kaplan (1964) for self-broadened half-widths for the pure rotational H_2O lines gave half-widths which varied from .566 to 0.61 cm^{-1} atm^{-1} and a temperature exponent n'' which varied from 1.04 to -.218.

Comparison of Anderson's theory with experimental values of the half-width, which is limited to a few cases, in general indicates fair agreement [Townes and Schalow (1955), Goody (1964a)]. However, Sanderson and Ginsburg (1963) have found experimentally, for three far infrared water vapor lines, self-broadened and nitrogen-broadened half-widths larger by a factor of 1.5 than the theoretical values of Benedict and Kaplan.

(6) Benedict Modification of Lorentz Line Shape

As the Lorentz line shape is theoretically valid only for frequencies near the line center, several experimental studies have been made to determine the shape in the wing of a collision-broadened line. For the HCl fundamental, Benedict, et al. (1956b) determined that for $\nu - \nu_0$ in the range of 1.5 to 40 cm^{-1} the line wing could best be described by

$$k(\nu) \approx \frac{1}{(\nu - \nu_0)^{m''}} , \tag{53}$$

where m'' is between 1.7 and 1.85, and ν represents wave number. The observed wing gives greater absorption than does a Lorentz wing ($m'' = 2$).

From absorption by the fundamental and first overtone of CO, Benedict, et al. (1962) have determined experimentally that the Lorentz line shape should be modified by an exponential multiplying factor dependent on $|\nu - \nu_0|$ for $|\nu - \nu_0| > d\,cm^{-1}$. The line shape is

$$k(\nu) = \frac{S}{\pi} \frac{\alpha_L}{(\nu - \nu_0)^2 + \alpha_L^2}, \qquad |\nu - \nu_0| \leq d \tag{54}$$

$$k(\nu) = \frac{S}{\pi} \frac{\alpha_L}{(\nu - \nu_0)^2 + \alpha_L^2} e^{-a'[|\nu - \nu_0| - d]^{b''}}, \qquad |\nu - \nu_0| \geq d \tag{55}$$

where the units of $k(\nu)$ and S are cm^{-1} atm^{-1} and cm^{-2} atm^{-1}, respectively. The transformation from mass absorption coefficient to absorption coefficient per unit length per unit pressure $k(\nu)$ will be discussed in section IIIA. For CO, the constants were found to be $d = 4\ cm^{-1}$, $b'' = 1$, and $a' = 0.015$. The line shape of Equation 55 is denoted as the Benedict modification of the Lorentz line shape. Due to the exponential factor, the Benedict modification drops off much faster in the wings than does the pure Lorentz line.

Bignell, et al. (1963) have observed less absorption than that given by the Lorentz line for the 15μ band of CO_2.

Winters, et al. (1964) have made an analysis of absorption in the spectral region short of the 4.17μ R-branch band head of the 4.26 CO_2 band. The absorption for wavelengths less than 4.17μ is due to the wings of strong lines in the R-branch. The line shapes determined from these measurements were of the same form as the Benedict modification of Equation 55. For self-broadened CO_2 the appropriate constants are $d = 5\ cm^{-1}$, $a' = 0.08$, and $b'' = 0.8$. In addition, measurements were made for carbon dioxide pressurized with nitrogen and also with oxygen. No detailed reduction exists for the foreign gas broadening; however, Winters, et al. suggest that values in the range $b'' = 0.46$ and $a' = 0.46$ would best fit the Benedict modification for atmospheric conditions. As the lowest CO_2 partial pressure of Winters, et al. was .25 atm, experimental evidence for conditions representative of the earth's atmosphere is not available.

Kyle, et al. (1965) have obtained numerous solar spectra in the 4.3μ CO_2 band at altitudes from 10 to 30 km along slant paths in the atmosphere. Comparison of theoretical slant path transmittances with experimental results gave satisfactory agreement at high altitudes for the Lorentz shape and at low altitudes for the Benedict modification.

From absorption measurements on the high wave number side of the head of the 3 ν_3 CO_2 band, Burch, et al. (1965, 1966) have determined that the observed absorption is less than that calculated for a Lorentz line. The authors found that the line shape varied with the type of broadening gas and

that the shape in this region (~7000 cm^{-1}) differed from that found by Winters, et al, in the region of 2400 cm^{-1}.

Bignell, et al. (1963) determined the Lorentz line shape giving the best agreement with H_2O extinction measurements of the 8-12μ window region. These observations tested the line shape very far into the wings (~100-600 cm^{-1}) of the 6.3μ vibration-rotation band and the pure rotational lines of H_2O. From sky emission measurements, Bolle (1965) has derived water vapor continuum absorption coefficients for window regions in the 7.5-26μ region. Comparison of theoretical continuum absorption coefficients with the experimental values indicated a Lorentz line shape.

The Lorentz line shape and the Benedict modification in the wings of a Lorentz line are the most applicable of the collisional line shapes in the infrared, with the Anderson theory being the most applicable method for calculating the line half-width. To date, no theoretical basis has been established for the Benedict modification. Further theoretical and experimental work is needed to obtain the applicable line shape for the wings of lines.

B. Doppler Broadening

The motion of an atom or molecule, through the Doppler effect, causes the frequency ($\bar{\nu}$) of emitted radiation to shift from the monochromatic frequency ($\bar{\nu}_0$) of emission of a stationary atom or molecule. The derivation of the absorption coefficient for Doppler broadening assumes (1) the velocities of the emitting atoms or molecules in the line of sight have a Maxwellian distribution, and (2) the intensity of the spectral line at frequency $\bar{\nu}$ is proportional to the number of atoms or molecules radiating at frequency $\bar{\nu}$. Using the Doppler principle, the absorption coefficient can then be derived (Aller, 1953)

$$k^m(\bar{\nu}) = \frac{S^m}{\bar{\nu}_0} \frac{c}{v_p \sqrt{\pi}} \exp\left[-\frac{c^2}{v_p^2}\left(\frac{\bar{\nu} - \bar{\nu}_0}{\bar{\nu}_0}\right)^2\right] , \tag{56}$$

where v_p is the most probable Maxwellian speed for a given temperature. Substituting for the most probable speed

$$v_p^2 = 2 k_b \frac{T}{M} , \tag{57}$$

the Doppler absorption coefficient in terms of frequency becomes

$$k^m(\bar{\nu}) = \frac{S^m}{\bar{\nu}_0} \sqrt{\frac{mc^2}{2\pi k_b T}} \exp\left[-\frac{mc^2}{2 k_b T}\left(\frac{\bar{\nu} - \bar{\nu}_0}{\bar{\nu}_0}\right)^2\right] . \tag{58}$$

In wave number units,

$$k(\nu) = \frac{S}{\nu_0}\sqrt{\frac{mc^2}{2\pi k_b T}}\exp\left[-\frac{mc^2}{2k_b T}\left(\frac{\nu-\nu_0}{\nu_0}\right)^2\right] \quad . \tag{59}$$

The Doppler half-width, at the point where the absorption coefficient equals one-half its maximum value, is

$$\alpha_D = \sqrt{\frac{2k_b T}{mc^2}\ln 2\,\nu_0^2} \quad , \tag{60}$$

which reduces to

$$\alpha_D = 3.58\times 10^{-7}\sqrt{\frac{T}{M}}\,\nu_0 \quad , \tag{61}$$

where M is the molecular weight. The corresponding equations in wavelength units are

$$k(\lambda) = \frac{S}{\lambda}\sqrt{\frac{mc^2}{2\pi k_b T}}\exp\left[-\frac{mc^2}{2k_b T}\left(\frac{\lambda-\lambda_0}{\lambda_0}\right)^2\right] \quad , \tag{62}$$

$$\alpha_D = 3.58\times 10^{-7}\sqrt{\frac{T}{M}}\,\lambda_0 \quad . \tag{63}$$

Figures 1 and 2 show the Doppler half-width graphed with T/M as a parameter in terms of wave number and wave length units, respectively.

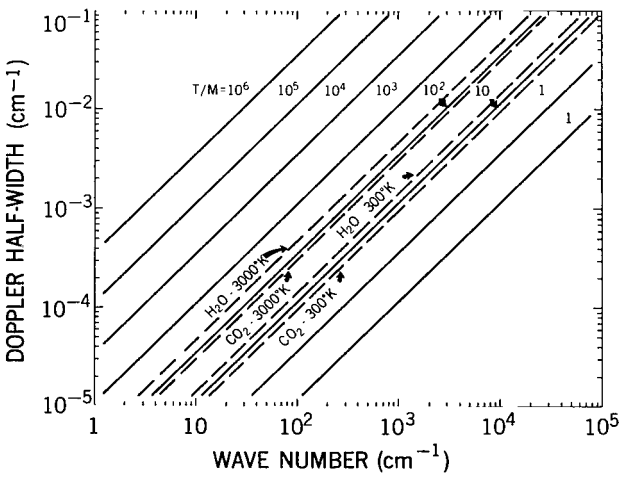

Figure 1—The Doppler half-width in wave number units is given over a range of wave numbers for different values of T/M. Special cases of T/M are given for H_2O and CO_2 at temperatures of 300 and 3000 °K.

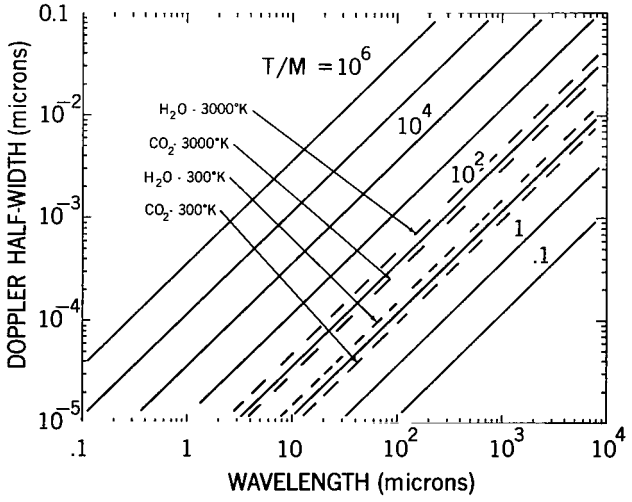

Figure 2—The Doppler half-width in wavelength units is given over a range of wavelengths for different values of T/M. Special cases of T/M are given for H_2O and CO_2 at temperatures of 300 and 3000 °K.

C. Collisional-Doppler Broadening

For physical conditions, as in the earth's stratosphere, where both the collisions of neighboring particles and the thermal motion of the emitter contribute significantly to the broadening of a line it is necessary to consider simultaneously the collisional and Doppler line shape. The absorption coefficient for a mixed line can be written (Aller, 1953)

$$k(\nu) = k_0 \frac{y'}{\pi} \int_{-\infty}^{\infty} \frac{e^{-t'^2}}{y'^2 + (x' - t')^2} dt' , \tag{64}$$

where

$$k_0 = \frac{S}{\alpha_D} \sqrt{\frac{\ln 2}{\pi}} , \tag{65}$$

$$y' = \frac{\alpha_L}{\alpha_D} \sqrt{\ln 2} , \tag{66}$$

$$x' = \frac{\nu - \nu_0}{\alpha_D} \sqrt{\ln 2} . \tag{67}$$

In the above expression, the collisional line shape is assumed to be Lorentzian. The integration over t' represents the integration over the different velocities of the absorbers in the line of sight, assuming the distribution of absorbers in terms of velocity is Maxwellian. The integration over velocity thus accounts for all of the radiation which is Doppler shifted to wave number ν. Equation 64 can be rewritten as

$$k(\nu) = k_0 H(y', x') , \tag{68}$$

with

$$H(y', x') = \frac{y'}{\pi} \int_{-\infty}^{\infty} \frac{e^{-t'^2}}{y'^2 + (x' - t')^2} dt' . \tag{69}$$

As $H(y', x')$ cannot be evaluated analytically, various methods of evaluation for different ranges of x' and y' have evolved (Penner, 1959); however, no method is suitable for the entire range of x' and y' occurring in a planetary atmosphere. Young (1965) has generated a method and developed it into a Fortran program for the evaluation of $H(y', x')$, covering a large range of x' and y', for

routine use on a digital computer. The evaluations of the mixed line shape considered in this paper have been made utilizing Young's program.

The quantity $k(\nu)/S$ for a mixed line is graphed as a function of wave number for a range of pressures for $\alpha_D = 0.00014\ cm^{-1}$ in Figure 3 and for $\alpha_D = 0.016\ cm^{-1}$ in Figure 4. Also shown are the $k(\nu)/S$ profiles for pure collisional and pure Doppler broadening. From Figures 3 and 4 it is evident that Doppler broadening determines the shape of the core and collisional broadening determines the shape of the wings of the mixed line shape. The calculations on which Figures 3 and 4 are based indicate that the mixed line shape should be used for pressures smaller than 100 mb and for distances from the line center less than $2.5\ cm^{-1}$. The exception to this is for very low pressures, where only pure Doppler broadening need be considered. Outside these ranges, only collisional broadening need be taken into account. The above limits of 100 mb and $2.5\ cm^{-1}$ are valid provided the ratio T/M is in the range of 4-20 and the wave number of interest is in the range of 500 to 2000 cm^{-1}.

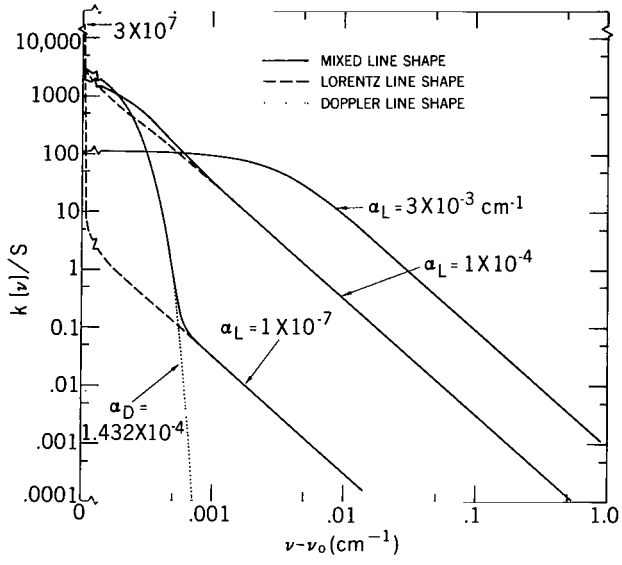

Figure 3—The ratio $k(\nu)/S$ is given as a function of $\nu - \nu_0$ for the mixed, the Lorentz and the Doppler line shapes for various values of α_L/α_D. The Doppler half-width is $1.432 \times 10^{-4}\ cm^{-1}$.

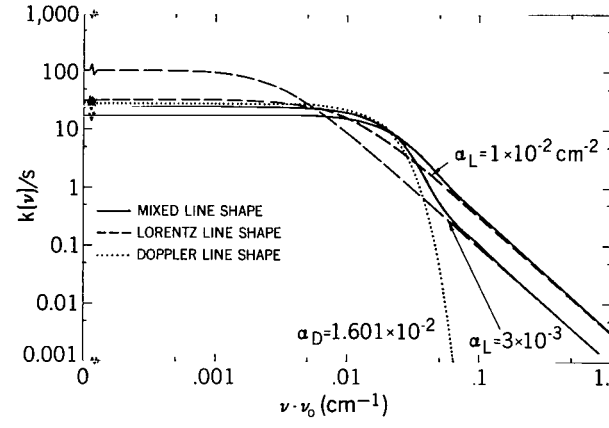

Figure 4—The ratio $k(\nu)/S$ is given as a function of $\nu - \nu_0$ for the mixed, the Lorentz and the Doppler line shapes for various values of α_L/α_D. The Doppler half-width is $1.601 \times 10^{-2}\ cm^{-1}$.

III. BASIC EQUATIONS

(A) Infrared Radiative Transfer Equation

The outgoing spectral radiance from a planetary atmosphere is computed for a slant path through concentrically stratified atmospheric layers. As shown in Figure 5, the atmospheric path along s is specified by the geometrical parameter r_0. The integration is from the top of the atmosphere to the level R_s which represents the lower boundary of the path. For a clear atmosphere, R_s denotes the planetary surface. Only the case where the atmospheric path intersects

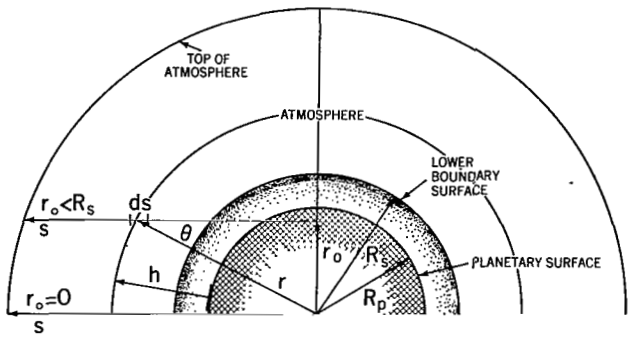

Figure 5—Slant path geometry through the atmosphere.

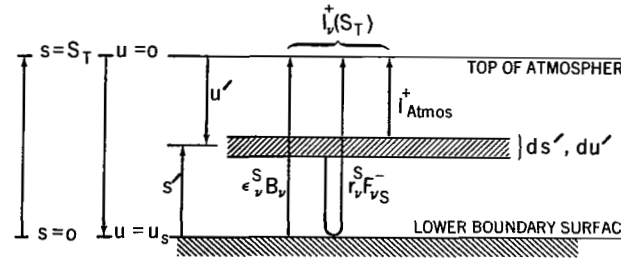

Figure 6—Illustration of radiation components contributing to outgoing planetary radiance.

the lower boundary surface is considered in Figure 5. A more detailed description of the atmospheric slant path is shown in Figure 6. For a pure absorbing atmosphere in local thermodynamic equilibrium, the outgoing spectral radiance $I_\nu^+(S_T)$ at level S_T (Chandrasekhar, 1960) is

$$I_\nu^+(S_T) = I_\nu^+(0)\, e^{-\int_0^{S_T} k^m(\nu)\rho_g\, ds} + \int_0^{S_T} B_\nu(s')\, e^{-\int_{s'}^{S_T} k^m(\nu)\rho_g\, ds}\, k^m(\nu)\rho_g\, ds' \quad , \tag{70}$$

where $k^m(\nu)$ is the mass absorption coefficient, B_ν is the Planck function, and ρ_g is the density of the absorber. To conform to the system of units generally in use with respect to the absorption coefficient, it is necessary to transform the mass absorption coefficient $k^m(\nu)$ into an absorption coefficient per unit length per unit pressure $k(\nu)$. The transformation is made by defining

$$k(\nu) = \frac{k^m(\nu)\,\rho_r}{p_r} \quad , \tag{71}$$

and

$$du = -p_r\left(\frac{\rho_g}{\rho_r}\right) ds \quad , \tag{72}$$

where p_r is the partial pressure of the absorber, u is the optical path length in cm atm, and ρ_r is the absorber density corresponding to reference conditions, usually taken at NTP. The absorption coefficient $k(\nu)$ has units of $cm^{-1}\ atm^{-1}$. With Equations 71 and 72 the product $k^m(\nu)\rho_g\, ds$ may be written as

$$k^m(\nu)\,\rho_g\, ds = -k(\nu)\, du \quad . \tag{73}$$

The absorption coefficient transformation also requires that the integrated absorption coefficient be redefined. The transformed integrated absorption coefficient S in units of $cm^{-2}\ atm^{-1}$ is

related to S^m (Equation 26)

$$S = \frac{\rho_r S^m}{p_r c} . \tag{74}$$

The factor c enters the conversion because of the change from frequency to wave number units in the absorption coefficient. Making the substitution of Equation 73 into Equation 70, the radiative transfer equation becomes

$$I_\nu^+(u = 0) = I_\nu^+(u_S)\, e^{-\int_0^{u_S} k(\nu)\, du} + \int_0^{u_S} B_\nu(u')\, e^{-\int_0^{u'} k(\nu)\, du}\, k(\nu)\, du' , \tag{75}$$

where the coordinate convention is as indicated in Figure 6. The transmittance between the levels u' and u'' in the atmosphere is given by

$$T_\nu(u'', u') = e^{-\int_{u''}^{u'} k(\nu)\, du} , \tag{76}$$

where $u'' < u'$. The radiative transfer equation can be written in terms of the spectral transmittance as

$$I_\nu^+(T_\nu = 1) = I_\nu^+(T_\nu^S)\, T_\nu(0, u_S) + \int_{T_\nu^S}^{1} B_\nu(T_\nu)\, dT_\nu(0, u') , \tag{77}$$

or after an integration by parts as (Plass, 1956)

$$I_\nu^+(T_\nu = 1) = I_\nu^+(T_\nu^S)\, T_\nu(0, u_S) + B_\nu(T_\nu = 1) - B_\nu(T_\nu^S)\, T_\nu(0, u_s) + \int_{B_\nu(T_\nu=1)}^{B_\nu(T_\nu^S)} T_\nu(0, u')\, dB_\nu(T_\nu) . \tag{78}$$

Assuming the underlying surface does not radiate as a blackbody, the outgoing radiance of the surface consists of two terms

$$I_\nu^+(T_\nu^S) = \epsilon_\nu^S B_\nu(T_\nu^S) + r_\nu^S F_{\nu_S}^- , \tag{79}$$

where r_ν^S is the reflectivity for a perfectly diffuse reflector, and $\pi F_{\nu_S}^-$ is the downward monochromatic radiant emittance. Because of the non-blackbody character of the surface, not all of the

radiation incident on the surface will be absorbed; some of the radiation will be reflected back up into the atmosphere. The reflected component of the outgoing radiance from the surface is given by the second term of Equation 79. The reflected component can be neglected for spectral regions where the downward atmospheric emission is small as in "window" regions, and where the surface emissivity is close to unity, as the surface reflectivity is then close to zero.

Including the pressure and temperature dependence of the absorption coefficient, the transmittance (Equation 76) can be written as

$$T_\nu (P, T, u'', u') = e^{-\int_{u''}^{u'} k(P,T,\nu)\, du} \quad . \tag{80}$$

The evaluation of this equation requires an integration along the variable pressure and temperature atmospheric slant path. Assuming an isothermal slant path ($T = T_I$), an approximation by Curtis (1952) and Godson (1953) allows the transmittance over a variable pressure path to be determined by using a mean value for the pressure. With the mean pressure given by

$$\bar{P} = \int_{u''}^{u'} P du \Big/ \int_{u''}^{u'} du \ , \tag{81}$$

the transmittance simplifies to

$$T_\nu(\bar{P}, T_I, u'', u') = e^{-k(\bar{P}, T_I, \nu)\,(u' - u'')} \quad . \tag{82}$$

The Curtis-Godson approximation thus equates the transmission along the variable pressure slant path with the transmission of a homogeneous path of length $u' - u''$ at constant pressure $\bar{P}$. In the weak and strong line limit, the Curtis-Godson approximation gives the same absorption as the exact expression. The Curtis-Godson approximation is more transparent at the line center, less transparent in the line wings, and gives a larger equivalent width than the corresponding exact expression (Goody, 1964a, Drayson, 1966). As one would expect, for a given atmospheric slab the error in the Curtis-Godson approximation reaches a maximum for intermediate values of Su. The maximum error also increases as the pressure difference over the atmospheric slab increases, becoming about 5% for end point pressures of 50 and 1000 mb (Drayson, 1966). In general, the conclusion is that the Curtis-Godson approximation is fairly accurate for carbon dioxide and water vapor transmission studies, but is not very good for ozone. These results have been discussed by Kaplan (1959), Goody (1964a, 1964b), and Drayson (1966).

The measured outgoing radiance for a spectral interval $\Delta\nu$ is

$$I^+_{\Delta\nu} (T_\nu = 1) = \int_{\Delta\nu} I^+_\nu (T_\nu = 1)\, d\nu = \int_{\Delta\nu} \phi_\nu\, I^+_\nu (T^S_\nu)\, T_\nu (0, u_S)\, d\nu + \int_{\Delta\nu} \int_{T^S_\nu}^{1} \phi_\nu\, B_\nu(T_\nu)\, dT_\nu (0, u')\, d\nu \ , \tag{83}$$

with ϕ_ν describing the spectral response of the measuring instrument. We can define the average transmittance for $\Delta\nu$

$$\overline{T}_{\Delta\nu} = \frac{\int_{\Delta\nu} T_\nu \, \phi_\nu \, X_\nu \, d\nu}{\int_{\Delta\nu} \phi_\nu \, X_\nu \, d\nu} \quad , \tag{84}$$

where X_ν represents I_ν^+ and B_ν of the first and second terms of Equation 83, respectively. Assuming I_ν^+ and B_ν are constant over $\Delta\nu$,

$$\overline{T}_{\Delta\nu} = \int_{\Delta\nu} T_\nu \, \phi_\nu \, d\nu \Big/ \int_{\Delta\nu} \phi_\nu \, d\nu \quad . \tag{85}$$

Equation 83 can be written in terms of the average transmittance, as defined by Equation 84,

$$I^+_{\Delta\nu}(\overline{T}_{\Delta\nu} = 1) = \overline{T}_{\Delta\nu}\,(0, u_s) \int_{\Delta\nu} \phi_\nu \, I_\nu^+ (\overline{T}^s_{\Delta\nu}) \, d\nu + \int_{\overline{T}^s_{\Delta\nu}}^{1} \int_{\Delta\nu} \phi_\nu B_\nu (\overline{T}_{\Delta\nu}) \, d\nu \, d\overline{T}_{\Delta\nu}(0, u') \quad . \tag{86}$$

(B) Optical Path Length

From Equation 72 the optical path length in cm atm for NTP conditions is

$$du = - \rho_g \, ds \Big/ \rho_{NTP} \quad . \tag{87}$$

The number of cm atm of the absorbing gas in a slant path can be found by taking the number of absorber molecules per unit area in the slant path, and determining the length per unit area which they occupy under normal temperature and pressure conditions. For CO_2 at NTP, one cm atm equals 0.00197 gm/cm^2. In the atmosphere the density of the absorbing gas can be represented as

$$\rho_g = q_m \, \rho_a \quad , \tag{88}$$

where q_m represents the mass fraction of the absorber and ρ_a, the total atmospheric density. With the ideal gas law and Equation 88 the optical path length becomes

$$du = - q_m \frac{M_a}{M_g} \frac{P}{P_{NTP}} \frac{T_{NTP}}{T} \, ds \quad , \tag{89}$$

where P and T represent the atmospheric pressure and temperature and M_a and M_g are the molecular weights of the atmosphere and the absorbing gas, respectively. Alternatively the above equation can be written in terms of the volume fraction of the absorber, $q_v = M_a/M_g\, q_m$, as

$$du = - q_v\, P/P_{NTP} \frac{T_{NTP}}{T}\, ds \quad . \tag{90}$$

In the Earth's atmosphere, carbon dioxide has an average value — average with respect to season, latitude and altitude — of $q_m = .0477$ gm/kg (Bolin and Keeling, 1963). For water vapor and ozone, q_m is highly variable with respect to altitude.

The water vapor content is usually specified in terms of the mixing ratio q_m^d, which is the ratio of the density of water vapor to the density of dry air. The optical path length is considered in units of precipitable centimeters (pr cm) - the length of a column of liquid water formed by condensing all the water vapor in a column along the slant path - the unit of conversion being 1 pr cm = 1245 cm atm. The number of pr cm is equal to the number of gm/cm² in the path. The optical path length for water vapor becomes

$$du = - \frac{q_m^d}{1245} \frac{M_a}{M_{H_2O}} \frac{P}{P_{NTP}} \frac{T_{NTP}}{T}\, ds \quad . \tag{91}$$

From Equation 87, the optical path length for O_3 in cm atm may be written as

$$du = - q_{O_3}\, ds \quad , \tag{92}$$

where q_{O_3} is in cm atm/km.

From the geometry of Figure 5, the relationship

$$ds = r(r^2 - r_0^2)^{-1/2}\, dr \tag{93}$$

may be obtained with $r_0 = \sin\theta\,(R_p + h)$, where R_p is the radius of the planet. The integrated optical path length from the top of the atmosphere to the point r is

$$CO_2: \quad u(\text{cm atm, NTP}) = - \int_{\infty}^{0} q_v \frac{P}{P_{NTP}} \frac{T_{NTP}}{T}\, 10^5\, ds\ (\text{km}) \quad . \tag{94}$$

$$H_2O: \quad u(\text{pr cm}) = - \int_{\infty}^{0} \frac{q_m^d \left(\frac{\text{gm}}{\text{kg}}\right) 10^{-3}}{1245} \frac{M_a}{M_{H_2O}} \frac{P}{P_{NTP}} \frac{T_{NTP}}{T}\, 10^5\, ds\ (\text{km}) \quad . \tag{95}$$

$$O_3: \quad u(\text{cm atm, NTP}) = - \int_{\infty}^{0} q_{O_3} \left(\frac{\text{cm atm}}{\text{km}}\right) \, ds \, (\text{km}) \, . \tag{96}$$

Assuming hydrostatic equilibrium for the atmosphere gives the pressure as a function of height,

$$P(r) = P_S \exp\left[- \int_{R_S}^{r} \frac{g(r) \, M_a \, 10^5 \, dr \, (\text{km})}{RT} \right] , \tag{97}$$

where P_s is the surface pressure, g is gravity, and R is the universal gas constant.

The next section is devoted to a description of the methods used to determine the average transmittance over a finite spectral interval. In section V, the development of the computer logic involving the equations discussed in this section will be covered.

IV. AVERAGE TRANSMITTANCE FOR A FINITE SPECTRAL INTERVAL

The average transmittance for a finite spectral interval, as defined by Equation 85, is

$$\overline{T}_{\Delta\nu} = 1/\Delta\nu \int_{\Delta\nu} T_\nu \, d\nu \, , \tag{98}$$

where ϕ_ν has been set equal to unity. The average transmittance may be determined semi-theoretically by using a band model, which can be evaluated analytically, to represent the vibration-rotation lines or by direct integration across the spectrum considering each vibration-rotation line individually. Which approach to use depends on the particular problem. Where high resolution is not demanded, the band models offer a practical solution which can be computed very fast. However, as the width of the spectral interval decreases to the order of five wave numbers or less, the computational time required by a band model such as the quasi-random model begins to approach that of the direct spectral integration. Serious limitations of the band models are (Drayson, 1966):

1. Representation of line strengths, positions, and collision broadened half-widths is not adequate.
2. Of necessity, the Curtis-Godson approximation must be used for the vertical integration.
3. Instrumental response functions and the mixed line shape cannot be simply taken into account.

The utilization of the band model approach, in particular the quasi-random model, and the direct spectral integration approach will be discussed in more detail in the following sections. First, however, a brief digression will be made to consider the equivalent width of a single line.

A. Equivalent Width for a Single Line

The equivalent width for a single line is

$$W = \int_{-\infty}^{+\infty} (1 - e^{-k(\nu)u})\, d\nu \quad . \tag{99}$$

With

$$k(\nu) = S\, b(\nu) \quad , \tag{100}$$

where $b(\nu)$ is the relative line shape subject to the normalization condition

$$\int_{-\infty}^{+\infty} b(\nu)\, d\nu = 1 \quad , \tag{101}$$

the equivalent width is

$$W = \int_{-\infty}^{+\infty} (1 - e^{-S\,u\,b(\nu)})\, d\nu \quad . \tag{102}$$

The equivalent width reduces to

$$W = Su \tag{103}$$

for small path length and/or weak lines (Green and Wyatt, 1965). The above expression, known as the weak line approximation, is independent of the line shape and half-width. For large values of Su/α, the equivalent width for a Lorentz line is

$$W = \sqrt{Su\,\alpha} \quad , \tag{104}$$

which is referred to as the square root approximation.

Equation 99 has been evaluated numerically for the Lorentz line shape and for the Benedict modified Lorentz line shape with the results shown in Figure 7. As one would anticipate, the exponential drop-off of the wings of the Benedict line shape causes the difference between the Lorentz and Benedict modification equivalent widths to increase as the pressure and absorber concentration increase, with the Benedict modification equivalent width always being smaller than

the corresponding Lorentz value. Equation 99 also has been evaluated numerically for the mixed line shape. The equivalent widths of a Lorentz line with $\alpha_L = 1 \times 10^{-4}$ cm^{-1} are compared with the corresponding values for several mixed line shapes (Figure 8). The Doppler half-widths for the mixed line shapes are assumed to be 1.432×10^{-4} and 1.601×10^{-2} cm^{-1}.

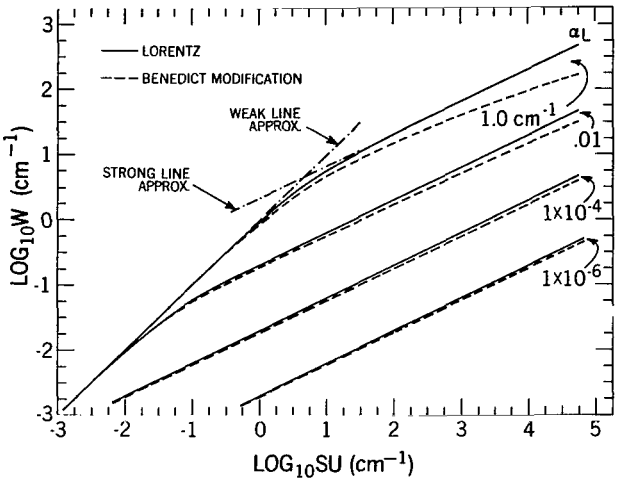

Figure 7—Curve of growth for Lorentz line shape and for Benedict modification of Lorentz line shape.

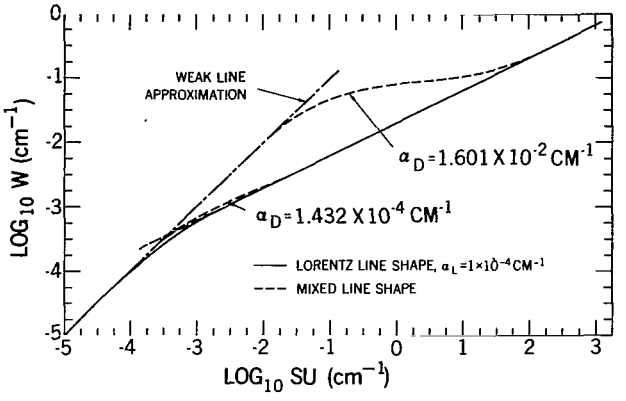

Figure 8—Curve of growth for Lorentz line shape and for mixed line shape.

B. Quasi-Random Model for Molecular Line Absorption

The various models (Elsasser, statistical, random Elsasser) that have been proposed to represent molecular band absorption, approximations to these models, and their regions of validity have been discussed by Plass (1958, 1960). Of these models, only the statistical model is of interest in the present study as it is essential to the development of the quasi-random model. The quasi-random model will be presented in some detail as the author has programmed the quasi-random model for the IBM 7094, thus allowing a check on the accuracy of the transmittance calculations of Wyatt, Stull and Plass (1962b, 1963).

(1) Theory and Computational Technique

The statistical model (Goody, 1952; Plass, 1958; Howard, Burch and Williams, 1955; Goody, 1964a) considers a spectral interval of width $\Delta\nu$ containing n total lines, with each individual line having intensity S_i and wave number ν_i occurring within $\Delta\nu$. Let $N(\nu_1 \cdots \nu_i \cdots \nu_n)\, d\nu_1 \cdots d\nu_i \cdots d\nu_n$ represent the probability that the i^{th} line occurs between ν_i and $\nu_i + d\nu_i$, and similarly $P(S_i)\, dS_i$ is the probability that the i^{th} line has an intensity between S_i and $S_i + dS_i$. If $\nu_1 \cdots \nu_n$, $S_1 \cdots S_n$ are mutually independent, the probability of finding the set of n lines with the distribution $\nu_1 \cdots \nu_n$, $S_1 \cdots S_n$ is

$$\sum_{i=1}^{n} N(\nu_i)\, P(S_i)\, d\nu_i\, dS_i \quad . \tag{105}$$

The average transmittance at wave number ν is found by averaging the transmittance at ν over the probability distribution of the set of n lines

$$\bar{T}(\nu) = \int_{\Delta\nu} \cdots \int_{\Delta\nu} \int_0^\infty \cdots \int_0^\infty \sum_{i=1}^{n} N(\nu_i)\, P(S_i) \exp\left[-S_i\, u\, b(\nu, \nu_i)\right] d\nu_i\, dS_i \,. \tag{106}$$

Assuming that the line positions are distributed at random in $\Delta\nu$ and that all the lines have the same intensity,

$$\bar{T}(\nu) = \left[\frac{\int_{\Delta\nu} e^{-S\, u\, b(\nu, \nu_i)}}{\Delta\nu} d\nu_i \right]^n \,. \tag{107}$$

The average transmittance $\bar{T}(\nu)$ is usually evaluated for the wave number ν_c occurring at the center of $\Delta\nu$, with the assumption that $\bar{T}(\nu_c)$ is equivalent to the average transmittance $\bar{T}_{\Delta\nu}$

$$\bar{T}_{\Delta\nu} = \int_{\Delta\nu} \bar{T}(\nu)\, d\nu \tag{108}$$

of the interval. The quasi-random model calculations of Wyatt, Stull and Plass (1962b, 1963) used the above assumption. The validity of this assumption will be discussed later.

The quasi-random model differs from other band models in several ways (Wyatt, Stull and Plass, 1962a):

a. Method of spectral division — To determine the average transmittance for the interval Δ, a subdivision of Δ into smaller intervals δ is made. The vibration-rotation lines occurring in an interval δ are assumed to have a random distribution of line positions. The average transmittances for the δ's within Δ are arithmetically averaged to obtain the average transmittance of Δ. In principle, the exact line positions are obtained by allowing δ to approach zero.

b. Intensity distribution — The lines in a subinterval δ are divided into subgroups, each subgroup covering one intensity decade. Wyatt, Stull and Plass have found that only the five strongest intensity decades need be retained in a subinterval. The intensity distribution is then simulated by the number of lines and the average intensity $\bar{S}$ for each decade. Considering the five intensity decades, Equation 106 gives the average transmittance at ν due to the lines in δ_j as

$$\bar{T}_j(\nu) = \sum_{i=1}^{5} \left\{ 1/\delta_j \int_{\delta_j} e^{-\bar{S}_i\, u\, b(\nu, \nu_i)}\, d\nu_i \right\}^{n_i} \,, \tag{109}$$

where the total number of lines in δ_j is

$$n_j = \sum_{i=1}^{5} n_i .$$

c. Wing effects — The contribution to the transmittance of a given subinterval from the wings of lines in adjacent subintervals is taken into account.

The total transmittance at wave number ν in subinterval δ_k is

$$\bar{T}_k(\nu) = \sum_{j=1}^{\infty} \bar{T}_j(\nu) \quad , \tag{110}$$

where $\bar{T}_j(\nu)$ is the contribution to $\bar{T}_k(\nu)$ from the n_j lines in interval δ_j. The direct contribution to $\bar{T}_k(\nu)$ occurs due to the n_k lines in subinterval δ_k when $j = k$. The wing contribution is due to all remaining intervals for which $j \neq k$. Combining Equations 109 and 110,

$$\bar{T}_k(\nu) = \sum_{j=1}^{\infty} \left[\sum_{i=1}^{5} \left\{ 1/\delta \int_{\delta} e^{-\bar{S}_i u b(\nu, \nu_i)} \, d\nu_i \right\}^{n_i} \right]_j . \tag{111}$$

From the above equation, the average transmittance for each subinterval δ can be evaluated. Determination of the quasi-random average transmittance for interval Δ is accomplished by arithmetically averaging the $\bar{T}_k(\nu)$'s of the subintervals contained in Δ.

To avoid errors introduced by the arbitrary division of the spectrum into subintervals δ, the quasi-random transmittance is calculated for an unshifted and shifted mesh. The two meshes are offset from each other by $\delta/2$ cm^{-1}. For an interval δ between ν_0 and $\nu_0 + \delta$, the resultant transmittance at $\nu_c = \nu_0 + \delta/2$ is then averaged from the two meshes

$$\bar{T}_k(\nu_c) = 1/3 \left[\bar{T}_k^s(\nu_0) + \bar{T}_k^u(\nu_c) + \bar{T}_k^s(\nu_0 + \delta) \right] , \tag{112}$$

where the superscripts s and u represent the shifted and unshifted meshes, respectively.

The main term to be evaluated in Equation 111 is the expression for the average transmittance for a single line,

$$\bar{T}_i(\nu) = 1/\delta \int_{\delta_i} e^{-\bar{S}_i u b(\nu, \nu_i)} \, d\nu_i \quad . \tag{113}$$

Introducing the following symbols

$$y = \nu_i - \nu_0 - \delta/2 \ , \tag{114}$$

$$z = \nu - \nu_0 - \delta/2 \ , \tag{115}$$

$$\xi_i = S_i \, u/\pi\alpha_L \ , \tag{116}$$

$$\rho = 2\alpha/\delta \ , \tag{117}$$

$$\eta = 2y/\delta \ , \tag{118}$$

$$\epsilon = 2z/\delta \ , \tag{119}$$

and assuming the Lorentz line shape,

$$\overline{T}_i(\nu) = 1/2 \int_{-1}^{1} \exp \left[\frac{-\rho^2 \xi_i}{(\epsilon - n)^2 + \rho^2} \right] d\eta \ . \tag{120}$$

The interval δ is considered to be between ν_0 and $\nu_0 + \delta$. In addition, ξ_{i_0} is defined by

$$\xi_{i_0} = S_i \, P_0/\pi \, \alpha_0(T) \ , \tag{121}$$

where $\alpha_0(T)$ is the half-width at pressure P_0 and temperature T, thus allowing Equation 116 to be rewritten as

$$\xi_i = \xi_{i_0} \, u/P \ . \tag{122}$$

The quantity ξ_{i_0} and the number of lines n_i have been determined semi-theoretically by Wyatt, Stull and Plass (1962b and 1963) for each of the five intensity decades for CO_2 and H_2O at 300°K, 250°K and 200°K and listed in coefficient tables. The tabulations are every 2.5 cm^{-1} for sub-intervals of δ = 5 cm^{-1}. The spectral range included is 505-10,000 cm^{-1} for CO_2, and 700-10,000 cm^{-1} for H_2O. From Equation 120, Wyatt, Stull and Plass (1962a) have evaluated the direct contribution to the transmittance in analytical form as

$$\overline{T}_i(\nu) = 1/2 \, (1 - \epsilon) \, \Omega(\xi_i, \zeta) + 1/2 \, (1 + \epsilon) \, \Omega(\xi_i, \zeta') \ , \tag{123}$$

where

$$\zeta = \rho/1 - \epsilon \ , \tag{124}$$

$$\zeta' = \rho/1 + \epsilon \ , \tag{125}$$

$$\Omega(\xi\zeta) = \exp\left[-\xi\zeta^2/(1+\zeta^2)\right] - \frac{1}{2}\zeta\xi \exp\left(-\frac{1}{2}\xi\right) \left[I_0\left(\frac{1}{2}\xi\right) + I_1\left(\frac{1}{2}\xi\right)\right](\pi - \psi)$$

$$+ 2\zeta \exp\left(-\frac{1}{2}\xi\right) \sum_{n=1}^{\infty} I_n\left(\frac{1}{2}\xi\right) \sin n\psi + \zeta\xi \exp\left(-\frac{1}{2}\xi\right) \sum_{n=1}^{\infty} \left[I_n\left(\frac{1}{2}\xi\right) + I_{n+1}\left(\frac{1}{2}\xi\right)\right] \frac{\sin n\psi}{n}, \tag{126}$$

where $\psi = 2 \tan^{-1} \zeta$, and I_n is the Bessel function of imaginary argument and order n. Young (1964) has shown that the direct contribution may be evaluated numerically by dividing the integration interval of Equation 120 into seven subintervals and applying seven-point Legendre-Gauss quadrature formula to each subinterval. The seven subintervals were chosen as

$$\eta = 0.0,\ 0.001,\ 0.005,\ 0.01,\ 0.05,\ 0.1,\ 0.5,\ 1.0.$$

In this work, Young's method was used with one exception, i.e., eight-point rather than seven-point quadrature formula was applied. The numerical and analytical integration agree exactly to six significant figures.

The average transmittance $\overline{T}_i(\nu)$ has been evaluated from Equation 120 for the center $\nu = \nu_c$ and for the lower boundary $\nu = \nu_0$ of the interval with the results given in Table 1. The large difference between $\overline{T}(\nu_c)$ and $\overline{T}(\nu_0)$ indicates that $\overline{T}(\nu)$ should be averaged with respect to

Table 1

Average Transmittance at Center and Boundary of Subinterval δ.

$\rho^2 \xi_i$	ρ	$\overline{T}(\nu_c)$	$\overline{T}(\nu_0)$
0.001	0.05	0.9724	0.9860
0.01	0.05	0.8454	0.9202
0.1	0.05	0.5413	0.7464
1.0	0.05	0.0897	0.3544
10.0	0.05	0.0	0.1108

frequency as discussed previously (Equation 108). In effect, this averaging with respect to ν is accomplished in a fashion by Wyatt, Stull and Plass (1962a) by the averaging over the two meshes.

The wing contribution is obtained by assuming $\alpha^2 << (\nu - \nu_0)^2$. Equation 120 then becomes for the Lorentz line shape

$$\bar{T}_i(\nu) = \frac{1}{2} \int_{-1}^{1} \exp\left[\frac{-\rho^2 \xi_i}{(\epsilon - \eta)^2}\right] d\eta \ , \tag{127}$$

which Wyatt, Stull, and Plass (1962) have evaluated as

$$\bar{T}_i(\nu) = \frac{1}{2}\left\{(\epsilon + 1)\exp\left[\frac{-A}{(\epsilon+1)^2}\right] - (\epsilon - 1)\exp\left[\frac{-A}{(\epsilon-1)^2}\right]\right\} - \frac{1}{2}\pi^{1/2} A^{1/2}\left[\operatorname{erf}\left(\frac{A^{1/2}}{\epsilon-1}\right) - \operatorname{erf}\left(\frac{A^{1/2}}{\epsilon+1}\right)\right], \tag{128}$$

where $A = \rho^2 \xi_i$. For the Benedict modification, the wing expression is

$$\bar{T}_i(\nu) = \frac{1}{2} \int_{-1}^{1} \exp\left[\frac{-\xi_i \rho^2 \exp\left[-a'(\delta/2)^{b''}|\epsilon - n|^{b''} + a'|d|^{b''}\right]}{(\epsilon - \eta)^2}\right] d\eta \ . \tag{129}$$

It should be noted that the above formulation of the Benedict modification used by Wyatt, Stull and Plass (1962a, 1962, 1963) is not the same as appears in Equation 55. The Wyatt, Stull and Plass formulation yields an absorption coefficient about 5-10% too large. In this investigation the Wyatt, Stull and Plass formulation has been used. The wing contributions of Wyatt, Stull and Plass 1962b, 1963) were calculated using the Lorentz line shape for H_2O and the Benedict modification for CO_2. As Equation 129 cannot be evaluated analytically Wyatt, Stull and Plass have assumed the transmittance at the center of the interval ($\eta = 0$) is representative of the average transmittance over the interval. The integration of Equation 129 can then be avoided. In this investigation, 8-point Legendre-Gauss quadrature formula was applied to the interval $\eta = -1$ to $\eta = +1$ for Equations 127 and 129. This technique allows the average transmittance to be determined to an accuracy of 5-6 significant figures. The wing transmittance due to lines in the nearest adjacent interval ($\epsilon = -2$) is shown in Figure 9 for both the Lorentz and Benedict modified line shapes. The average transmittance at the center of the interval for the Benedict modified line shape, as determined by the 8-point quadrature formula, is indicated in Figure 9 by the small dots. Comparison of the average transmittance with the transmittance for $\eta = 0$ gives an indication of the error introduced by Wyatt, Stull, and Plass in assuming

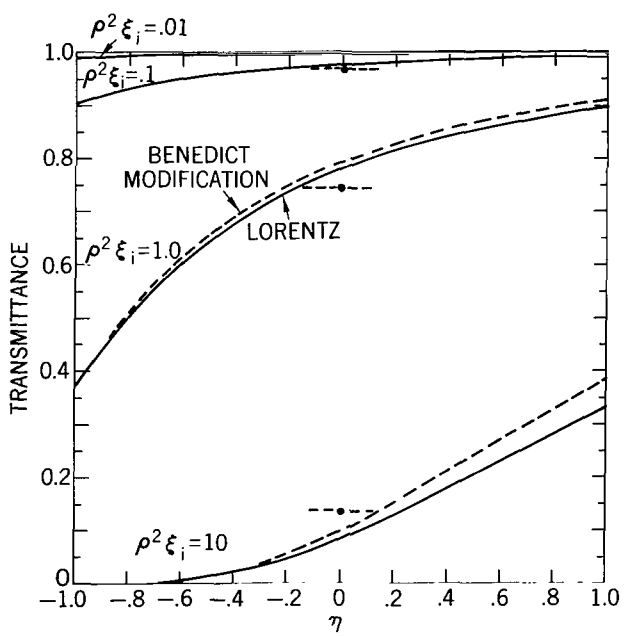

Figure 9—Wing transmittance due to lines occurring in adjacent subinterval ($\epsilon = -2$).

that the average transmittance can be approximated by the transmittance at $\eta = 0$. This comparison is given in Table 2. The differences are significant enough to warrant inclusion of the numerical averaging. In their work, Wyatt, Stull and Plass used values of $a' = 0.0675$ and $b'' = 0.7$ for the Benedict modification parameters, which differ slightly from the values of $a' = 0.08$ and $b'' = 0.08$ given by Winters, et al. (1964).

Table 2
Average Wing Transmittance $\bar{T}(\nu)$ due to Lines in Adjacent Subinterval.

$\rho^2\xi_i$	$\eta = 0$	Quad. Avg.
.001	.9998	.9997
.01	.9977	.9968
.1	.9772	.9691
1.0	.7939	.7455
10.0	.0995	.1336

The wing contribution for a given interval is due to wings of lines occurring in intervals both to the high wave number side ($\epsilon = +2, 4, 6, \cdots$) and the low wave number side ($\epsilon = -2, -4, -6, \ldots$) of the given interval. For a gas at a specified temperature, pressure and optical path length, an interval at some maximum epsilon ϵ_M may be defined such that the contributions of lines in intervals with $+\epsilon > +\epsilon_M$ and with $-\epsilon < -\epsilon_M$ will have a negligible effect on the wing contribution of the given interval at $\epsilon = 0$. Considering only the strongest line intensity decade ($i = 1$) for $\eta = 0$, the wing transmittance may be written as

$$\bar{T}(\nu) = \left\{ \exp\left[\frac{-\rho^2 \xi_1}{|\epsilon|^2} \right] \right\}^{n_1} . \tag{130}$$

Setting $\bar{T}(\nu) = 0.999$, ϵ_M is defined by

$$\epsilon_M^2 = \frac{-n_1 \rho^2 \xi_1}{\ln (0.999)} , \tag{131}$$

which can be simplified to

$$\epsilon_M^2 = \text{const}\, n_1 \xi_{1_0} Pu . \tag{132}$$

Selecting the maximum combination of $n_1 \xi_{0_1}$ from the coefficient tables and inserting into Equation 132 gives

$$\epsilon_M^2 = \text{const Pu} \ . \tag{133}$$

With P and u specified, ϵ_M can be determined. The wave number ν_M corresponding to ϵ_M can be determined using the relations in Equations 115-119. The parameter ϵ_M thus specifies the number of intervals on either side of a given interval that must be considered to insure that all lines which could possibly contribute to the wing contribution of the given interval have been taken into account. The above expression is valid only for a Lorentz line shape; a similar expression can be derived for the Benedict modification.

2. Apparent Error in Wyatt, Stull and Plass Quasi-Random Transmittance Tables

Using the numerical evaluation techniques discussed in the previous section, the quasi-random model was programmed on the IBM 7094 digital computer. Dr. Plass kindly provided magnetic tapes containing the coefficient tables of ξ_{i_0} and n_i for H_2O at 300, 250 and 200°K and for CO_2 at 300 and 200°K. As a side result, this investigation allows an independent check on the accuracy of the Wyatt, Stull and Plass (WSP) transmittance tables. In all cases, agreements with the WSP transmittance tables should be exact to at least three significant figures since the same input data and the same formulation is used.

Exact agreement was found for H_2O, with one exception. For values of Pu greater than approximately unity, the transmittance values calculated in this investigation are lower than the corresponding WSP values, the disagreement increasing with increasing values of Pu. This is illustrated for the case ν = 1002.5 cm^{-1}, P = 1, T = 300°K in Figure 10.

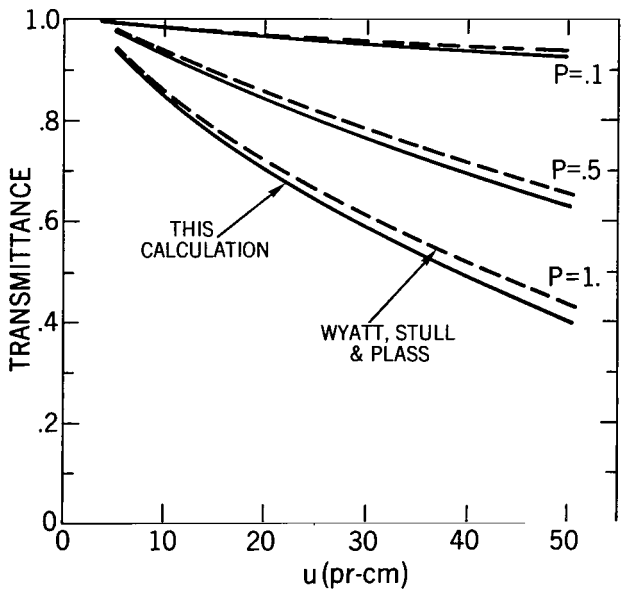

Figure 10—Comparison of water vapor transmittances for ν = 1002.5 cm^{-1} and T = 300°K.

For CO_2, disagreement was found for all the cases that were considered. In general, the disagreement correlates with the amount of wing contribution with the disagreement increasing as the wing contribution becomes a larger fraction of the total transmittance. In Figure 11 the transmittance for ν = 605 cm^{-1}, P = 1, and T = 300°K is graphed as a function of u. The transmittance values of this calculation are more transparent than the corresponding values of WSP, with the difference between the two values increasing with increasing u. A second comparison of CO_2 transmittances is illustrated in Figure 12 for the R branch lines of the 4.3μ band for P = 1, T = 300°K and for several values

of u. From this figure the correlation of the difference between the two sets of transmittances with the amount of wing contribution is very evident.

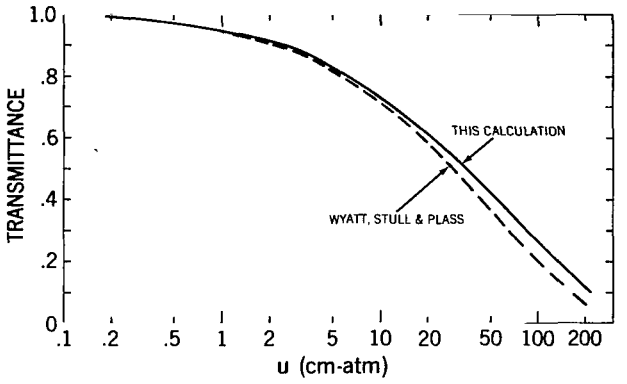

Figure 11—Comparison of carbon dioxide transmittances as a function of u for $\nu = 605$ cm^{-1}; P = 1 and T = 300°K.

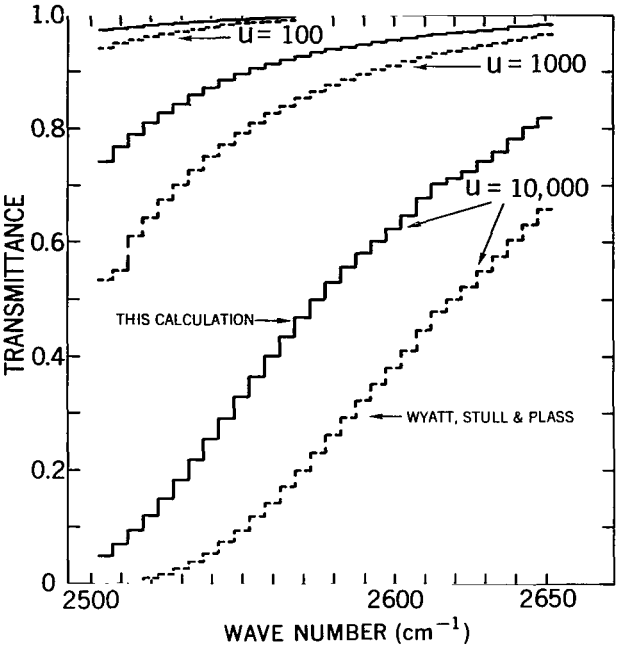

Figure 12—Comparison of carbon dioxide transmittances as a function of wave number for various values of u with P = 1 and T = 300°K.

The reason for the disagreement for the H_2O and CO_2 calculations is not known at the present time. However, there seems to be a strong possibility that the CO_2 transmittances of WSP may be in error. Stull* has indicated that instead of using the wing contribution for a given interval, the wing contributions of the two adjacent intervals may have been used, thus overestimating the absorption. A few checks by the author have indicated that inducing this type of error into the present calculations would give much better, although not identical, agreement with WSP.

3. Comparison of Quasi-Random Transmittances to Experimental Data

As the quasi-random transmittances are normalized to the low spectral resolution experimental data by the normalization constants $C_\nu^{\nu'}(T)$ (Wyatt, Stull and Plass, 1962b, 1963), one would expect that the quasi-random transmittances would in turn give good agreement with the experimental data. As a check, the quasi-random integrated absorptance has been calculated for several cases for H_2O and CO_2.

For the 6.3μ H_2O band Burch, et al. 1962, have measured the integrated absorptance for the spectral intervals 1250 to 1590 cm^{-1} and 1590 to 2100 cm^{-1} for a range of pressures and H_2O concentrations. The largest path length was 0.077 pr cm. A comparison of the calculated and measured integrated absorptance is given in Table 3. The fourth and seventh columns represent

*V. R. Stull. Private communication, 1965.

Table 3

Comparison of Quasi-Random and Experimental Integrated Absorptances for the 6.3μ H_2O Band.

			$\int A d\nu$ 1250-1590 cm^{-1}			$\int A d\nu$ 1590-2100 cm^{-1}		
Sample	Pe	u	Exp.	α_L = .10	α_L = .16	Exp.	α_L = .100	α_L = .115
	atm	pr cm						
1	.0184	.0017	12.3	9.6	15.0	12.7	13.4	15.4
2	.0232	.0018	14.9	10.9	17.1	14.4	15.4	17.6
3	.0345	.0019	17.0	13.4	20.9	16.4	18.9	21.6
4	.0530	.0019	21.1	16.2	25.0	22.4	22.9	26.1
5	.1167	.0017	30.0	21.3	32.6	30.3	30.3	34.5
6	.3540	.0019	50.9	35.1	51.8	50.9	50.3	56.7
7	1.0171	.0018	79.4	48.9	69.0	79.4	71.2	79.1
8	.0184	.0034	18.2	13.7	21.4	13.6	19.1	21.9
9	1.0171	.0036	102	70.1	94.8	114.	101	112
10	.0447	.0041	30.6	22.3	34.2	31.3	31.4	35.7
11	.0580	.0047	38.0	26.8	40.6	39.2	37.7	42.7
12	.0755	.0048	45.5	30.3	45.6	48.8	42.7	48.3
13	.1382	.0045	56.7	37.6	55.7	59.5	53.4	60.2
14	.0447	.0081	47.3	31.5	47.4	53.1	43.9	49.7
15	.0580	.0092	54.0	37.4	55.6	59.8	52.2	59.0
16	.0755	.0095	63.9	42.3	62.3	69.9	59.4	66.9
17	.1382	.0089	76.6	52.3	75.3	80.7	74.0	82.8
18	.0447	.0161	63.7	43.9	64.6	70.5	60.8	68.4
19	.0580	.0183	72.1	51.9	75.2	80.2	72.0	80.7
20	.0755	.0190	86.6	58.7	83.9	96.5	81.7	91.3
21	.1382	.0176	100	71.5	99.4	117.	101.	112.
22	.0447	.0322	78.9	60.5	86.4	99.5	83.1	92.8
23	.0580	.0364	90.4	70.8	99.2	108.	97.6	108
24	.0755	.0378	110.	79.5	110	125.	110.	122
25	.1382	.0352	131.	96.0	128	153.	135	148
26	.0487	.0045	33.8	24.3	37.1	38.1	34.1	38.8
27	.0491	.0089	48.1	34.3	51.4	55.3	47.8	54.1
28	.0496	.0179	69.7	48.2	70.4	79.2	66.7	74.9
29	.0500	.0359	93.0	66.4	93.8	109.	91.3	102
30	1.0658	.0102	153	113	141	181	164.	176
31	1.0632	.0198	190	144	172	226.	211	224
32	1.0605	.0389	220	178	204	273	263	275
33	1.0592	.0770	256	212	234	319	315	325

the experimental values of $\int A d\nu$, with the fifth and eighth columns representing the theoretical calculations for $\alpha_L = 0.10$, which is the value used by WSP. It is evident from the comparison that the theoretical values are systematically too small, especially for the 1250-1590 cm^{-1} interval. Trial and error calculations with different values of α_L have indicated that values of $\alpha_L = 0.16$ and 0.115 for the intervals 1250-1590 cm^{-1} and 1590-2100 cm^{-1} respectively give fair agreement with the experimental data. The above half-widths were used only for the direct contribution with the half-width for the wing contribution kept at 0.10 cm^{-1}. The calculated integrated absorptances for the half-widths of .16 and .115 are given in columns six and nine of Table 3. The half-widths given should not be considered as representing the actual average half-width of the respective position of the absorption band, but rather as a parameter adjusted to normalize the theoretical and experimental transmittances. In addition to the above comparison, the integrated absorptance for the entire 6.3μ band was compared to experimental measurements of Burch, et. al. (1955) which covered a wider range of optical path length. Using the half-widths of 0.16 and 0.115, satisfactory agreement was found.

Table 4
Comparison of Quasi-Random and Experimental Integrated
Absorptances for the 15μ CO_2 Band.

P_e (atm)	u (cm-atm)	$\int A d\nu$ (cm^{-1})		
		Experimental	Theoretical (Young)	Theoretical (This Calculation)
0.00051	0.58	3.37	5.8	2.4
0.00137	1.53	8.86	10.1	6.3
0.00496	5.56	21.7	26.7	20.1
0.00827	9.20	32.6	39.3	30.4
0.0205	5.73	34.6	43.3	34.4
0.0397	5.73	43.8	54.0	42.8
0.0837	5.73	54.7	67.3	53.6
0.2052	5.73	69.5	83.6	68.1
0.3999	5.73	81.9	94.0	79.2
1.0089		95.3	103.9	93.2

Values of $\int A d\nu$ for the 15μ band of CO_2 are given Table 4. Column 3 represents the experimental measurements of Burch, et. al. (1962). The integrated absorptances of column 4 are theoretical calculations of Young (1964) using the quasi-random model but different line strengths and column 5 represents the results of the present calculation for a half-width of 0.60 cm^{-1}. For the range of conditions considered in Table 4, the agreement between the present results and the experimental values can be considered satisfactory.

4. Modification for Doppler Broadening

Including the effect of the mixed line shape, the average transmittance for a single line (Equation 113) becomes

$$\overline{T}_i(\nu) = \frac{1}{\delta} \int_{\delta_i} e^{-k_{0_i} H(y', x') u} \, d\nu_i \, . \tag{134}$$

The above expression is evaluated using 8 point Legendre-Gauss quadrature formula for each of seven subintervals in the same manner as for the direct contribution of the pure Lorentz line. As discussed in Section IIc, the mixed line shape is used for pressures less than 100 mb and for distances from the line center less than 2.5 cm^{-1}. A comparison of the average transmittance for a Lorentz line and for a mixed line is presented in Table 5.

Table 5

Quasi-Random Transmittance for Lorentz Line Shape and for Mixed Line Shape, T = 300°K.

ν (cm^{-1})	Pressure	Optical Path Length	Transmittance	
			Lorentz	Mixed
585	100 mb	100 cm-atm	.7722	.7722
640	100 mb	100 cm-atm	.0605	.0605
665	100 mb	100 cm-atm	.0005	.0005
585	10 mb	10 cm-atm	.9745	.9738
640	10 mb	10 cm-atm	.7702	.7681
665	10 mb	10 cm-atm	.3528	.3501
585	10 mb	100 cm-atm	.9073	.9059
640	10 mb	100 cm-atm	.4169	.4146
665	10 mb	100 cm-atm	.0709	.0706
585	1 mb	10 cm-atm	.9902	.9864
640	1 mb	10 cm-atm	.9175	.9043
665	1 mb	10 cm-atm	.6791	.6578
585	.001 mb	10,000 cm-atm	.9894	.9142
640	.001 mb	10,000 cm-atm	.9172	.8522
665	.001 mb	10,000 cm-atm	.6789	.6197

C. Direct Spectral Integration

Drayson (1966) has developed a computer program to determine atmospheric transmittances by direct spectral integration across the absorption band, using theoretically calculated line positions and strengths. Other features of his program are: (1) the mixed line shape is used, and (2) the inclusion of the integration of the absorption coefficient along the atmospheric slant path, thus avoiding the use of the Curtis-Godson approximation. The initial calculations by Drayson have been made for the 15μ CO_2 absorption band.

Drayson has kindly provided the author with a copy of his program. With only slight modification the program has been made compatible with the IBM 7094. In the development of his program, Drayson has divided the 15μ CO_2 absorption lines into 982 strong and 1008 weak lines. This portion of the program was changed so that all the lines were considered as strong lines. The results obtained with this program will be covered in a later section.

V. PROGRAMMING LOGIC

The logical development of the computer program for determining the outgoing spectral radiance, using the quasi-random transmittance, will be discussed in this section. The program is modular in form, consisting of three basic sections:

1. Atmos 1 — For an input model atmosphere, Atmos 1 calculates the optical path length and the average pressure from a given level in the atmosphere to the top of the atmosphere as a function of height for each absorbing gas considered. The input model atmosphere specifies the temperature, the water vapor distribution and the ozone distribution as a function of height. The atmospheric slant path is specified by θ and h (Figure 5). Initially, Atmos 1 numerically integrates the hydrostatic equation for a zenith angle of 0° from the surface to the top of the atmosphere using 0.1 km intervals. As the integration is carried out, the quantity ds (Equation 93) plus the temperature and pressure at the mid-point of each 0.1 km interval is computed and stored. Using the above stored quantities along with the vertical gas distributions, the optical path length (Equations 94, 95, 96) is integrated from the top of the atmosphere to the lower boundary surface. At the same time the average effective pressure (Equation 81) is computed as a function of height. A matrix of height vs optical path length vs average effective pressure is written on magnetic tape for each absorbing gas, considered for a number of pre-selected heights, to serve as an input data tape for the second section of the program. The number of height levels in the matrix is arbitrary, subject only to the restriction that the product of the number of spectral intervals times the number of atmospheric levels cannot exceed 13000 for H_2O or 15000 for CO_2.

2. Atmos 2 — Using the Curtis-Godson approximation, Atmos 2 calculates the quasi-random transmittance for each spectral interval of interest for each atmospheric level of the input height matrix produced by Atmos 1. The widths of the spectral intervals were chosen as $\Delta = \delta = 5$ cm^{-1}, which means that the average transmittance for Δ is based on the assumption of random line

positions in Δ. In this sense the quasi-random model is not really being used, as the quasi-random model differs from a pure random model in the assumption of random line positions only for $\Delta > \delta$. The width of $\Delta = 5\ cm^{-1}$ was chosen so that the coefficient tables of Wyatt, Stull, and Plass (1962b, 1963) could be used. In principle, of course, Δ can be chosen to be any value. Atmos 2 requires the center wave number of the initial ν_I and final ν_F spectral interval to be specified.

The transmittances are evaluated, considering the integrated absorption coefficients to be at an isothermal temperature along the atmospheric slant path. The isothermal temperature which best represents the temperature variation along the slant path must be chosen from 200 and 300°K for CO_2 and from 200, 250 and 300°K for H_2O. With the optical path length, the isothermal temperature and the average effective pressure known, the quasi-random transmittance can be evaluated using the formulation given in section IVB1.

The quasi-random transmittances for a given temperature, pressure, and optical path length are calculated as follows. To insure that the contributions of all lines are taken into account, all intervals from $\nu_I - \nu_M$ to $\nu_F + \nu_M$ must be considered. For the above intervals, the coefficients ξ_{0_i} and η_i, corresponding to temperature T_I for both the unshifted and shifted meshes, are read from magnetic tape and put in core storage. The direct contribution is then computed for each 5 cm^{-1} interval from ν_I to ν_F using the numerical quadrature of Equation 120. Next, the wing contribution is computed starting with the interval at $\nu_I - \nu_M$ and subsequently considering all intervals until the interval $\nu_I + \nu_M$ is reached. For a given interval, the associated coefficients were used to calculate the wing contribution to the transmittances at the center of all the other intervals from ν_I to ν_F. The wing contribution was computed for higher and lower wave numbers until the contribution exceeded 0.999. In each interval of interest, the wing contribution was multiplied into the values previously calculated. When the computation of the wing contribution was completed, the direct and wing contribution for each interval of interest were multiplied together. The same procedure was then used for the shifted mesh. The quasi-random transmittance is then obtained by averaging the transmittances of the unshifted and shifted meshes according to Equation 112. The transmittances are computed for each wave number range of interest starting with the level in the matrix representing the ground, and subsequently evaluating the transmittances for each level in the matrix until the top of the atmosphere is reached. The output of Atmos 2 consists of a height vs transmittance matrix for each 5 cm^{-1} interval. This data is put on magnetic tape to serve as input data for the third section of the program.

3. Atmos 3 — Solves the radiative transfer equation for each 5 cm^{-1} interval. Atmos 3 reads the height vs transmittance matrix for a given spectral interval from the input magnetic tape. The outgoing radiance for this interval is then determined by integrating the radiative transfer equation, in the form of Equation 77, from the top of the atmosphere to the lower boundary surface. The integration is done numerically for atmospheric layers of 0.1 km thickness. The transmittance for each atmospheric level is determined by interpolation from the height vs transmittance matrix. The spectral response and spectral surface emittance must be specified as input parameters for Atmos 3. If more than one absorbing gas must be taken into account, the total transmittance is taken as the product of the transmittances for each individual gas.

Each of the above sections represents a separate Fortran IV program. The three sections cannot be combined into a single program as Atmos 2 utilizes all the available core storage of the IBM 7094. An IBM 7094 listing for the Atmos 1, Atmos 2 and Atmos 3 programs may be found in Appendix C, Appendix D and Appendix E, respectively.

The description given above has been for transmittances as determined from the quasi-random model. However, the modular form allows one section to be modified or even completely replaced without affecting the remaining sections. This is extremely beneficial as Atmos 1 and Atmos 3 can be considered relatively permanent programs whereas Atmos 2 will undergo frequent changes as improved techniques for computing atmospheric transmission become available and are implemented. For example, the atmospheric transmission of Drayson, discussed in Section IVC, represents a considerable improvement over the quasi-random band model and the Curtis-Godson approximation. For the 15μ CO_2 band, this program essentially replaces Atmos 1 and Atmos 2 and it has been modified to write on magnetic tape the height vs transmittance matrix required by Atmos 3.

VI. OUTGOING INFRARED RADIANCES FOR THE EARTH AND MARS

The outgoing infrared radiances have been computed at 5 cm^{-1} intervals for several typical model atmospheres of the Earth and Mars in the spectral range 500 to 2000 cm^{-1}. The transmittances for this spectral range have been assembled from a variety of sources. The high spectral resolution transmittances discussed in the previous sections were used in the manner described in Table 6.

Table 6
Sources of High Spectral Resolution Transmittances.

Gas	Band	Spectral Range	Source
CO_2	15μ	500 - 860 cm^{-1}	Drayson (1966), direct sp. integ.
CO_2	5.2, 9.4, 10.4μ	865 - 2000 cm^{-1}	Plass (1963), quasi-random model
H_2O	6.3μ	1000 - 2000 cm^{-1}	Plass (1962b), quasi-random model

As a temporary measure, the transmission of the 9.1 and 9.6μ bands of ozone and the rotational lines of water vapor has been included at a spectral resolution much lower than 5 cm^{-1}. As the higher spectral resolution data become available for these spectral regions, they will be incorporated into the radiance calculations. These transmittances were determined using generalized absorption coefficients. For the 9.1 and 9.6μ ozone bands and the water vapor rotational lines, the generalized absorption coefficients of Elsasser (1960) and Moller and Raschke (1963), respectively, were used.

A. Earth

The model atmospheres chosen to represent the Earth's atmosphere in this investigation have been described previously by Hanel, Bandeen and Conrath (1963). The models were modified in several ways: (1) the water vapor distributions were assumed to be constant in height above the tropopause at the value occurring at the tropopause, (2) the 1962 U. S. Standard temperature profile was substituted for the 1959 ARDC Standard temperature profile, and (3) the 1959 ARDC Standard water vapor distribution was scaled so that the total amount of H_2O in the vertical was approximately 1 pr cm. Several characteristic properties of the models are listed in Table 7.

Table 7

Surface Temperatures and Total Gas Content for One Air Mass.

Atmosphere	Surface Temperature	Water vapor u(pr cm)	Carbon dioxide u(cm-atm)	Ozone u(cm-atm)
Tropical	305.30°K	4.63	250.11	0.24
1962 U.S. Std	288.15°K	0.97	250.04	0.36
Arctic Winter	246.00°K	0.14	249.93	0.34

Hovis (1965, 1966a, 1966b, 1966c*) has made total reflectance measurements of some common surface minerals, iron oxides, and different types of igneous rocks in the wavelength interval 0.5 to 22μ. Emissivities derived from these measurements are shown in Figure 13 for selected materials from each of the above categories. The solid curve represents soil from the Mojave Desert of California; the dashed curve, limonite of particle size less than 0.105 mm from Caracas, Venezuela; the dotted curve, granite of particle size less than 0.038 mm; and the dot-dash curve, sand from Daytona Beach, Florida, with particle sizes in the range 0.25 to 0.50 mm. The most pronounced infrared spectral features are the residual ray reflections in the 8 to 10μ and 18 to 23μ region. Less pronounced is the water of hydration feature at 6.3μ. The features for wavelengths less than 5μ are not relevant to this investigation. The measurements of Hovis indicate that the emissivity depends strongly on the particle size of the sample.

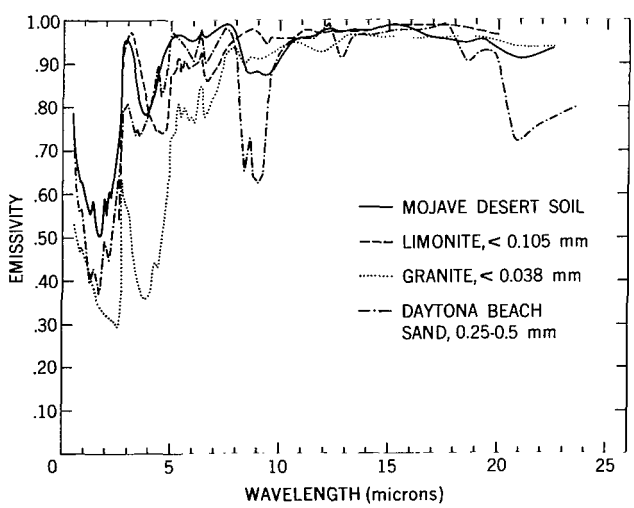

Figure 13—Spectral emissivity of surface materials (Hovis, 1965, 1966a, 1966b, 1966c*).

*W. A. Hovis, Jr. Private communication, 1966.

The computed theoretical thermal emission spectra for the 1962 U. S. Standard, Tropical and Arctic Winter model atmospheres are shown in Figures 14, 15, and 16 respectively for the case of vertical viewing. The vertical scale for all three figures is brightness temperature, the blackbody temperature which is necessary to produce the outgoing radiance in a 5 cm^{-1} interval. The surface emissivity for the three models was assumed to be blackbody. In addition, the thermal emission spectra were computed for the 1962 U. S. Standard model considering the surface emissivities of Mojave Desert soil and of Daytona Beach sand. These spectra are also presented in Figure 14. No instrumental effects have been considered in these computations.

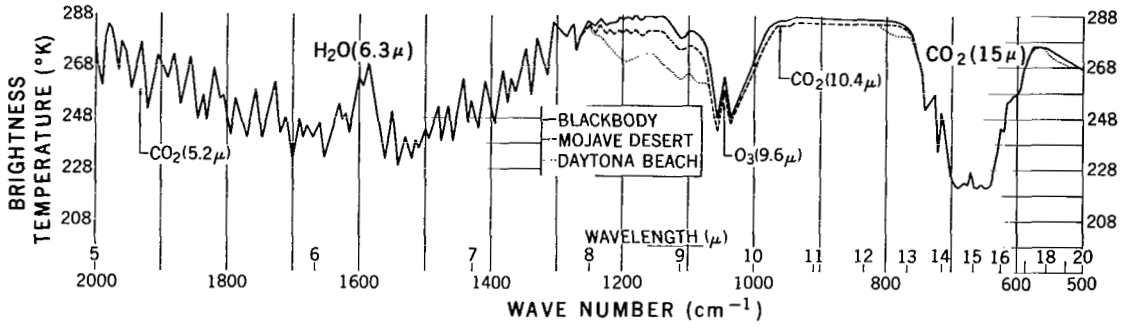

Figure 14—Theoretical thermal emission spectra, 1962 U. S. Standard Model Atmosphere. The effect of surface emissivity on the spectrum is illustrated.

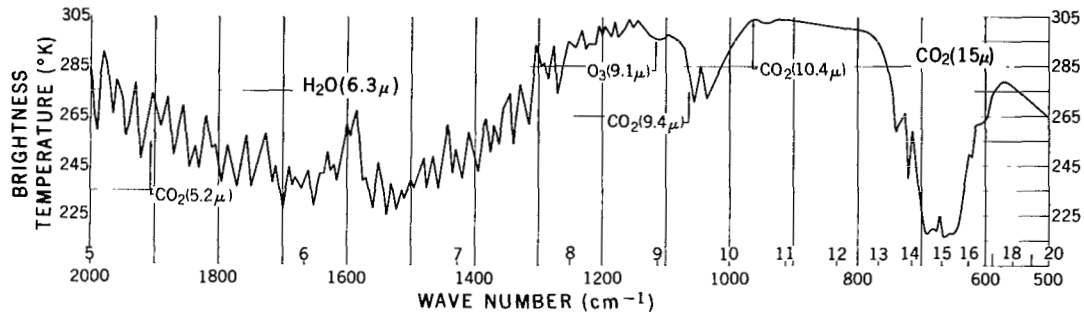

Figure 15—Theoretical thermal emission spectrum, Tropical Model Atmosphere.

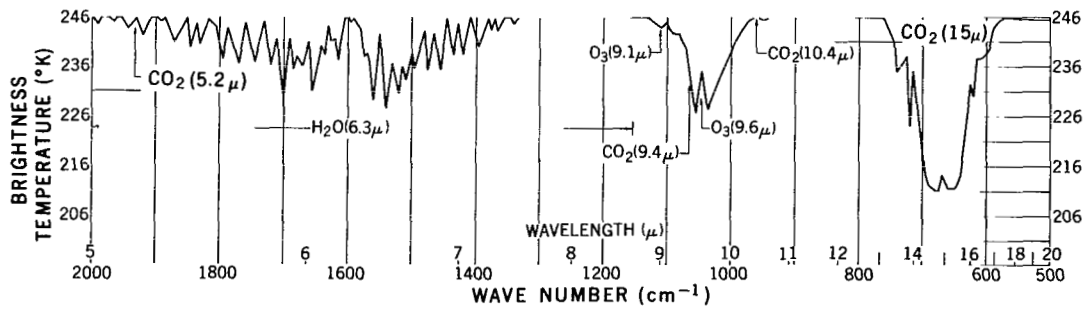

Figure 16—Theoretical thermal emission spectrum, Arctic Winter Model Atmosphere.

In Figures 14, 15, and 16 the most pronounced spectral features are the 6.3μ H_2O, 9.6μ O_3, and 15.0μ CO_2 absorption bands and the H_2O rotational lines which dominate most of the spectral range from 5 to 20μ. Minor absorption due to the 5.2μ CO_2, 9.1μ O_3, 9.4μ CO_2, and 10.4μ CO_2 absorption bands is also evident in the spectra. The minor constituents CH_4, with an absorption band at 7.7μ, and N_2O, with absorption bands at 7.8μ, 8.5μ and 17.0μ, have not been included in the present calculations. The ground transmission spectra, corresponding to the three model atmospheres, are given in Figure 17. The transmittances in the 9 to 11μ region are somewhat inaccurate as the "continuum" H_2O absorption has not been considered and because the generalized absorption coefficients used for O_3 overestimate the absorption of the 9.6μ O_3 band (Elsasser, 1960).

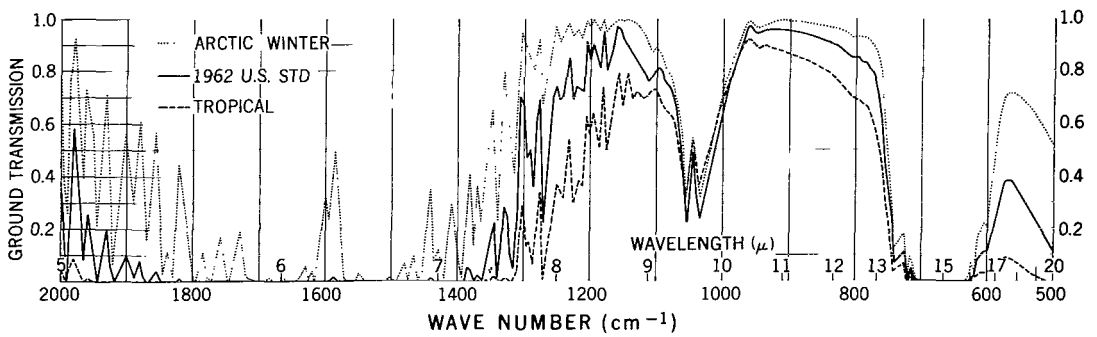

Figure 17—Ground transmission spectra of model atmospheres.

Considerable spectral structure can be seen in the 6.3μ H_2O and 15.0μ absorption bands. Similar structure is not evident in the 9.6μ O_3 band and the H_2O rotational structure because the low spectral resolution absorption data were used. The outgoing radiance was computed for 5 cm^{-1} spectral intervals with the center wave number of each interval being 5 cm^{-1} apart (500 cm^{-1}, 505 cm^{-1}, 510 cm^{-1}, $\cdots$). Because of this procedure some spectral resolution is lost when the strongest absorption features do not coincide with the center wave number of an interval. For example, this has occurred for the 618 cm^{-1} CO_2 band in the 15.0μ region. The 618 cm^{-1} and the 721 cm^{-1} CO_2 bands are approximately equal in strength yet do not appear so in the spectra. The 15μ CO_2 band is shown on an expanded wave number scale in Figure 18. In this presentation the

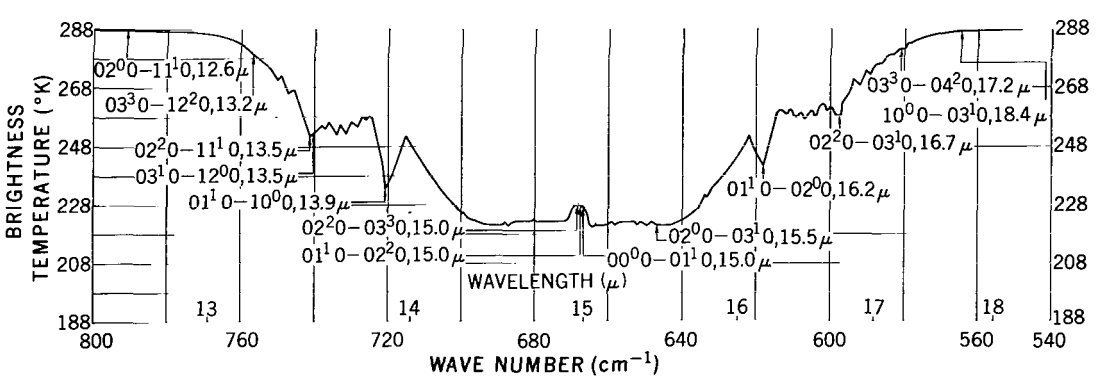

Figure 18—Theoretical thermal emission spectrum of 15μ CO_2 absorption band, 1962 U. S. Standard Model Atmosphere. The brightness temperature has been computed every 1 cm^{-1}.

outgoing radiance was computed for 5 cm^{-1} intervals every 1 cm^{-1}. The 15μ CO_2 band is due mainly to the ν_2 fundamental and about fourteen overtone and combination bands of C^{12} O^{16} O^{16}. The lower and upper state and transition wavelength (Young, 1964) is denoted for each of these bands in Figure 18.

As mentioned previously, the effect of surface emissivity is illustrated in Figure 14. The solid curve represents a blackbody surface; the dashed curve, Mojave Desert soil; and the dotted curve, Daytona Beach sand. The major effect is in the 8 to 9μ "window" where the residual ray reflection has decreased the brightness temperature by about 4°K for the Mojave Desert soil surface and by 4 to 14°K for the Daytona Beach sand surface. In the 11μ "window" the brightness temperature has been decreased by about 2°K.

B. Mars

Two Mars model atmospheres with different surface pressures (5 and 15 mb) were considered. The models include about 45 m-atm of CO_2 (Cann, Davies, Greenspan and Owen, 1965), 14μ of precipitable water (Kaplan, 1964) and a surface temperature of 230°K. Current estimates of the total amount of CO_2 are somewhat higher. From the $\nu_1 + 2\nu_2 + 3\nu_3$ CO_2 band at 1.05μ in the Martian spectrum, Belton and Hunten (1966) have derived a CO_2 abundance of 60 ± 26 m-atm while Gray (1966), from a personal communication by Schorn, has given 60 to 80 m-atm as the best current estimate of the Martian CO_2 abundance. In these calculations the value of 45 m-atm has been used. From near infrared spectroscopic observations Kuiper (1952) has set an upper limit of 0.05 cm-atm for O_3 in the Martian atmosphere. Prabhakara and Hogan (1965) have used photochemical theory to determine the total amount of Martian O_3 as approximately 0.03 cm atm. In addition, Prabhakara and Hogan determined that this amount of O_3 was small enough so that absorption by the 9.6μ O_3 band need not be considered. From recent ultraviolet spectral measurements of Mars from a rocket, Evans (1965) has determined an upper limit of 0.004 cm atm for O_3 (Rea, 1965). In these calculations the effects of O_3 have been neglected. The temperature profiles, based on the above parameters, were calculated* under the assumption of radiative and convective equilibrium and are shown in Figure 19.

The computed spectra are presented in Figure 20 for a blackbody surface with surface pressures of 5 and 20 mb. With the exception of the 15μ CO_2 band, the Martian spectrum is essentially featureless in the 5-20μ region. Because of low H_2O abundance, the 6.3μ H_2O band shows only weak absorption. The interval from 875 to 2000 cm^{-1} is shown in Figure 21 with the temperature scale expanded. The parallel structure of the upper state bands of CO_2 at 9.4 and 10.4μ and the perpendicular structure of the $3\nu_3$ band at 5.2μ can be clearly seen. Under the assumed conditions, water vapor shows a maximum absorption of about ten per cent or in terms of brightness temperature not exceeding several degrees. Consequently it will be difficult to identify H_2O in

*R. A. Hanel and F. Bartco. Private communication, 1965.

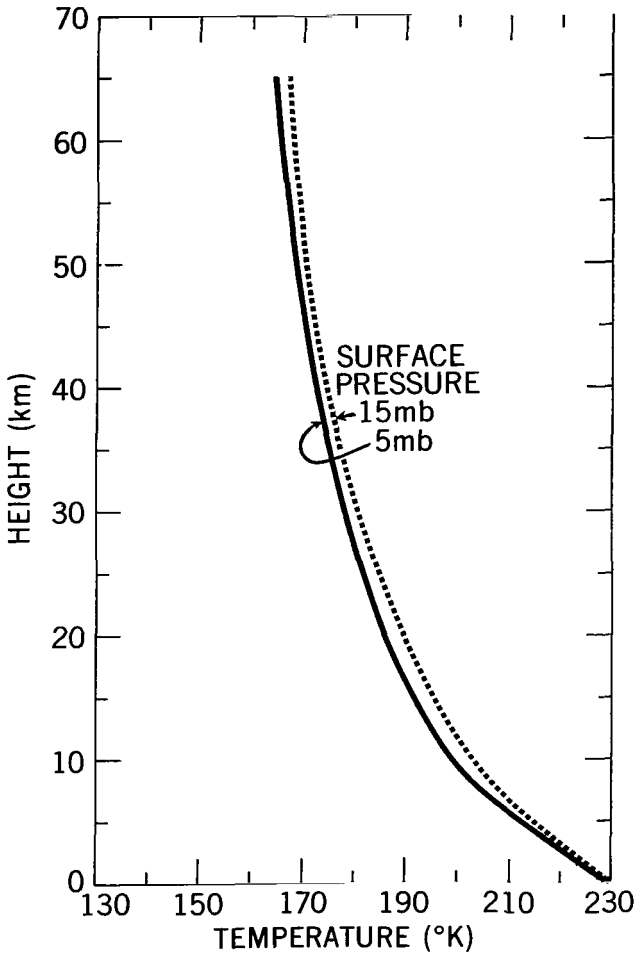

Figure 19—Temperature profiles for Martian atmosphere (Hanel and Bartko, 1965).

the Martian spectrum and even more difficult to determine its abundance. Fortunately the band spreads over 600 to 700 cm^{-1} and shows considerable rotational structure. This allows the use of statistical methods to obtain information about H_2O from the observed spectrum. Atmospheric H_2O has been identified using a cross-correlation technique* in which the H_2O ground transmission is cross-correlated with the computed brightness temperature spectrum. A power spectrum analysis* of the ground transmittance of H_2O, corresponding to the spectra of Figure 21, indicates a periodicity of about 17 cm^{-1} in the rotational structure. More will be discussed later concerning the 17 cm^{-1} periodicity. The 15μ CO_2 band is shown on an expanded wave number scale in Figure 22 for the Mars model atmosphere with a surface pressure of 5 mb.

On comparison, several distinct differences can be discerned in the Earth (Figures 14 and 18) and Mars (Figures 20 and 22) spectra. The most significant difference is due to the low abundance of H_2O and lack of O_3 on Mars. A second difference can be seen in the Q branch of the 15μ CO_2 band. The strongly absorbing Q branch absorbs fairly high in the atmosphere and thus,

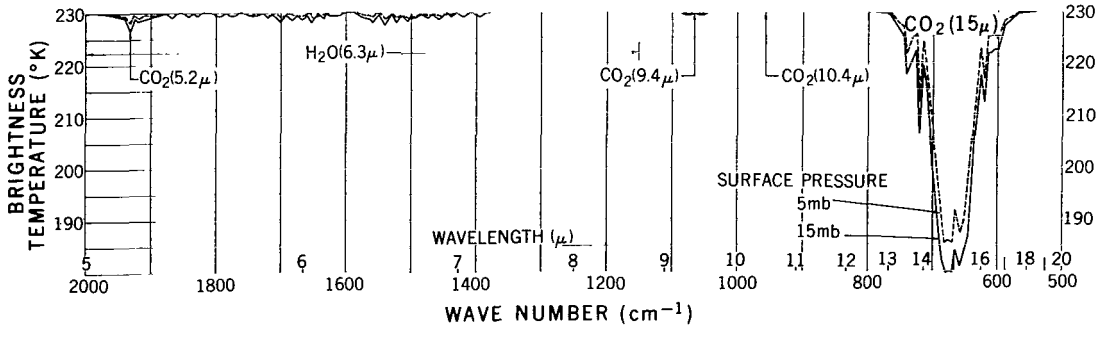

Figure 20—Theoretical thermal emission spectra for Mars. The effect of surface pressure is illustrated.

*B. J. Conrath. Private communication, 1967.

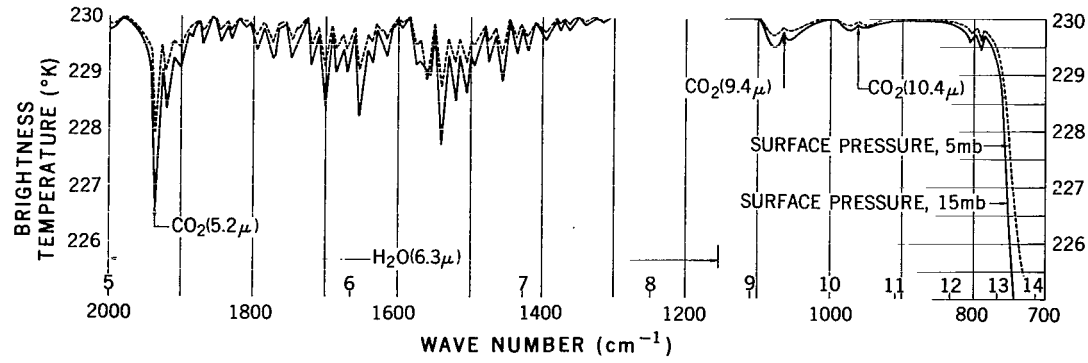

Figure 21—A portion of the spectra (700 - 2000 cm^{-1}) shown in Figure 20 with an expanded brightness temperature scale to better exhibit the water vapor absorption features.

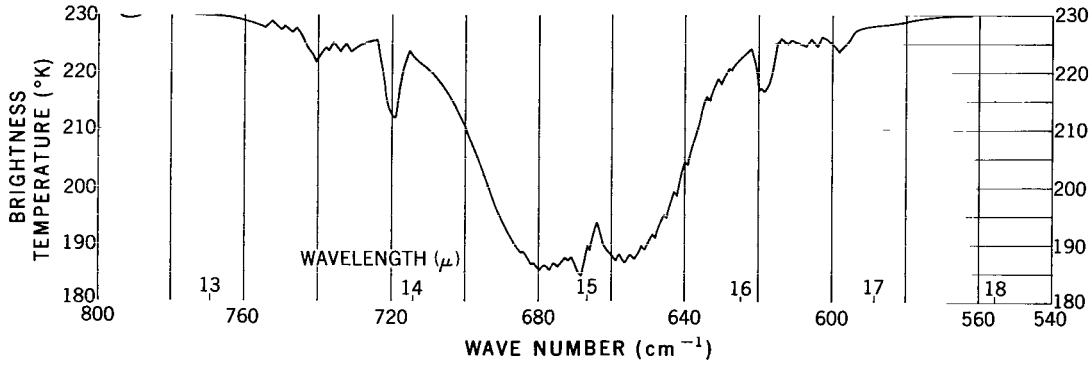

Figure 22—Theoretical thermal emission spectrum of 15μ CO_2 absorption band for Mars model with surface pressure of 5 mb. The brightness temperature has been computed every 1 cm^{-1}.

for the Earth, most of the absorption and subsequent re-emission at the Q branch occurs in the stratosphere where the temperature is increasing. The re-emission at higher temperatures leads to an increasing brightness temperature. For the Mars model, "seeing" higher in the atmosphere corresponds to cooler temperatures, and the brightness temperature decreases. Thus qualitatively the general shape of the temperature profile in the region of Q branch absorption can be determined by observing the shape of the Q branch in the spectrum.

Due to the high concentration of CO_2, the absorption by the CO_2 bands in the 5 to 20μ region is pressure dependent. Thus the procedure of using the two limiting absorption laws (weak band - strong band) for determining both the atmospheric CO_2 abundance and surface pressure cannot be made in this spectral region. However, several techniques utilizing curves of growth analyses are available to determine both surface pressure and atmospheric CO_2 abundance. These include the measurement of the equivalent widths of two different CO_2 bands (e.g., the 5.2, 9.4, 10.4 and 15μ bands) or of resolvable spectral intervals within a given CO_2 band (e.g., the 15μ band).

For the Mars model of 5 mb surface pressure, the effect of surface emissivity on the thermal emission spectra has been considered. The computed spectra are shown in Figure 23 with the

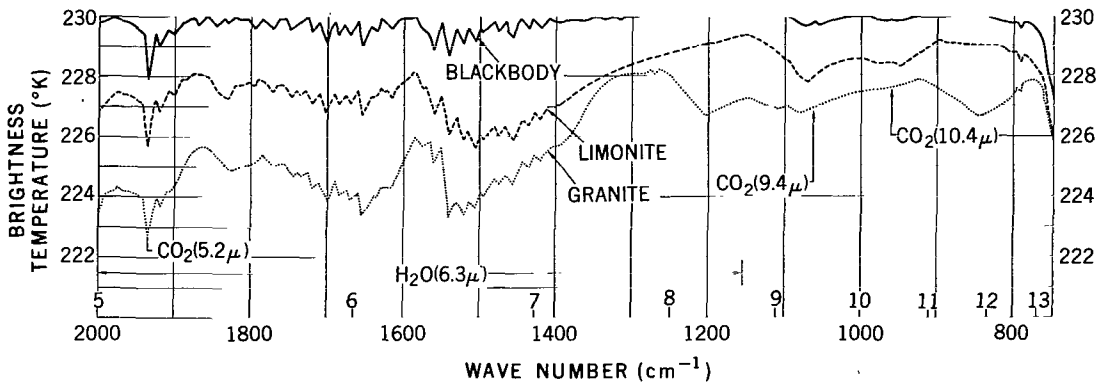

Figure 23—Theoretical thermal emission spectra for Mars model with surface pressure of 5 mb. The effect of surface emissivity is illustrated.

solid curve representing the blackbody surface; the dashed curve, limonite; and the dotted curve, granite. The limonite and granite samples were chosen mainly to study the effects of the strong water of hydration feature at 6.3μ on the thermal emission spectrum.

Whether limonite and/or granite is representative of certain areas of the Martian surface is unsettled. The main evidence for believing that the Martian desert areas are composed of limonite is:

(1) Color — Sharonov (1961) has found that limonite best matches both the brightness and color index of the Martian bright areas.

(2) Monochromatic albedo — Sagan, Phaneuf and Ihnat (1965) have compared Russell-Bond monochromatic albedos for Mars with laboratory samples in the spectral region 0.3 to 4μ. The best correlation was obtained with a pulverized limonite.

(3) Polarimetric — Dollfus (1961) has attempted to match a curve of polarization versus phase angle, obtained from measurements of Martian desert areas in the visible part of the spectrum, with laboratory samples. The best comparison was obtained with the limonite sample. The reduction of the observational data assumed a surface pressure of 90 mb. The recent measurements of surface pressure by Kaplan, Münch and Spinrad (1964), Evans (1965) and Kliore, Cain, Levy, Eshelman, Fjeldbo and Drake (1965) have indicated a surface pressure less than 25 mb. Considering the change in surface pressure alters the polarization curve so that surface materials other than limonite will give the observed polarization (Younkin, 1966).

Arguments against the existence of large amounts of limonite on the Martian surface are:

(1) Mean density — Van Tassel and Salisbury (1964) reason that it is unlikely that the surface composition of a terrestrial planet would be mainly hydrated iron oxides, and that the low mean density of Mars compared to that of Earth indicates that the metal content of Mars is low.

(2) Near-infrared spectral reflectance — Laboratory reflectance data of powdered mixtures of geothite and hematite have been obtained by Draper, Adamcik and Gibson (1965) which indicate an absorption feature around 0.9μ with an increasing reflectance toward longer wavelengths. From reflectance measurements of the complete Martian disk, Younkin (1966) finds no indication of this absorption feature or of the increasing reflectance.

(3) Limb darkening at 4920 and 6430 Å — Coulson (1965) has compared the limb darkening of a planet with a limonite surface with Mars observations at 4920 and 6430 Å. For angles near the limb, considerable disagreement was found.

Sinton and Strong (1959) obtained Martian spectra in the 8 to 13μ region. From these spectra the CO_2 bands at 9.4, 10.4 and 12.6μ were identified, and it was also concluded that less than 20% of the Martian surface materials contained silicates. The conclusion concerning silicates was based on the absence in the spectrum of residual ray features in the 8 to 9μ region. However, Van Tassel and Salisbury (1964) have shown that fine-grained silicates and powdered limonite emit like gray-bodies with little indication of the residual ray features. Low thermal conductivities, derived from the diurnal variation of surface temperature, suggest the Martian surface material is small grained (Leovy, 1965).

The spectra of Figure 23 corresponding to the limonite and granite samples do not match the observed spectra of Sinton and Strong (1959). The granite surface does not compare because of the emissivity features in the region of 850 cm^{-1}. The limonite surface comparison fails because the emissivity features in the region of 9.4 and 10.4μ enhance the absorption by the 9.4 and 10.4μ CO_2 absorption bands with respect to that of the 12.6μ band. Thus the strengths of the three bands would not be in the observed ratio. Smaller grained samples of limonite and granite, different surface materials or combinations of surface materials probably would give a better comparison with observations. However, the purpose here is not to reproduce the observed spectra of Sinton and Strong, but to illustrate the magnitude of the effect of surface emissivity on the spectrum. It can be seen that the surface emissivity is the dominant parameter in determining the shape of the spectrum and that the brightness temperature may be considerably lower than the radiating temperature of the surface.

For the 6.3μ H_2O band, the main effect of the surface water of hydration features of limonite and granite is to lower the predicted brightness temperatures without seriously affecting the band contour or the 17 cm^{-1} periodicity of the rotational structure. The band contour and rotational structure is fairly preserved because the surface emissivity changes only slowly with wave number, as it exhibits no rotational structure. To identify H_2O in the atmosphere of Mars from measurements in this spectral region requires that any surface water of hydration be taken into account. One possible method for identifying atmospheric H_2O under these conditions depends on the rotational structure of the atmospheric H_2O which is not present in the surface water of hydration. Qualitatively, the 17 cm^{-1} periodicity of the rotational structure should allow a separation of the effects of atmospheric H_2O and surface water of hydration. This also has been accomplished* using cross correlation techniques.

*B. J. Conrath. Private communication, 1967.

VII. CONCLUSIONS

The main object of this investigation has been to theoretically calculate the outgoing spectral radiance from a planetary atmosphere for spectral intervals of 5 cm^{-1}. The theoretical radiances provide an aid both in the interpretation of high spectral resolution planetary radiation data and in instrument design. The high spectral resolution spectra presented for the model atmospheres of Earth and Mars show that considerable information is available to recover atmospheric and surface parameters.

Other more detailed results are:

(1) An apparent error in the transmittance tables of Wyatt, Stull and Plass (1962b, 1963) was found. Disagreement with the WSP tables is mainly for the CO_2 calculations. It was also found that the theoretically calculated integrated absorptances for the 6.3μ absorption band were systematically smaller than the corresponding experimental values.

(2) For the Earth, the effect of surface emissivity in the 10.5 to 11.5μ "window" is to lower the brightness temperature about 2°K.

(3) Identification of the minor constituent H_2O in Mars' atmosphere from the weak absorption of the 6.3μ band will be very difficult. The difficulty increases due to possible surface water of hydration.

The direction of future efforts is very clear. The atmospheric absorption by all molecules of importance should be calculated using the techniques of Drayson (1966), thus eliminating the band model approximations and Curtis-Godson approximation. The pressure-broadened line half-width should be considered as a function of rotational quantum number and in addition it is important to determine the appropriate pressure-broadened line shape.

ACKNOWLEDGMENTS

The author would like to express his appreciation to Mr. Matty Shimizu and Mr. Oliver Clark for their programming efforts, to Dr. Barney Conrath for helpful discussions on the contents of this paper, and to Mr. S. Roland Drayson and Dr. Charles Young for their assistance in providing the computer program for direct spectral integration.

Goddard Space Flight Center
National Aeronautics and Space Administration
Greenbelt, Maryland, January 10, 1967
160-44-04-02-51

REFERENCES

1. Aller, L. H., "Astrophysics - The Atmospheres of the Sun and Stars, 2nd edition," New York: The Ronald Press Company, 1963.

2. Anderson, P. W., "Pressure Broadening in the Microwave and Infra-red Regions," *Phys. Rev.* 76(5):647-661, 1949.

3. Belton, M. J., and Hunten, D. M., "The Abundance and Temperature of CO_2 in the Martian Atmosphere," *Astrophys. J.* 145(2):454-467, 1966.

4. Benedict, W. S., Herman, R., Moore, G. E., and Silverman, S., "The Strengths, Widths and Shapes of Infrared Lines," I General Considerations, *Can. J. Phys.* 34(8):830-849, 1956.

5. Benedict, W. S., Herman, R., Moore, G. E., and Silverman, S., "The Strengths, Widths and Shapes of Infrared Lines," II The HC1 Fundamental, *Can. J. Phys.* 34(8):850-875, 1956.

6. Benedict, W. S., and Kaplan, L. D., "Calculations of Line Widths in H_2O-N_2 Collisions," *J. Chem. Phys.* 30(2):388-399, 1959.

7. Benedict, W. S., Herman, R., Moore, G. E., and Silverman, S., "The Strengths, Widths, and Shapes of Lines in the Vibration-Rotation Bands of CO," *Astrophys. J.* 135(1):277-297, 1962.

8. Benedict, W. S., and Kaplan, L. D., "Calculation of Line Widths in H_2O-H_2O and H_2O-O_2 Collisions," *J. Quant. Spectr. Radiat. Transfer* 4(3):453-469, 1964.

9. Bignell, K., Saiedy, F., and Sheppard, P. A., "On the Atmospheric Infrared Continuum," *J. Opt. Soc. Am.* 53(4):466-479, 1963.

10. Bloom, S., and Margenau, H., "Quantum Theory of Spectral Line Broadening," *Phys. Rev.* 90(5):791-794, 1953.

11. Böhm, K., 1960: "Basic Theory of Line Formation," In: *Stellar Atmospheres*, Edited by Jesse L. Greenstein. The University of Chicago Press, 1960.

12. Bolin, B., and Keeling, C. D., 1963: "Large-Scale Atmospheric Mixing as Deduced from the Seasonal and Meridional Variations of Carbon Dioxide, *J. Geophys. Res.* 68(13):3899-3920, 1963.

13. Bolle, Hans-Jugen, 1965: "Investigation of the Infrared Emission Spectrum of the Atmosphere and Earth," Final Report, Contract AF 61(052)-488, Air Force Cambridge Research Laboratories, 1965.

14. Breene, R. G., Jr., "Line Shape," *Rev. Mod. Phys.* 29(6):94-143, 1957.

15. Breene, R. G., Jr., "The Shift and Shape of Spectral Lines," Oxford: Pergamon Press, 1961.

16. Burch, D. E., Gryvnak, D., Singleton, E. B., France, W. L., and Williams, D., "Infrared Absorption by Carbon Dioxide, Water Vapor, and Minor Atmospheric Constituents," AFCRL-62-698, Air Force Cambridge Research Laboratories, Bedford, Massachusetts, July 1962.

17. Burch, D. E., Patty, R. R., and Gryvnak, D. A., Abstract - "Shapes of the Extreme Wings of CO_2 Absorption Lines," *J. Opt. Soc. Am.* 55(5):606, 1965.

18. Burch, D. E., and Gryvnak, D. A., "Laboratory Investigation of the Absorption and Emission of Infrared Radiation," *J. Quant. Spectr. Radiat. Transfer* 6(3):229-240, 1966.

19. Cann, M. W. P., Davies, W. D., Greenspan, J. A., and Owen, T. C., "A Review of Recent Determinations of the Composition and Surface Pressure of the Atmosphere of Mars," Contract NAS5-9037, September 1965.

20. Chandrasekhar, S., "Radiative Transfer," Dover, 393 pp, 1960.

21. Ch'en, Shang-Yi, and Takeo, M., 1957: "Broadening and Shift of Spectral Lines due to the Presence of Foreign Gases," *Rev. Mod. Phys.* 29(1):20-73, 1957.

22. Coulson, K. L., and Cray, E. L., "Reflecting and Polarizing Properties of Surface and Atmospheric Models of Mars," Presented at American Geophysical Union, Washington, D. C., April 22, 1965. Abstract in *Trans. Am. Geophys. Union* 46(1):143, 1965.

23. Curtis, A. R., "Discussion of a Statistical Model for Water Vapor Absorption," *Royal Meteorol. Soc. Quart. J.* 78(338):638-640, 1952.

24. Curtis, A. R., and Goody, R. M., "Spectral Line Shape and its Effect on Atmospheric Transmission," *Royal Meteorol. Soc. Quart. J.* 80(343):58-67, 1954.

25. Curtis, A. R., and Goody, R. M., Reply to G. N. Plass re "Spectral Line Shape and its Effect on Atmospheric Transmission," *Royal Meteorol. Soc. Quart. J.* 80(345):454-455, 1954.

26. Debye, P., "Polar Molecules," New York: The Chemical Catalogue Co. Inc., 1929. Reprint, Dover: Dover Publications, 1960.

27. Dollfus, A., Polarization studies of planets in "The Solar System III: Planets and Satellites," (Kuiper, G. P., and Middlehurst, B. M., eds.), 343-399, Chicago: University of Chicago Press, 1961.

28. Draper, A. L., Adamcik, J. A., and Gibson, E. K., "Comparison of the Spectra of Mars and a Goethite-Hematite Mixture in the 1 to 2 Micron Region," *Icarus* 3(1):63-65, 1964.

29. Drayson, S. R., "Atmospheric Transmission in the CO_2 Bands Between 12μ and 18μ," *App. Opt.* 5(3):385-392, 1966.

30. Elsasser, W. M., and Culbertson, M. F., "Atmospheric Radiation Tables," *Meteorological Monographs* 4(23):1-43, 1960.

31. Evans, D. C., "Ultraviolet Reflectivity of Mars," *Science* 149(3687):969-972, 1965.

32. Foley, H. M., "The Pressure Broadening of Spectral Lines," *Phys. Rev.* 69(11, 12):616-628, 1946.

33. Godson, W. L., "The Evaluation of Infrared Radiative Fluxes Due to Atmospheric Water Vapor," *Royal Meteorol. Soc. Quart. J.* 79(341):367-379, 1953.

34. Goody, R. M., "A Statistical Model for Water-Vapour Absorption," *Royal Meteorol. Soc. Quart J.* 78(336): 165-169, 1952.

35. Goody, R. M., "Atmospheric Radiation." Vol. I: Theoretical Basis, Oxford: Clarendon Press, 1964.

36. Goody, R. M., "The Transmission of Radiation Through an Inhomogeneous Atmosphere," *J. Atmos. Sci.* 21(6):575-581, 1964.

37. Gray, L. D., "Transmission of the Atmosphere of Mars in the Region of 2μ," *Icarus* 5(4): 390-398, 1966.

38. Green, A. E. S., and Wyatt, P. J., "Atomic and Space Physics," Reading: Addison-Wesley Publishing Company, Inc., 1965.

39. Hanel, R. A., Bandeen, W. R., and Conrath, B. J., "The Infrared Horizon of the Planet Earth," *J. Atmos. Sci.* 20(2):73-86, 1963.

40. Hanel, R. A., and Chaney, L., "The Infrared Interferometer Spectrometer Experiment (IRIS)," Vol. I: Martian fly-by mission, GSFC Document X-650-64-204, also NASA TM X-55070, 1964.

41. Hanel, R. A., and Chaney, L., "The Infrared Interferometer Spectrometer Experiment (IRIS)," Vol. II: Meteorological Mission, GSFC Document X-650-65-75, also NASA TM X-55218, 1965.

42. Hilleary, D. T., Heacock, E. L., Morgan, W. A., Moore, R. H., Mangold, E. C., and Soules, S. D., "Indirect Measurement of Atmospheric Temperature Profiles from Satellites. III The Spectrometers and Experiments," *Monthly Wea. Rev.* 94:367-377, June 1966.

43. Holstein, T., "Pressure Broadening of Spectral Lines," *Phys. Rev.* 79(4):744, 1950.

44. Hovis, W. A., Jr., "Infrared Reflectivity of Iron Oxide Minerals," *Icarus* 4(4):425-430, 1965.

45. Hovis, W. A., Jr., "Optimum Wavelength Intervals for Surface Temperature Radiometry," *App. Opt.* 5(5):815-818, 1966.

46. Hovis, W. A., Jr., and Callahan, W. R., "Infrared Reflectance Spectra of Igneous Rocks, Tuffs and Red Sandstone from 0.5 to 22 Microns," *J. Opt. Soc. Am.* 56(5):639-643, 1966.

47. Howard, J. N., Burch, D. L., and Williams, D., "Near-Infrared Transmission Through Synthetic Atmospheres," Geophysical Research Papers No. 40, AFCRC-TR-55-213, AD87679, Geophysics Research Directorate, Air Force Cambridge Research Center, Bedford, Massachusetts, November 1955.

48. Kaplan, L. D., "A Method for Calculation of Infrared Flux for Use in Numerical Models of Atmospheric Motion; In: *The Atmosphere and the Sea in Motion*, Scientific Contributions to the Rossby Memorial Volume, ed. by Bert Bolin, New York: Rockefeller Inst. Press, 1959.

49. Kaplan, L. D., Münch, G., and Spinrad, H., "An Analysis of the Spectrum of Mars," *Astrophys. J.* 139(1):1-15, 1964.

50. Kleman, B., and Lindholm, E., "The Broadening of Na Lines by Argon," *Ark. Astron. och Fys.* 32B(10), 1945.

51. Kliore, A., Cain, D. L., Levy, G. S., Eshleman, V. R., Fjeldbo, G., and Drake, F. R., "Occultation Experiment: Results of the First Direct Measurements of Mars' Atmosphere and Ionosphere," *Science* 149(3689):1243-1248, 1965.

52. Kuiper, G. P., "Planetary Atmospheres and their Origin," In: *The Atmospheres of the Earth and Planets*, Chicago: Univ. of Chicago Press, 1952.

53. Kyle, T. G., Murcray, D. G., Murcray, F. H., and Williams, W. J., "Absorption of Solar Radiation by Atmospheric Carbon Dioxide," *J. Opt. Soc. Am.* 55(11):1421-1426, 1965.

54. Leovy, C., "Note on Thermal Properties of Mars," Memorandum RM-4551, Rand Corporation, Santa Monica, California, April, 1965. *Icarus* 5(1):1-6, 1966.

55. Lindholm, E., "Zur Theorie der Verbreiterung von Spektrallinien," *Ark. Mat. Astron. och Fys.* 28B(3):1941.

56. Lindholm, E., "Pressure Broadening of Spectral Lines," *Ark. Mat. Astron. och Fys.* 32A(17), 1945.

57. Lorentz, H. A., "The Absorption and Emission Lines of Gaseous Bodies," *Proc. R. Acad. Sci.* (Amsterdam), 8, 591-611, 1906.

58. Margenau, H., "Theory of Pressure Effects of Foreign Gases on Spectral Lines," *Phys. Rev.* 48(9):755-765, 1935.

59. Margenau, H., and Watson, W. W., "Pressure Effects on Spectral Lines," *Rev. Mod. Phys.* 8(1): 22-53, 1936.

60. Margenau, H., and Lewis, M., "Structure of Spectral Lines from Plasmas," *Rev. Mod. Phys.* 31(3):569-615, 1959.

61. Michelson, A. A., "On the Broadening of Spectral Lines," *Astrophys. J.* 2(9):251-263, 1895.

62. Moller, F., and Raschke, E., 1963: "Evaluation of Tiros III Radiation Data," Interim report No. 1, NASA-CR-112, 1964. Meteorologisches Institut der Universitaet Muenchen.

63. Penner, S. S., "Quantitative Molecular Spectroscopy and Gas Emissivities," Reading: Addison-Wesley Publishing Company, Inc., 1959.

64. Plass, G. N., and Warner, D., "Influence of Line Shift and Asymmetry of Spectral Lines on Atmospheric Heat-Transfer," *J. Met.* 9(5):333-339, 1952.

65. Plass, G. N., and Warner, D., "Pressure Broadening of Absorption Lines," *Phys. Rev.* 86(1): 138-139, 1952.

66. Plass, G. N., "Spectral Line Shape and its Effect on Atmospheric Transmissions," *Royal Meteorol. Soc. Quart. J.* 80(345):452-454, 1954.

67. Plass, G. N., "Infrared Radiation in the Atmosphere," *Am. J. Phys.* 24 (5):303-321, 1956.

68. Plass, G. N., "Models for Spectral Band Absorption," *J. Opt. Soc. Am.* 48: 690-703, 1958.

69. Plass, G. N., "Useful Representations for Measurements of Spectral Band Absorption," *J. Opt. Soc. Am.* 50(9):868-875, 1960.

70. Prabhakara, C., and Hogan, J. S., Jr., "Ozone and Carbon Dioxide Heating in the Martian Atmosphere," *J. Atmos. Sci.* 22(2):97-109, 1965.

71. Rea, D. G., "The Atmosphere and Surface of Mars - A Selective Review." Presented at the lunar and planetary seminar, California Institute of Technology, Space Sciences Laboratory, University of California, Berkeley, California, September 1965.

72. Sagan, C., Phaneuf, J. P., and Ihnat, M., "Total Reflection Spectrophotometry and Thermogravimetric Analysis of Simulated Martian Surface Materials," *Icarus* (1):43-61, 1965.

73. Sanderson, R. B., and Ginsburg, N., "Line Widths and Line Strengths in the Rotational Spectrum of Water Vapor," *J. Quart. Spectr. Radiat. Transfer* 3(4):435-444, 1963.

74. Sharonov, V. V., "A Lithological Interpretation of the Photometric and Colorimetric Studies of Mars." Translation in *Soviet Astron.* - AJ, 5, 199, 1961. Original in *Astronom. Zhornal* 38(2):267-272.

75. Sinton, W. M., and Strong, J., "Radiometric Observations of Mars," *Astrophys. J.* 131(2):459-469, 1960.

76. Spitzer, L., Jr., "Stark-Effect Broadening of Hydrogen Lines," I. Single encounters, *Phys. Rev.* 55(8):699-708, 1939.

77. Spitzer, L., Jr., "Stark-Effect Broadening of Hydrogen Lines," II. Observational profiles, *Phys. Rev.* 56(1):39-47, 1939.

78. Spitzer, L., Jr., "Impact Broadening of Spectral Lines," *Phys. Rev.* 58(4):348-357, 1940.

79. Smith, W. V., Lackner, H. A., and Volkov, A. B., "Pressure Broadening of Linear Molecules," II. Theory, *J. Chem. Phys.* 23(2):389-396, 1955.

80. Townes, C. H., and Schawlow, A. L., "Microwave Spectroscopy," New York: McGraw-Hill, 1955.

81. Traving, G., "Über die Theorie der Druckverbreiterung von Spektrallinien," Karlsruhe: G. Braun, 1960.

82. Tsao, C. J., and Curnutte, B., "Line-Widths of Pressure Broadened Spectral Lines," *J. Quant. Spectr. Radiat. Transfer* 2(1):41-91, 1962.

83. Unsold, A., "Physik der Sternatmosphären," Berlin: Springer Verlag, 1955.

84. Van Tassel, R. A., and Salisbury, J. W., "The Composition of the Martian Surface," *Icarus* 3(3):264-269, 1964.

85. Van Vleck, J. H., and Weisskopf, V. F., "On the Shape of Collision Broadened Lines," *Rev. Mod. Phys.* 17(2, 3):227-236, 1945.

86. Van Vleck, J. H., and Margenau, H., "Collision Theories of Pressure Broadening of Spectral Lines," *Phys. Rev.* 76(8):1211-1214, 1949.

87. Weisskopf, V., "Zur Theorie der Kopplungsbreite und der Stossdampfung, *Zeitschrift für Physik* 75(5, 6):287-301, 1932.

88. Weisskopf, V., "Die Breite den Spektrallinien in Gasen," *Physikalische Zeitschrift* 34(1):1-24, 1933.

89. White, H. E., "Introduction to Atomic Spectra," New York: McGraw-Hill, 1934.

90. Winters, B. H., Silverman, S., and Benedict, W. S., "Line Shape in the Wing Beyond the Band Head of the 4.3μ Band of CO_2," *J. Quant. Spectr. Radiat. Transfer* 4(4):527-537, 1964.

91. Woolley, R. v.d. R., and Stibbs, D. W. N., "The Outer Layers of a Star," Oxford, 1953.

92. Wyatt, P. J., Stull, V. R., and Plass, G. N., "Quasi-Random Model of Band Absorption," *J. Opt. Soc. Am.* 52(11):1209-1217, 1962.

93. Wyatt, P. J., Stull, V. R., and Plass, G. N., "The Infrared Transmittance of Water Vapor," Report SSD-TDR-62-127, Vol. 2, Aeronutronic Div., Ford Motor Co., Newport Beach, California, September, 1962. Also, *Appl. Optics* 3(2):229-241, 1964.

94. Wyatt, P. J., Stull, V. R., and Plass, G. N., "The Infrared Transmittance of Carbon Dioxide," Report SSD-TDR-62-127, Vol. 3, Aeronutronic Div., Ford Motor Co., Newport Beach, California January 1963. Also, *Appl. Optics* 3(2):243-254, 1964.

95. Young, C., "A Study of the Influence of Carbon Dioxide on Radiative Transfer in the Stratosphere and Mesosphere." Technical Report, Dept. of Meteorology and Oceanography, College of Engineering, University of Michigan, March, 1964.

96. Young, C., "Calculation of the Absorption Coefficient for Lines with Combined Doppler and Lorentz Broadening," *J. Quant. Spectr. Radiat. Transfer* 5(3):549-552, 1965.

97. Younkin, R. L., "A Search for Limonite Near-Infrared Spectral Features on Mars," *Astrophys. J.* 144(2):809-818, 1966.

Appendix A

List of Symbols

$a(\omega)$ - Spectral amplitude of emitted radiation.

a' - Constant in Benedict modification of Lorentz line shape.

$b(\nu)$ - Relative line shape.

b' - Impact parameter.

b_0' - Weisskopf impact parameter.

b'' - Constant in Benedict modification of Lorentz line shape.

c - Velocity of light, 2.997925×10^{10} cm sec^{-1}.

d - Constant in Benedict modification of Lorentz line shape.

e - Charge of electron, 1.60210×10^{-19} coul.

f - Final quantum state of transition.

f' - Oscillator strength.

g - Gravitational acceleration.

h - Height above planetary surface.

$\hbar$ - Planck constant/2π.

i - Initial quantum state of transition.

k - Absorption coefficient per unit length per unit pressure, cm^{-1} atm^{-1}.

k^m - Mass absorption coefficient, cm^2/gm.

k_b - Boltzmann's constant, 1.38054×10^{-16} erg deg^{-1}.

k_0 - Mixed line parameter, Equation 64.

m - Mass.

m' - Quantum number.

m'' - Coefficient, Equation 53.

m_f - Degeneracy index for state f.

n - Number of lines.

n_i - Number of lines in i^{th} intensity decade.

n_j - Total number of lines in subinterval δ_j.

n' - Quantum number.

n'' - Temperature coefficient, Equation 52.

n''' - Constant, Equation 13.

p - Partial pressure.

q_v - Volume fraction, ratio of absorber pressure to total pressure.

q_m - Mass fraction, ratio of absorber density to total density.

q_m^d - Mixing ratio, ratio of density of water vapor to density of dry air.

q_{0_3} - Vertical distribution parameter for O_3, cm-atm/km.

r - Geocentric distance.

r' - Distance between radiating and perturbing particle.

r_0 - Geometrical parameter.

r_v^s - Spectral reflectivity of planetary surface.

s - Slant path for integration of optical path length.

s' - Dummy integration variable.

t - Time.

t' - Dummy variable.

u - Optical path length.

u', u'' - Optical path length at arbitrary level in atmosphere.

u_s - Optical path length from top of atmosphere to planetary surface.

v - Molecular velocity.

v_r - Relative velocity of perturbing particle.

$\bar{v}_r$ - Mean relative velocity.

v_p - Most probable speed of Maxwellian distribution.

x' - Mixed line shape parameter, Equation 67.

x - Complex displacement of electron.

$\ddot{x}$ - Acceleration along x.

x_0 - Displacement at t = 0.

y - Change of variable parameter, Equation 114

y' - Mixed line shape parameter, Equation 66.

z - Change of variable parameter, Equation 115.

A - Change of variable parameter.

B - Self-broadening coefficient.

B_ν - Planck function.

$C_\nu^{\nu'}(T)$ - Normalization constant.

C - Constant, Equation 13.

D - Optical collision diameter.

$\pi F_{\nu_s}^-$ - Downward monochromatic radiant emittance.

G - Instantaneous power radiated by an accelerating electron.

G_T - Total radiated power.

$H(y', x')$ - Relative mixed line shape.

$I^e(\omega)$ - Spectral emission intensity per oscillator.

$I_\nu^e(\omega)$ - Spectral emission intensity per unit volume.

I_T^e - Integrated emission intensity.

$I_\nu^+(s)$ - Outgoing spectral radiance at level s.

$I_\nu^+(u)$ - Outgoing spectral radiance at level u.

$I_{\Delta\nu}^+(\overline{T}_{\Delta\nu} = 1)$ - Outgoing spectral radiance in interval $\Delta\nu$ at level where $\overline{T}_{\Delta\nu} = 1$.

I_n - Bessel function of imaginary argument and order n.

J - Rotational quantum number.

J_2 - Total quantum state of perturbing particle.

M - Molecular weight.

M_a - Molecular weight of atmosphere.

M_g - Molecular weight of absorbing gas.

M' - Constant, Equation 44.

M_2 - Magnetic quantum number of perturbing particle.

N - Number of colliding particles/unit volume.

N' - Number of absorbing particles/unit volume.

$N(\nu_i)$ - Probability distribution function for line position ν_i.

P - Total pressure.

P_e - Effective pressure.

P_s - Surface pressure.

P_0 - Reference pressure.

$\bar{P}$ - Mean pressure over variable pressure path.

$P(s_i)$ - Probability distribution function for line of strength S_i.

R - Universal gas constant, 8.3143×10^7 erg deg^{-1} $mole^{-1}$.

R_p - Planetary radius.

R_s - Lower integration boundary.

S_T - Level representing top of atmosphere.

S - Integrated absorption coefficient, cm^{-2} atm^{-1}, wave number units.

S^m - Integrated absorption coefficient, cm^2 gm^{-1} sec^{-1}, frequency units.

$S(b', J_2)$ - Probability of induced transition.

$\bar{S}$ - Average integrated absorption coefficient.

T - Temperature.

T_B - Time between collisions.

T_{B_0} - Mean time between collisions.

T_0 - Reference temperature.

T_I - Isothermal temperature.

$V_1(t)$ - Perturbing potential due to collision.

W - Equivalent width.

x - Dummy variable.

α - Mean half-width, collisional broadening.

α_L - Mean half-width, for Lorentz line shape.

α_D - Half-width of Doppler line shape at half-maximum.

$\alpha_L(v)$ - Half-width of Lorentz line for molecular velocity v.

α_w - Weisskopf half-width.

α_0 - Half-width at reference conditions.

β - Line shift.

γ - Force constant.

δ - Spectral sub-interval.

δ_A - Line shift in Anderson theory.

ϵ - Change of variable parameter, Equation 119.

ϵ_M - Specifies number of spectral intervals to be considered on either side of interval of interest.

ϵ_ν^s - Spectral emissivity of surface.

ζ, ζ' - Change of variable parameter, Equations 124, 125.

η - Change of variable parameter, Equation 118.

η' - Total phase change.

θ - Zenith angle at level s.

λ - Wavelength.

λ_0 - Natural wavelength.

μ - Dipole moment.

ν - Wave number, cm^{-1}.

ν_I - Center wave number of starting interval δ.

ν_F - Center wave number of final interval δ.

ν_0 - Natural wave number.

$\overline{\nu}$ - Frequency.

$\overline{\nu}_0$ - Natural frequency.

$\Delta\overline{\nu}$ - Frequency increment.

ξ_i - Change of variable parameter, Equation 116.

ξ_{i_0} - Defined by Equation 121.

ρ - Change of variable parameter, Equation 117.

ρ_a - Total atmospheric density.

ρ_g - Absorber gas density.

ρ_{J_2} - Boltzmann distribution for perturbing particle in state J_2.

ρ_r - Absorber density at reference condition.

τ - End time of time interval.

ϕ_ν - Spectral response of measuring instrument.

ψ - Change of variable parameter.

ω - Angular frequency.

ω_0 - Natural angular frequency.

$\omega_{m'n'}$ - Transition frequency between states m' and n'.

ω' - Dummy variable.

ω'_0 - Perturbed angular frequency.

$\Delta\omega$ - Angular frequency increment.

$\Delta\omega'$ - Instantaneous total phase shift.

Δ - Spectral division.

Λ - Collision cross-section.

Λ_e - Effective collision cross-section.

Λ_{J_2} - Partial collision cross-section.

$T_\nu(u'', u')$ - Spectral transmittance between level u'' and u'.

T_ν^s - Spectral transmittance at lower boundary surface.

$\overline{T}(\nu)$ - Average transmittance at ν.

$\overline{T}_j(\nu)$ - Contribution to transmittance at ν from n_j lines in δ_j.

$\overline{T}_k(\nu)$ - Total average transmittance at ν in interval δ_k.

$\overline{T}_{\Delta\nu}$ - Average transmittance over interval $\Delta\nu$.

$\overline{T}_k^s(\nu)$ - Average transmittance at ν in interval δ_k, shifted mesh.

$\overline{T}_k^u(\nu)$ - Average transmittance at ν in interval δ_k, unshifted mesh.

Φ - Probability distribution for time between collisions.

$\Omega(\xi_i, \zeta)$ - Defined by Equation 126.

Appendix B

Theoretical Brightness Temperatures and Weighting Functions for the Tiros VII and Nimbus II 15μ Carbon Dioxide Absorption Band Channels

Both the Tiros VII and Nimbus II meteorological satellites carried a radiometric experiment which responded to thermal radiation in the 15μ CO_2 absorption band. The spectral response of the instrument on each satellite can be found in the "Tiros VII Radiation Data Catalog and Users' Manual" (1964) and the "Nimbus II Users' Guide" (1966).

The radiometers are calibrated in terms of brightness temperature T_{BB}, which is related to the measured effective radiance $\bar{N}$ through the expression

$$\bar{N} = \int_{\nu=0}^{\nu=\infty} \phi_\nu \, B_\nu(T_{BB}) \, d\nu \, , \tag{B1}$$

where ϕ_ν is the instrumental spectral response. The outgoing radiation measured by the instrument can be written as

$$\bar{N}(\text{Top}) = \sum_{i=1}^{N} \bar{N}_{\Delta\nu_i} \, , \tag{B2}$$

where $\bar{N}_{\Delta\nu_i}$ is the effective radiance from the i^{th} spectral interval $\Delta\nu$ and the summation covers the spectral range over which the instrument responds.

The effective radiance for each spectral interval can be obtained from Equation 86 of the main text in terms of height along the vertical h as

$$\bar{N}_{\Delta\nu}(\text{Top}) = \bar{T}_{\Delta\nu}(h = 0) \int_{\Delta\nu} \phi_\nu \, I_\nu^+(h = 0) \, d\nu + \int_{h=0}^{\text{Top}} \int_{\Delta\nu} \phi_\nu B_\nu(h) \, d\nu \frac{\partial \bar{T}_{\Delta\nu}(h)}{\partial s} \frac{\partial s \, (h, \theta)}{\partial h} \, dh \, . \tag{B3}$$

The above equation can be rewritten as

$$\bar{N}_{\Delta\nu}(\text{Top}) = \bar{T}_{\Delta\nu}(0) \int_{\Delta\nu} \phi_\nu \, I_\nu^+(0) \, d\nu + \int_0^{\text{Top}} \psi'(h) \, dh \, , \tag{B4}$$

where $\psi'(h)$ is given by

$$\psi'(h) = \frac{\partial \bar{T}_{\Delta\nu}(h)}{\partial s} \frac{\partial s(h, \theta)}{\partial h} \Bigg) \int_{\Delta\nu} \phi_\nu B_\nu(h) \, d\nu \, . \tag{B5}$$

The quantity $\psi'(h)$ represents the thermal emission contribution of each atmospheric layer to the observed outgoing radiation. A normalized weighting function $\psi(h)$ which can be defined by

$$\psi(h) = \psi'(h)/\bar{N}(Top) \tag{B6}$$

represents the contribution of each atmospheric layer relative to the total outgoing radiation.

The effective radiance $\bar{N}(Top)$ and the weighting function $\psi(h)$ have been calculated for a set of model atmospheres for the Earth using the direct spectral integration program of Drayson (1966). The temperature profiles, the weighting functions for vertical viewing and the weighting functions for a ground zenith angle of 70° are shown in Figures B1 and B2 for the Tiros VII and Nimbus II radiometers respectively. Brightness temperatures for these cases are presented in Table B1.

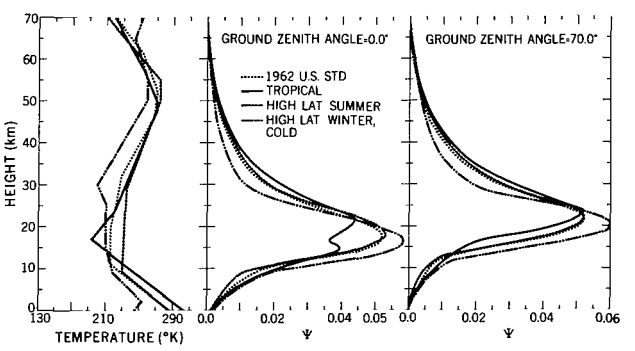

Figure B1—Temperature profiles used in the calculations are shown at left. The weighting functions are shown for vertical viewing and for a ground zenith angle of 70° for the Tiros VII 15μ absorption band channel.

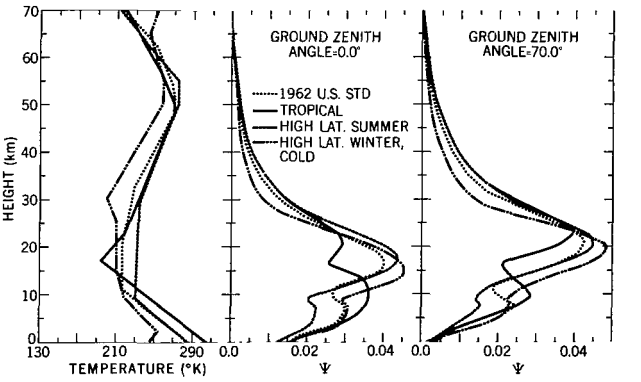

Figure B2—Temperature profiles used in the calculations are shown at left. The weighting functions are shown for vertical viewing and for a ground zenith angle of 70° for the Nimbus II 15μ absorption band channel.

Table B1

Brightness Temperatures for Tiros VII and Nimbus II 15μ Absorption Band Channel.

Model	Tiros VII		Nimbus II	
	$\theta = 0°$	$\theta = 70°$	$\theta = 0°$	$\theta = 70°$
High lat., summer	235°K	236°K	237°K	236°K
Tropical	220°K	224°K	228°K	226°K
1962 U.S. Std.	223°K	224°K	227°K	225°K
High lat., winter	212°K	211°K	217°K	214°K

REFERENCES

1. Drayson, S. R., "Atmospheric transmission in the CO_2 bands between 12μ and 18μ," *App. Opt.* 5(3):385-391, March 1966.

2. "TIROS VII Radiation Data Catalog and Users' Manual," Vol. I (June 19, 1963 - September 30, 1963). Goddard Space Flight Center, Greenbelt, Maryland, September 30, 1964.

3. "Nimbus II Users' Guide," Goddard Space Flight Center, Greenbelt, Maryland, July 1966.

Appendix C

Atmos 1 – IBM 7094 Fortran IV Program for Computing Optical Path Length

```
$ID J01T        V.K.   OUTGOING ATMOS RADIATION  SECT 1-OPTICAL PATH
$PAUSE
$DATE           012766
$EXECUTE        IBJOB
$IBJOB          GO
$IBFTC ATMOS1   M94,XR7,NODECK,NOLIST,NOREF
      COMMON G0,XMINH,P1,RAD,CAPK,C1,C2,DELR,DELH0,HT,XMAXH,HC,T0,IGAS,I
     1ATM/ZA/IXA,DATA(200)/ZB/IXB,DATB(100)/ZC/IXC,DATC(100)
      COMMON/ZD/HT3,LAYER1,LAYER2,THLAY1,THLAY2,THLAY3
      DIMENSION PLKA(4),PLKB(4),PLK1(4),XTA(7,90,6),WORDS(11)
      DIMENSION PRESS(100),TEMP(100),HH(100),HMIN(100),PRESH(100),PREHH(
     1100),XP(1200),XT1(1200),XDEL(1200),X(1200),X1(1200)
      DIMENSION XT2(1200),XPBOT(1200)
 1    FORMAT(3I3)
 2    FORMAT(1H0,10X,F8.2,6X,F12.9,6X,F7.2,6X,F12.7,6X,F12.7,6X,F11.7,6X
     1,F12.4/27X,F7.2,8X,F12.6,6X,1PE12.5,5X,1PE12.5,5X,0PF8.5,
     26X,0PF12.4/27X,1PE13.6,5X,1PE13.6)
 3    FORMAT(I3)
 4    FORMAT(10(F5.2))
 5    FORMAT(5(F3.1,F7.5))
 6    FORMAT(1H ,10X,4HK = F11.7,3X,7HK(1) = F4.2,3X,7HK(2) = F4.2)
 7    FORMAT(I3,I3,I3,I3,(E13.7))
 8    FORMAT(11A6)
 9    FORMAT(1H ,10X,8HANGLE = F6.2,3X,7HXMINH= F8.2,3X,26HLOWER INTEGRA
     1TION LIMIT = F7.2)
 10   FORMAT(F5.2)
 11   FORMAT(1H ,4I5)
 12   FORMAT(F6.2,I3,(F10.6))
 13   FORMAT(3E12.6,F6.2,E12.6,F6.2)
 14   FORMAT(1H ,10X,12HCASE NUMBER I3)
 15   FORMAT(1H0,4(1PE13.6,5X)/)
 16   FORMAT(1H0,4HPLK=1PE13.6)
 17   FORMAT(1H0,5HSF = F7.3)
 18   FORMAT(1H ,10X,F12.6,3X,F12.6,3X,F12.6,3X,F12.6,3X,F12.6,3X,F12.6,
     13X,F12.6)
 19   FORMAT(1H1,8X,16H     HT-BTLAY   ,15H   AVET(H20)   ,15H   AVEP(H2
     10)   ,15H  DEPTH(H20)   ,15H   AVET(CO2)   ,15H   AVEP(CO2)   ,15H
     2  DEPTH(CO2)   )
 23   FORMAT(F8.6,F4.2,F4.2,I1)
 24   FORMAT(1H1,8HMID-HT   ,9H MID-TEMP,12H   MID-PRESS,8H  RHO1  ,11H
     1 PEFF1   ,8H  AVET1 ,11H    AVEP1  ,12H DEPTH1-BLAY,7H PRAT  ,11H
     2  PEFF2   ,8H AVET2  ,11H  AVEP2    ,12H DEPTH2-BLAY/50X,13H(WATER
     3 VAPOR),29X,17H(CARBON DI-OXIDE)//)
 25   FORMAT(1H ,10X,4HKK= F11.4,3X,7HKK(1)= F4.2,3X,7HKK(2)= F4.2)
 26   FORMAT(1H ,   F7.3,2X,F6.2,4X,F8.3,3X,F6.3,1X,F8.3,3X,F5.1,4X,F8.3
     1,1X,F9.6,4X,E9.3,3X,F6.1,3X,F5.1,3X,F8.3,3X,F11.4)
 28   FORMAT(5(3X,F5.2,2X,F9.4))
 29   FORMAT(1H1,10X,62HOUTGOING ATMOSPHERIC RADIATION    SECT 1   OPTIC
     1AL PATH LENGTH)
 31   FORMAT(6E12.5)
 32   FORMAT(12F6.2)
 33   FORMAT(5X,I4,F10.2,E15.5,E12.4,E10.5,E10.5)
 34   FORMAT(5X,E10.5,F10.2)
 35   FORMAT(5X,4I5,E12.5,E12.5,F10.2,F12.4)
 36   FORMAT(5X,I5,F10.5,I5,F10.5)
```

```
 40   FORMAT(1H0,6X,4HGRAV,3X,7HSURF PR,3X,8HSTD TEMP,2X,6HRADIUS,2X,9HG
     1AS CONST,1X,4HDELR,2X,4HIGAS,1X,4HJGAS,1X,4HIATM,1X,4HJTAN,1X,2HLA
     2)
 41   FORMAT(1H ,E10.4,  2F10.3,F10.4,E11.4,F6.3,2I5,2I4)
 50   FORMAT(5F6.2,2I5,3F5.2)
 51   FORMAT(F5.2,F10.1,F10.2)
 52   FORMAT(1H ,F6.2,F10.2,F10.3)
 5601 FORMAT(1H1)
 5605 FORMAT(1H ,I3)
C     OUTPUT TAPE ON A5 FOR HEIGHT*ANGLE*TRANSMITTANCE MATRIX
      NUM1=0.
      HT2=0.0
      READ(2,3) NUM
 20   READ(2,3) JTAN
      READ(2,50)RAD,XMINH,DELR,HT,HT4,LAYER1,LAYER2,THLAY1,THLAY2,THLAY3
      READ(2,10) ANGLE
      READ(2,8) (WORDS(I),I=1,11)
      READ(2,13) G0,P1,P0,XMOL,RD,T0
      READ(2,23) CCAPK,CC1,CC2,JGAS
      READ(2,23)CCPK,C1,C2,IGAS
      IVERT=-1
      IF(IVERT) 60,60,70
C     HEIGHT VS TEMPERATURE READ IN, IVERT=-1**************************
   60 READ(2,3)IXA
      READ(2,4) (DATA(I),I=1,IXA)
      WRITE(3,28)(DATA(I),I=1,IXA)
      GO TO 80
C     PRESSURE VS TEMPERATURE READ IN,  IVERT=+1************************
   70 READ(2,3)IXA
      READ(2,31) (PRESS(I),I=1,IXA)
      READ(2,32) (TEMP(I),I=1,IXA)
C     CONVERSION FROM PRESSURE TO HEIGHT*********************************
      HMIN(1)=0.0
      CONST=8.317E+07/(XMOL*G0)
      DO 100 I=2,IXA
      TERM=(CONST*(TEMP(I)+TEMP(I-1))*(PRESS(I)-PRESS(I-1)))/(PRESS(I)+P
     1RESS(I-1))
      TERM=TERM/1.E+05
      HMIN(I)=HMIN(I-1)+TERM
      WRITE(3,33)I,TEMP(I),PRESS(I),CONST,TERM,HMIN(I)
 100  CONTINUE
      DO 115 I=1,IXA
      HH(I)=HMIN(IXA)-HMIN(I)
      DATA(I)=TEMP(I)
      WRITE(3,34)HH(I),DATA(I)
 115  CONTINUE
      DO 120 I=1,IXA
      IXAA=IXA+1-I
      IXA1=2*I-1
      IXA2=2*I
      DATA(IXA1)=HH(IXAA)
      DATA(IXA2)=TEMP(IXAA)
      PRESH(I)=PRESS(IXAA)
      PREHH(I)=1013.25*PRESH(I)
      WRITE(3,35)I,IXAA,IXA1,IXA2,PRESH(I)    ,DATA(IXA1),DATA(IXA2),PREH
     1H(I)
 120  CONTINUE
      IXXX=2*IXA
      IH=HMIN(IXA)
      IH=IH-1
      HT4=FLOAT(IH)
      HT=HT4
      WRITE(3,36) IH,HT4,IH,HT
      IXA=2*IXA
```

```
   80 READ(2,3)IXB
      READ(2,5) (DATB(I),I=1,IXB)
      WRITE(3,28) (DATB(I),I=1,IXB)
      READ(2,3)IXC
      READ(2,5) (DATC(I),I=1,IXC)
      WRITE(3,28) (DATC(I),I=1,IXC)
      JTA=1
      CAPK=(XMOL)/(12.45*18.)
      CCAPK=CCAPK*(1.E+05)
   30 ANG=ANGLE*.017453294
      HT3=HT4
      ITA=0
      NUM1 = NUM1 + 1
      CALL SLITE(0)
      IDELR1=(DELR*1000./2.)+.05
      IDELR=DELR*1000.+.5
      IH=0
      R0=(RAD+XMINH)*SIN(ANG)
      SUM=0.
      SUMBOT=0.0
C     PRESSURE INTEGRATION**************************************************
      WRITE(3,5601)
      N=1
      X(1)=0.0
      X1(1)=0.005
      H1=.005
      H=0.0
      DEL=0.
      DELL=0.005
      GO TO 608
  600 IF(N-51)601,602,605
  601 IH=IH+10
      IH1=IH+05
      X(N)=FLOAT(IH)/1000.
      X1(N)=FLOAT(IH1)/1000.
      DELL=.01
      DEL=DELL
      GO TO 608
  602 IH=IH+10
      IH1=IH+50
      X(N)=FLOAT(IH)/1000.
      X1(N)=FLOAT(IH1)/1000.
      DELL=.055
      DEL=.01
      H1=X1(N)
      H=X(N)
      GO TO 608
  605 IH=IH+IDELR
      IH1=IH+IDELR1
      X(N)=FLOAT(IH)/1000.
      X1(N)=FLOAT(IH1)/1000.
      DELL=FLOAT(IDELR)/1000.
      DEL=DELL
      H1=X1(N)
      H=X(N)
  608 CALL INTA(H1,TH1)
      CALL INTA(H,THBOT)
      XT1(N)=TH1
      XT2(N)=THBOT
      GR= G0*(RAD/(H1+RAD))**2
      GRBOT=G0*(RAD/(H+RAD))**2
      SUM=SUM+DELL*(GR*XMOL)*(1.E+05)/(RD*TH1)
      SUMBOT=SUMBOT + DEL *(GRBOT*XMOL)*(1.E+05)/(RD*THBOT)
      XP(N)=P1*(2.71828182**(-SUM))
      XPBOT(N)=P1*(2.71828182**(-SUMBOT))
```

```
      R=RAD+X(N)
      IF(R-R0)610,610,612
  610 R=R0
      H=R0-RAD
      IH=H*1000.
      GO TO 600
  612 XDEL(N)=(R/SQRT(R**2-R0**2))*DELL
      IHT=(HT-DELR)*1000.
      N=N+1
      IF(IH-IHT)600,604,604
  604 NOLAY=N-1
      IPR1=0
      WRITE(3,5605)NOLAY
      IPR2=IPR1+55
      WRITE(3,29)
      WRITE(3,14)NUM1
      WRITE (3,8) (WORDS(I),I=1,11)
      WRITE(3,9) ANGLE,XMINH,HT2
      WRITE(3,6)CAPK,C1,C2
      WRITE(3,25) CCAPK,CC1,CC2
      WRITE(3,40)
      WRITE(3,41)G0,P1,T0,RAD,RD,DELR,IGAS,JGAS,IATM,JTAN
      WRITE(3,24)
      DELU=0.
      TSUM1=0.
      PSUM1=0.
      SUM2=0.
      DELUU=0.
      TSUM2=0.
      PSUM2=0.
      SUM22=0.
      SUM4=0.
      SUM44=0.
C     OPTICAL DEPTH COMPUTATION*********************************************
      DO 650 M=1,NOLAY
      N=NOLAY-M+1
      H=X(N)
      H1=X1(N)
      TH1=XT1(N)
      PR=XP(N)
      DELS=XDEL(N)
      CALL INTB(H1,RHOI)
      CALL INTC(H1,RHOJ)
      SUM4=DELS*RHOI*((PR/P0)**C1)*((T0/TH1)**C2)
      DELU1=SUM4*CAPK
      DELU=DELU+DELU1
      TSUM1=TH1*DELU1+TSUM1
      CALL PPEFV(RHOI,PR,IGAS,CAPK,PEFF1)
      PSUM1=PEFF1*DELU1+PSUM1
      SUM2=SUM2+SUM4
      DEPT1=CAPK*SUM2
      AVET1=TSUM1/DELU
      AVEP1=PSUM1/DELU
      SUM44=DELS*RHOJ*((PR/P0)**CC1)*((T0/TH1)**CC2)
      DELU2=SUM44*CCAPK
      DELUU=DELUU+DELU2
      TSUM2=TH1*DELU2+TSUM2
      CALL PPEFV(RHOJ,PR,JGAS,CCAPK,PEFF2)
      SUM22=SUM22+SUM44
      DEPT2=CCAPK*SUM22
      PSUM2=PEFF2*DELU2+PSUM2
      AVET2=TSUM2/DELUU
      AVEP2=PSUM2/DELUU
      PRAT=PR/P0
```

```
 780  IPR1=IPR1+1
      IF(IPR2-IPR1) 782,782,784
 782  IPR2=IPR1+55
      WRITE(3,24)
 784  WRITE(3,26)    H1,TH1,PR,RHOI,PEFF1,AVET1,AVEP1,DEPT1,PRAT,PEFF2,
     1AVET2,AVEP2,DEPT2
      IF(H-HT3)750,750,650
C     OPTICAL DEPTH MATRIX*********************************************
 750  ITA=ITA+1
      PUNCH 51,H,XT2(N),XPBOT(N)
 752  XTA(1,ITA,JTA)=H
      XTA(2,ITA,JTA)=AVET1
      XTA(3,ITA,JTA)=AVEP1
      XTA(4,ITA,JTA)=DEPT1
      XTA(5,ITA,JTA)=AVET2
      XTA(6,ITA,JTA)=AVEP2
      XTA(7,ITA,JTA)=DEPT2
      IHT3=HT3
      IF(IHT3-0)706,706,756
756   IF(ITA-LAYER1)762,758,758
758   IF(ITA-LAYER2)764,766,766
762   HT3=HT3-THLAY1
      GO TO 777
764   HT3=HT3-THLAY2
      GO TO 777
 766  HT3=HT3-THLAY3
 777  IHT3=HT3
      IF(IHT3-0)770,770,655
 770  HT3=0.
 655  IF(HT2-H)650,706,706
 650  CONTINUE
 706  IF(JTA-JTAN)720,708,708
 720  JTA=JTA+1
      READ(2,10) ANGLE
      GO TO 30
 708  IDONE=1
      LA=ITA
      WRITE(5,8)(WORDS(I),I=1,11)
      WRITE(5,12)P1,IXA,(DATA(I),I=1,IXA)
      WRITE(5,7) HT2,NUM,JTAN,LA,(((XTA(KT,MT,NT),KT=1,7),MT=1,LA),NT=1,
     1JTAN)
      WRITE(3,19)
      WRITE(3,11) HT2,NUM,JTAN,LA
      WRITE(3,18) (((XTA(KT,MT,NT),KT=1,7),MT=1,LA),NT=1,JTAN)
      NUM=NUM-1
      IF(NUM) 710,710,20
 710  WRITE(3,52) (X(N),XT2(N),XPBOT(N),N=1,NOLAY)
      STOP
      END
```

67 CARDS

```
$IBFTC PPEFV   M94,XR7,NODECK,NOLIST,NOREF
      SUBROUTINE PPEFV(RHO,PR,IGAS,CAPK,PEFF)
      PB1=1.3
      PB2=6.3
      IF(IGAS-2) 10,20,30
 10   PEFF=PR+(PB1-1.)*CAPK*10.**(-5)*PR
      GO TO 40
 20   PEFF=PR+(PB2-1.)*10.**(-3)*RHO*12.45*CAPK*PR
      GO TO 40
 30   PEFF=PR
 40   RETURN
      END
```

12 CARDS

```
$IBMAP INTA     100,NODECK
 INTA  SAVE
       SXA      SAV4,4
       CLA      IXA
       ALS      18
       STD      MOD+2
       CLA      4,4
       STA      TEM
       CLA*     3,4
 MOD   TSX      TIN1,4
       PZE      DATA
       PZE      1,,**
 SAV4  AXT      **,4
       STO*     TEM
       RETURN   INTA
 ZA    CONTRL   ZA
       USE      ZA
 IXA   BSS      1
 DATA  BSS      100
       USE      PREVIOUS
 TEM   BSS      1
 INTB  SAVE
       SXA      SAV4,4
       CLA      IXB
       ALS      17
       STD      MOD1+2
       CLA      4,4
       STA      TEM1
       CLA*     3,4
 MOD1  TSX      TIN1,4
       PZE      DATB
       PZE      1,,**
       LXA      SAV4,4
       STO*     TEM1
       RETURN   INTB
 ZB    CONTRL   ZB
       USE      ZB
 IXB   BSS      1
 DATB  BSS      100
       USE      PREVIOUS
 TEM1  BSS      1
 INTC  SAVE
       SXA      SAV4,4
       CLA      IXC
       ALS      17
       STD      MOD2+2

       CLA    4,4
       STA      TEM2
       CLA*     3,4
 MOD2  TSX      TIN1,4
       PZE      DATC
       PZE      1,,**
       LXA      SAV4,4
       STO*     TEM2
       RETURN   INTC
 ZC    CONTRL   ZC
       USE      ZC
 IXC   BSS      1
 DATC  BSS      100
       USE      PREVIOUS
 TEM2  BSS      1
       END
```

62 CARDS

```
$IBMAP TIN1     125,M94,NODECK
*       INTERPOLATION SUBROUTINE     TIN1
*       FAP
        ENTRY TIN1
 TIN1   STO     TIN1+98
        SXD     TIN1+87,1
        SXD     TIN1+88,2
        SXD     TIN1+89,4
        CLA     2,4
        STO     TIN1+94
        ADD     TIN1+91
        PAX     0,1
        SXD     TIN1+29,1
        ALS     1
        STA     TIN1+95
        CLA     TIN1+94
        ARS     17
        SUB     TIN1+95
        PAX     0,1
        SXD     TIN1+31,1
        ADD     TIN1+95
        PAX     0,1
        ADD     1,4
        STA     TIN1+23
        STA     TIN1+41
        STA     TIN1+43
        CLA     TIN1+98
        CAS     0,1
        TIX     *-1,1,2
        TRA     TIN1+26
        CLA     TIN1+94
        LBT
        TRA     TIN1+41
        TIX     TIN1+31,1,0
        LXD     TIN1+90,1
        TXL     TIN1+33,1,0
        LXD     TIN1+31,1
        PXD     0,1
        ARS     18
        CHS
        ADD     TIN1+23
        STA     TIN1+54
        ADD     TIN1+91
        STA     TIN1+52
        TRA     TIN1+50
        CLA     0,1
        TXI     TIN1+43,1,2
        FAD     0,1
        LRS     35
        FMP     TIN1+92
        CAS     TIN1+98
        TXI     TIN1+29,1,-1
        TXI     TIN1+29,1,-1
        TXI     TIN1+29,1,-3
        LXD     TIN1+90,2
        LXA     TIN1+95,1
        CLA     0,1
        STO     COM+1,2
        CLA     0,1
        FSB     TIN1+98
        STO     COM,2
        TXI     TIN1+58,2,-2
        TIX     TIN1+52,1,2
        CLA     COM
```

```
        STO     COM,2
        LXA     TIN1+94,4
        LXD     TIN1+93,2
        TXI     TIN1+64,2,-2
        PXD     0,2
        PDX     0,1
        CLA     COM+2,1
        FSB     COM,2
        TZE     TIN1+79
        STO     TIN1+97
        LDQ     COM,2
        FMP     COM+3,1
        STO     TIN1+96
        LDQ     COM+2,1
        FMP     COM+1,2
        FSB     TIN1+96
        FDP     TIN1+97
        STQ     COM+3,1
        TXI     TIN1+66,1,-2
        CLA     COM+2,2
        STO     COM+2,1
        TIX     TIN1+63,4,1
        CLA     COM+1,1
        LXD     TIN1+87,1
        LXD     TIN1+88,2
        LXD     TIN1+89,4
        TRA     3,4
        HTR
        HTR
        HTR
        HTR
        HTR     1,0,0
        DEC     .5
        HTR     0,0,2
        HTR
        HTR
        HTR
        HTR
        HTR
        PZE
        PZE
 COM    BSS     40
        END
'
001
001
 6371.0000.00000.10070.00064.00003200036002.00001.000.5
.0
           EARTH,ARCT WINT-HIGH LAT WINT COLD, GRD ZA=00.0, QH2O=C STRAT
9.806650E+021013.250E+0001013.25E+0028.9700008.317E+07273.18
.000314  1.0 1.01
.1292   01.001.02
076
00000246.0001.0250.0002.0254.0003.0248.9004.0243.9
005.0238.8007.0228.6008.0223.6009.0218.5010.0217.2
014.0211.8015.0210.4015.5210.0024.5210.0025.0209.4
026.0207.5028.0203.8029.0201.9030.0200.0031.0202.9
035.0214.5040.0229.0045.0243.5049.0255.1049.5256.6
050.0258.0050.5258.0055.0258.0055.5257.4056.0256.7
058.0254.1060.0251.5062.0248.9064.0246.3066.0246.4
070.0251.8075.0258.6080.0248.6
032
000.348   1.0.30    2.0.26    3.0.22    3.7.19
4.0.17    5.0.1     6.0.059   6.3.05    7.0.026
```

```
8.0.01     9.0.0051  10..0024  112.0011  115.0011
700.0011
004
0001.0     80.1.0
'
```

```
EOF E SY
  133 CARDS
```

Appendix D

Atmos 2 – IBM 7094 Fortran IV Program for Computing Quasi-random Transmittance for Water Vapor

```
$ID J01T        V KUNDE  OUTGOING ATMOS RAD  SECT 2-TRANS,MIXED LINE,H2O
$PAUSE
$DATE           010666
$EXECUTE        IBJOB
$IBJOB          GO,MAP
$IBFTC ATMOS2   M94,XR7,NODECK,LIST
      COMMON/AZ/A(5),NA(5)
      COMMON/AA/WORDS(11),WWAVEI,WAVEF,INTER,HT2 ,HT3,ANGLE,NUM,JTAN,LA
      COMMON/ZA/IXA,DATA(200)
      COMMON/TT/TRAN(300)
      DIMENSION XINOT(5),XILINE(5),XIST(5),          TIS(5),
     1CLA(7),CLB(7),CPA(4),CPX(4),AIJS(5),TIJS(5),CLA1(7),CLB1(7)
     2,H2O(13000),TRAND(300),TRANW(300),TRANS(300),TRAN1(300)
     3,GEOM(7,56,3),AA(15),AG(6)
      DIMENSION CLAII(7),CLBII(7)
  999 FORMAT(F6.2,I3,(F10.6))
 1000 FORMAT(1H0,30X,44HBASIC PARAMETERS FOR OBTAINING TRANSMITTANCE)
 1001 FORMAT(F3.2,F5.1,F5.2,F5.3,F2.1,F5.3,F5.2,F12.6,F5.1,F5.1,I2)
 1002 FORMAT(1H0,5X,16HPRESSURE(ATM) = 1PE12.6,3X,17HTEMPERATURE(K) = 0P
     1F10.2, 3X,16HDEPTH(PR CM ) = 1PE10.4,3X,09HHET     = 0PF8.2/6X,15HI
     2NITIAL WAVE  = 0PF13.1,3X,17HFINAL WAVE      = 0PF10.1,3X,16HWAVE I
     3NCR.     = 0PF10.1,3X,09HDWAVE  = 0PF8.1/6X,16HSTAN. PR(ATM) = 0PF1
     42.4,3X,17HSTAN. TEMP.     = 0PF10.2,3X,16HHALF WIDTH     = 0PF10.4/6
     5X,16HEMAX           = 0PF12.1,3X,17HCAIJ           = 1PE10.4)
 1004 FORMAT(1H0,46X,31HQUASI=RANDOM BAND TRANSMITTANCE/52X,15HWATER VAP
     1OR GAS/51X,18HLORENTZ LINE SHAPE)
 1005 FORMAT(1H0,46X,31HQUASI=RANDOM BAND TRANSMITTANCE/46X,24HMIXED LOR
     1ENTZ LINE SHAPE/52X,15HWATER VAPOR GAS)
 1007 FORMAT(1H ,5X,16HCXI            = 1PE12.6,3X,17HZETA           = 1P
     1E10.4,3X,16HZETA2          = 1PE10.4)
 1008 FORMAT(1H1)
 1009 FORMAT(1H0/(5X,7HWAVE = F6.1,5(3X,1PE9.2,0PF5.1))/(26X,7HAIJ  = 1P
     15E13.6))
 1010 FORMAT(11A6)
 1017 FORMAT(1H0,10X,30HERROR FROM STATEMENT NUMBER = I5)
 1020 FORMAT(1H0,10X,39HCOMPUTATION OF DIRECT CONTRIBUTION PART)
 1021 FORMAT(20X,6HOM1 = F9.6,3X,5HOM = F9.6,3X,7HOM11 = F9.6/)
 1028 FORMAT(1H0/(10X,37HCOMPUTATION OF WING CONTRIBUTION PART)/)
 1029 FORMAT(1H0,10X,14HCASE NUMBER = I2)
 1030 FORMAT(5(F10.6))
 1031 FORMAT(1H ,5X,16HBE1            = F12.5, 3X,17HBE2             = F10
     1.5,3X,16HBE3           = 0PF10.5/6X,16HPB1           = 0PF12.3,3X,
     217HPB2             = 0PF10.3)
 1032 FORMAT(14(F4.3))
 1033 FORMAT(8(F8.8))
 1040 FORMAT(14(F5.3))
 1041 FORMAT(1H ,/06X,9HDIRECT = 7(F5.3,1X,F5.3,3X)/20X,4(F9.8,1X,F9.8,3
     1X))
 1042 FORMAT(1H ,03X,9H  WING = 7(F5.3,1X,F5.3,3X)/20X,4(F9.8,1X,F9.8,3X
     1))
 1043 FORMAT(1H0,07X,17H WING -- MIDPOINT/)
 1048 FORMAT(1H ,09X,7HITEMP= I3,3X,8HITEMP1= I3,3X,8HIWAVEU= I10,3X,7HL
     1UPU1= I10,3X,7HLOWU1= I10,3X,8HIWAVEL= I10)
```

```
 1049 FORMAT(1H1,40X,19HDIRECT CONTRIBUTION)
 1050 FORMAT(1H ,1X////40X,17HWING CONTRIBUTION)
 1051 FORMAT(1H ,4X,4HWAVE,3X,6HLAMBDA,2X,5HTRANS,6X,4HWAVE,3X,6HLAMBDA,
     12X,5HTRANS,6X,4HWAVE,3X,6HLAMBDA,2X,5HTRANS,6X,4HWAVE,3X,6HLAMBDA,
     22X,5HTRANS,6X,4HWAVE,3X,6HLAMBDA,2X,5HTRANS)
 1052 FORMAT(1H ,5(2X,F7.1,F8.3,F9.5))
 1053 FORMAT(1H ,1X////40X,19HTOTAL TRANSMITTANCE)
 1054 FORMAT(1H ,3X///  40X,19HFINAL TRANSMITTANCE)
 1058 FORMAT(1H0,10HSTOP AT = I6)
 1061 FORMAT(I3,I3,I3,I3,(E13.7))
 1062 FORMAT(E13.7)
 1063 FORMAT(1H1,I3,I3,I3,I3,7(E13.7,3X))
 1065 FORMAT(5F5.2)
 1066 FORMAT(1H1,20X,71HOUTGOING ATMOSPHERIC RADIATION      SECT2 H2O-QUA
     1SI-RANDOM TRANSMITTANCE)
C      A5--GEOMETRY MATRIX TAPE
C      A6--BLANK TAPE
C      A8--COEFFICIENT TABLE FOR WATER VAPOR-250 WORDS' RECORD-PACKED
C      B7--OUTPUT TAPE FOR THIS PROGRAM-THIS TAPE WILL BE USEDIN ATMOS3
C      IDOP=-1,LORENTZ LINE SHAPE****************************************
       CALL KNUMIX(X,Y,OUT,1)
       READ(2,1030) BE1,BE2,BE3,PB1,PB2
       READ(2,1032) (CLA(J),J=1,7),(CLB(J),J=1,7)
       READ(2,1033) (CPA(J),J=1,4),(CPX(J),J=1,4)
       READ(2,1040)(CLA1(J),J=1,7),(CLB1(J),J=1,7)
       READ(2,1001)HWIDTH,WAVEI,TNOT,PR,DWAVE,PRNOT,TEMPO,PATH,WAVEF,
      1DNU,IWRITE
C      READ TAPE A5--GEOMETRY MATRIX*************************************
 1080 READ(5,1010) (WORDS(I),I=1,11)
       READ(5,0999)P1,IXA,(DATA(I),I=1,IXA)
       READ(5,1061) HT2 ,NUM,JTAN,LA,(((GEOM(KT,MT,NT),KT=1,7),MT=1,LA),
      1NT=1,JTAN)
       WRITE(3,1063)IATM,NUM,JTAN,LA,(((GEOM(KT,MT,NT),KT=1,7),MT=1,LA),
      1NT=1,JTAN)
       READ(2,1065) (AG(JJ),JJ=1,JTAN)
       LAST=-1
       HT3=GEOM(1,1,1)
       IDOP=-1
       IBLS=-1
       ICASE=1
       ISE=1
       IER=1
C      REMEMBER DIMENSION FOR H2O(I) IS 13000.
       DO 1096 J=1,13000
       H2O(J)=0.
 1096 CONTINUE
 1090 MT=LA
       ANGLE=AG(ICASE)
       IXB=MT*2
       IXB1=MT
       ISEC=-1
 1095 WAVEO=WAVEI
       PATH=GEOM(4,MT,ICASE)
       HET=GEOM(1,MT,ICASE)
       TNOT=GEOM(2,MT,ICASE)
       TNOT=249.
       PR=GEOM(3,MT,ICASE)/1013.25
       PATH1=PATH
 1097 IK=-1
       IWORD=0
       WAVET=WAVEO
       ISH1=WAVEO*10.
       ISH2=WAVEO
       ISH2=ISH2*10
```

```
C      TEST FOR SHIFTED OR UNSHIFTED WAVE NUMBER ************************
       IF(ISH1-ISH2)1870,1098,1099
 1098  IFT1=-1
       IFT2=1
       ISB=-1
       SLUMB=0.
       GO TO 1100
 1099  WAVET=WAVEO-2.5
       SLUMB=1861.
       ISB=1
       IFT1=1
       IFT2=-1
C      TEMP=300 - TNOT LARGER THAN 250***********************************
C      TEMP=250.,FOR TNOT WITHIN THE RANGE OF 225.AND 275.
C      TEMP=200., TNOT LESS THAN 225.
 1100  IF(TNOT-275.) 1105,1110,1110
 1105  IF(TNOT-225.) 1120,1115,1115
 1110  TEMP=300.
       ITEMP=1
       GO TO 1300
 1115  TEMP=250.
       ITEMP=0
       GO TO 1300
 1120  TEMP=200.
       ITEMP=-1
 1300  ITT=1
C      RANGE OF WING CONTRIBUTION***************************************
       MAX=(4.8000*(10.)**5*PR*PATH)**(.5)/2.
       EMAX=(MAX+1)*2
       CXI=PATH/PR
       ZETA=(2.0/DWAVE)*HWIDTH*(PR/PRNOT)*(TEMPO/TEMP)**.5
       ZETA2=ZETA*ZETA
       CAIJ=ZETA2*CXI
       WRITE(3,1066)
       WRITE(3,1029)ICASE
       WRITE(3,1010) (WORDS(I),I=1,11)
       IF(IDOP)1220,1220,1225
 1220  WRITE(3,1004)
       GO TO 1230
 1225  WRITE(3,1005)
 1230  CONTINUE
       WRITE(3,1000)
       WRITE(3,1002) PR,TEMP,PATH,HET,WAVEI,WAVEF,DNU,DWAVE,PRNOT,TEMPO,
      1HWIDTH,EMAX,CAIJ
       WRITE(3,1007)CXI,ZETA,ZETA2
       WRITE(3,1041) (CLA(J),CLB(J),J=1,7),(CPA(J),CPX(J),J=1,4)
       WRITE(3,1042) (CLA1(J),CLB1(J),J=1,7),(CPA(J),CPX(J),J=1,4)
C      CHECK CORE IF INPUT DATA THERE***********************************
 1294  IWAVEU=(WAVEF+2.5*EMAX)*10.
       IWAVEL=(WAVEI-2.5*EMAX)*10.
       IF(IWAVEL-7000) 1303,1304,1304
 1303  IWAVEL=7000
 1304  IF(IWAVEU-100000) 1306,1306,1305
 1305  IWAVEU=100000
 1306  IWORDS=(IWAVEU-IWAVEL)*2/10+10
       INTER=(WAVEF-WAVEI)/5.0+1.
       WRITE(3,1048) ITEMP,ITEMP1,IWAVEU,LUPU1,LOWU1,IWAVEL
       IF(ISEC) 2000,1870,1307
 1307  IF(ITEMP-ITEMP1)2000,1308,2000
 1308  IF(IWAVEU-LUPU1) 1309,1309,2000
 1309  IF(LOWU1-IWAVEL) 1310,1310,2000
C      UNSHIFTED OR SHIFTED MESH ****************************************
 1310  IF(ITT-2)1325,1340,1312
 1312  IER=1310
       GO TO 1870
```

```
 1325 WAVE=WAVEO
      IFT=IFT1
      GO TO 1400
 1340 WAVE=WAVEO+DWAVE/2.
      WAVEI=WAVEI+DWAVE/2.
      WAVEF=WAVEF+DWAVE/2.
      IFT=IFT2
C     PREPARE TO READ INPUT DATA FROM CORE*******************************
 1400 OM1=1.
      IJJ=1
      IR=1
      IST1=-1
      IWAVE=WAVE*10.0
      IST=-1
      GO TO 1900
C     DETERMINATION OF DIRECT CONTRIBUTION TO TRANSMITTANCE*************
 1405 WAVE=WAVE+DWAVE
      IWAVE=WAVE*10.
      OM1=1.0
      IF(WAVE-1590.0) 6301,6301,6303
 6301 HWIDTH=0.16
      GO TO 6304
 6303 HWIDTH=0.115
 6304 ZETA=(2.0/DWAVE)*HWIDTH*(PR/PRNOT)*(TEMPO/TEMP)**.5
      ZETA2=ZETA*ZETA
      CAIJ=ZETA2*CXI
      GO TO 1900
 1410 DO 1420 J=1,5
      XIST(J)=XINOT(J)*CAIJ
 1420 CONTINUE
      IF(IWRITE)1415,1870,1421
 1421 WRITE(3,1009)WAVE,(XINOT(JN),XILINE(JN),JN=1,5),(XIST(JN),JN=1,5)
      WRITE(3,1020)
C     DIRECT CALCULATION*************************************************
C     LEG GAUSS QUAD,  7 SUBINT, 8 POINT
 1415 J=1
 1422 CXIST=XIST(J)
      IF(IDOP)1423,1423,1416
 1416 IF(PR-0.029607)3000,1423,1423
C     DIRECT CALCULATION,LORENTZ LINE SHAPE*****************
 1423 SUM=0.
      IOM=1
 1424 JOM=1
 1426 IF(IOM-7) 1430,1430,1428
 1428 GO TO 1480
 1430 CLAI=CLA(IOM)
      CLBI=CLB(IOM)
      DLBA=CLBI-CLAI
      PBA=CLBI+CLAI
      SUM1=0.
 1432 IF(JOM-4) 1436,1436,1434
 1434 SUM=SUM+DLBA*SUM1/2.
      IOM=IOM+1
      GO TO 1424
 1436 CPAJ=CPA(JOM)
      CPXJ=CPX(JOM)
      GMIN1 =(-DLBA*CPXJ+PBA)/2.
      GPUS1=(DLBA*CPXJ+PBA)/2.
      GPUS=GPUS1*GPUS1
      GMINUS=GMIN1*GMIN1
      SUM1=SUM1+CPAJ*(EXP(-CXIST/(GPUS+ZETA2))+EXP(-CXIST/(GMINUS+ZETA2
     1)))
      JOM=JOM+1
      GO TO 1432
```

```
C     DIRECT CALC.,MIXED LINE SHAPE, 7 SUBINT, 8 POINT******************
 3000 CLBII(1)=2.5
      CLAII(1)=1.25
      CLBII(2)=1.25
      CLAII(2)=0.2500
      CLBII(3)=0.2500
      CLAII(3)=0.1250
      CLBII(4)=0.1250
      CLAII(4)=0.0250
      CLBII(5)=0.0250
      CLAII(5)=0.0125
      CLBII(6)=0.0125
      CLAII(6)=0.0025
      CLBII(7)=0.0025
      CLAII(7)=0.0
      SUM=0.
      IOM=1
 3003 JOM=1
      BOLTZ=1.38054E-16
      PROTON=1.67252E-24
      XMOL=18.
      VEL=2.997925E+10
      CONST=SQRT(2.*ALOG(2.)*BOLTZ/PROTON)/VEL
      DOPHW=CONST*SQRT(TEMP/XMO)*WAVE
      XLORHW=HWIDTH*(PR/PRNOT)*SQRT(TEMPO/TEMP)
      Y=(XLORHW/DOPHW)*SQRT(ALOG(2.))
      PI=3.1415927
      QUAN=(PI*Y*CXIST)/(SQRT(PI)*ZETA2)
 3005 IF(IOM-7)3015,3015,3010
 3010 GO TO 1480
 3015 CLAI=CLAII(IOM)
      CLBI=CLBII(IOM)
      DLBA=CLBI-CLAI
      PBA=CLBI+CLAI
      SUM1=0.
 3025 IF(JOM-4)3035,3035,3030
 3030 SUM=SUM+DLBA*SUM1/5.
      IOM=IOM+1
      GO TO 3003
 3035 CPAJ=CPA(JOM)
      CPXJ=CPX(JOM)
      XP=(DLBA*CPXJ+PBA)/2.
      XP=XP*SQRT(ALOG(2.))/DOPHW
      CALL KNUMIX(XP,Y,OUT,2)
      OUTP=OUT
      XM=(-DLBA*CPXJ+PBA)/2.
      XM=XM*SQRT(ALOG(2.))/DOPHW
      CALL KNUMIX(XM,Y,OUT,2)
      OUTM=OUT
      XTRANP=EXP(-QUAN*OUTP)
      XTRANM=EXP(-QUAN*OUTM)
      SUM1=SUM1+CPAJ*(XTRANP+XTRANM)
      JOM=JOM+1
      GO TO 3025
 1480 OM=1.-SUM
 1481 N1=XILINE(J)
      OM11=1.0
 1485 IF(N1-20) 1486,1486,1490
 1490 OM11=(1.-OM)**20*OM11
      N1=N1-20
      GO TO 1485
 1486 OM11=(1.-OM)**N1*OM11
      OM1=OM1*OM11
      IF(IWRITE)1488,1870,1487
```

```
 1487 WRITE(3,1021) OM1,OM,OM11
 1488 IF(OM1) 1870,1494,1482
 1482 IF(J-5) 1483,1494,1870
 1483 J=J+1
      GO TO 1422
 1494 TRAND(IJJ)=OM1
      IF(IJJ-INTER) 1495,1496,1496
 1495 IJJ=IJJ+1
      GO TO 1405
 1496 IF(IWRITE) 1504,1870,1492
 1492 WRITE(3,1049)
      WRITE(3,1051)
      IRET=1
      GO TO 1830
C     DETERMINATION OF WING CONTRIBUTION TO TRANSMITTANCE***************
 1504 IF(ITT-2)1506,1508,1868
 1506 WAVEI=WAVEI
      IFT=IFT1
      GO TO 1509
 1508 IFT=IFT2
 1509 IF(IFT) 1501,1870,1502
 1501 TLOW=700.
      TUP=10000.
      GO TO 1510
 1502 TLOW=702.5
      TUP=10002.5
C     INTERVAL CONTAINING LINES ******************************
 1510 TWAVE=WAVEI-2.5*EMAX
      DO 1511 JI=1,IJJ
      TRANS(JI)=1.0
 1511 CONTINUE
      IST=-1
      IST1=-1
      GO TO 1518
 1514 TWAVE=TWAVE+DWAVE
 1518 IF(TWAVE-TLOW) 1520,1520,1521
 1520 TWAVE=TLOW
 1521 IF(TWAVE-TUP) 1528,1528,1522
 1522 IJJ=INTER
      GO TO 1759
 1528 LWAVE=TWAVE*10.
      IWAVE=TWAVE*10.
      IR=-1
      GO TO 1900
C     INCREMENT TO HIGHER WAVENUMBER *************************
 1530 DNU=50.
      IDNU=DNU
      ISIDE=+1
      IWAVEF=WAVEF*10.
      IWAVEI=WAVEI*10.
      LWAVE=(LWAVE+IDNU)
      IEPSI=IABS(4*(LWAVE-IWAVE)/100)
      EPSI=FLOAT(IEPSI)
      IF(LWAVE-IWAVEF)1535,1535,1539
 1535 IF(IWAVEI-LWAVE)1570,1570,1530
 1539 LWAVE=TWAVE*10.
C     INCREMENT TO LOWER WAVENUMBER **************************
 1540 DNU=-50.
      IDNU=DNU
      ISIDE=-1
      LWAVE=(LWAVE+IDNU)
      IF(7000-LWAVE)1542,1542,1514
 1542 IEPSI=IABS(4*(LWAVE-IWAVE)/100)
      EPSI=FLOAT(IEPSI)
      IF(IWAVEI-LWAVE) 1545,1545,1514
```

```
 1545 IF(LWAVE-IWAVEF) 1570,1570,1540
C     WING CALCULATION*****************************************************
 1570 J=1
      HWIDTH=.10
      ZETA=(2.0/DWAVE)*HWIDTH*(PR/PRNOT)*(TEMPO/TEMP)**.5
      ZETA2=ZETA*ZETA
      CAIJ=ZETA2*CXI
      TIJ1=1.0
C     CHECK ON MIDPOINT OR AVERAGE CALC. FOR WING*************
 1580 IF(IBLS) 1584,1870,1582
C     MIDPOINT CALCULATION*************************************
 1582 XIST=XINOT(J)*CAIJ
      EPAB=ABS(EPSI)
      CORR=EXP(-BE2*(DWAVE/2.)**BE3*EPAB**BE3+BE2*(5.0)**BE3)
      TIJ=EXP(-(XIST*CORR)/(EPAB*EPAB))
      TIJS(J)=TIJ
      AIJS(J)=XIST*CORR
      GO TO 1701
C     LEG GAUSS QUAD. 1 INT, 8 POINT***************************
 1584 AIJ=XINOT(J)*CAIJ
      AIJS(J)=AIJ
      GO TO 1980
 1585 EPSI=EPSI
      EPSI1=EPSI
      AIJS(J)=AIJ
      CXIST=AIJ
      SUM=0.
      IOM=1
 1586 JOM=1
 1588 IF(IOM-1)1592,1592,1590
 1590 GO TO 1630
 1592 CLAI=CLA1(IOM)
      CLBI=CLB1(IOM)
      DLBA=CLBI-CLAI
      PBA=CLBI+CLAI
      SUM1=0.
 1594 IF(JOM-4) 1598,1598,1596
 1596 SUM=SUM+DLBA*SUM1/4.
      IOM=IOM+1
      GO TO 1586
 1598 CPAJ=CPA(JOM)
      CPXJ=CPX(JOM)
      GMIN1=EPSI1-(-DLBA*CPXJ+PBA)/2.
      GPUS1=EPSI1-(DLBA*CPXJ+PBA)/2.
      GPUS=GPUS1*GPUS1
      GMINUS=GMIN1*GMIN1
      SUM1=SUM1+CPAJ*(EXP(-CXIST/(GPUS       ))+EXP(-CXIST/(GMINUS)))
      JOM=JOM+1
      GO TO 1594
 1630 TIJ=SUM
      TIJS(J)=TIJ
 1701 N1=XILINE(J)
      TIJ11=1.0
 1702 IF (N1-20)1704,1704,1706
 1706 TIJ11=TIJ**20*TIJ11
      N1=N1-20
      GO TO 1702
 1704 TIJ11=TIJ**N1*TIJ11
      TIS(J)=TIJ11
 1705 TIJ1=TIJ1*TIJ11
      J=J+1
      IF(J-6)1580,1720,1720
 1720 IWAVEI=WAVEI*10.
      IJJ=(LWAVE-IWAVEI+50)/50
      IF(TIJ1-.999)  1722,1754,1754
```

```
 1722 TRANW(IJJ)=TIJ1*TRANS(IJJ)
      TRANS(IJJ)=TRANW(IJJ)
      IF(ISIDE)1540,1870,1530
 1754 IF(ISIDE) 1758,1870,1539
 1758 IF(TWAVE-WAVEF-2.5*EMAX)1514,1759,1759
 1759 IF(IWRITE)1763,1870,1760
 1760 WRITE(3,1050)
      WRITE(3,1051)
      IRET=2
      GO TO 1832
 1763 IF(ITT-2)1766,1788,1870
 1766 DO 1768 IJJ=1,INTER
      TRAN1(IJJ)=TRAND(IJJ)*TRANS(IJJ)
 1768 CONTINUE
      IF(IWRITE)1780,1870,1770
 1770 WRITE(3,1053)
      WRITE(3,1051)
      IRET=3
      GO TO 1834
 1780 IF(IREAD-1)1782,1785,2005
 1782 IER=1780
      GO TO 1870
 1785 ITT=ITT+1
      GO TO 1310
 1788 DO 1790 IJJ=1,INTER
      TRAND(IJJ)=TRAND(IJJ)*TRANS(IJJ)
 1790 CONTINUE
      IF(IWRITE)1800,1870,1792
 1792 WRITE(3,1053)
      WRITE(3,1051)
      IRET=4
      GO TO 1830
C     AVERAGE OVER TWO MESHES*********************************************
 1800 DO 1805 IJJ=2,INTER
      TRAN(IJJ)=(TRAN1(IJJ)+TRAND(IJJ-1)+TRAND(IJJ))/3.
 1805 CONTINUE
      WRITE(3,1054)
      WRITE(3,1051)
      IRET=5
      GO TO 1845
C     WRITE INSTR FOR TRANS MATRIX****************************
 1830 DO  1831 JI=1,IJJ
      TRAN(JI)=TRAND(JI)
 1831 CONTINUE
      GO TO 1845
 1832 DO 1833 JI=1,IJJ
      TRAN(JI)=TRANS(JI)
 1833 CONTINUE
      GO TO 1845
 1834 DO 1829 JI=1,IJJ
      TRAN(JI)=TRAN1(JI)
 1829 CONTINUE
      GO TO 1845
 1845 IU=IJJ/5
      IU=IU+1
      DO 1847 IA=1,IU
      JJ=1
      DO 1846 II=1,5
      IAA=IA+IU*(II-1)
      IF(IRET-5) 1852,1850,1870
 1850 WAVEI=WAVEO
      WAVEF=WAVEO+(FLOAT(INTER)-1.)*5.
 1852 AA(JJ)=WAVEI+FLOAT(IAA*5)-5.
      JJ=JJ+1
```

```
      AA(JJ)=10000./AA(JJ-1)
      JJ=JJ+1
      AA(JJ)=TRAN(IAA)
      JJ=JJ+1
 1846 CONTINUE
      WRITE(3,1052) (AA(JJ),JJ=1,15)
 1847 CONTINUE
      IF(IRET-2)1504,1763,1848
 1848 IF(IRET-4)1780,1800,1868
 1868 ISE=1
C     WRITE ON TAPE6 OF TRANSMISSION VALUES FOR A GIVEN LAYER **********
      TRAN(1)=FLOAT(IATM)
      WRITE(6,1062) TRAN(1),(TRAN(IJJ),IJJ=2,INTER)
      MT=MT-1
C     TEST FOR TOP LAYER IN GEOMETRY MATRIX ******************
      IF(0-MT)1095,1861,1861
 1861 WRITE(3,1029) ICASE
      MT=MT+1
C     TEST FOR ANOTHER ANGLE *********************************
      IF(ICASE-JTAN) 2130,2128,2128
 1864 ISTOP=1864
      REWIND 6
      CALL READ2
      WRITE(3,1058) ISTOP
      STOP
 1870 WRITE(3,1017) IER
      STOP
C     READ INPUT DATA FROM CORE ******************************
 1900 IF(IST)1905,1870,1952
 1905 ID=DWAVE*10.
      IW=1
      IF(IFT)1910,1870,1920
 1910 IWAVES=IWAVE1
      GO TO 1930
 1920 IWAVES=IWAVE2
 1930 IF(IWAVE-IWAVES)1932,1950,1940
 1932 IER=1930
      GO TO 1870
 1940 IWAVES=IWAVES+ID
      IW=IW+1
      GO TO 1930
 1950 IWN=(IW-1)*5+1
      IF(IBOSI) 1952,1870,1956
 1952 IF(IFT) 1956,1870,1954
 1954 IF(IST) 1955,1870,1956
 1955 IWN=IWN+6000
 1956 DO 1960 JST=1,5
      A(JST)=H2O(IWN)
      IWN=IWN+1
 1960 CONTINUE
      CALL UNPAK
      DO 1962 JST=1,5
      XINOT(JST)=A(JST)
      XILINE(JST)=NA(JST)
 1962 CONTINUE
      IF(IST1) 1976,1870,1974
 1974 IWN=IWN-10
 1976 IST=1
      IF(IR) 1530,1870,1410
 1980 IF(AIJ) 1978,1983,1981
 1978 IER=1980
      GO TO 1870
 1981 AIJA=-AIJ/(EPSI*EPSI)
      SUM=EXP(AIJA)
```

```
      TIJ=SUM
      XIL1=XILINE(J)
      SUMN1=EXP(AIJA*XIL1)
      IF(SUMN1-1.00)1585,1982,1982
 1982 TIJ11=SUMN1
      TIJS(J)=AIJA
      GO TO 1705
 1983 TIJ11=1.
      TIJS(J)=TIJ11
      GO TO 1705
C     READ INPUT DATA FROM TAPE*****************************************
 2000 IF(IWORDS-13000)2002,2004,2004
 2002 IBOSI=-1
      EPDN=(WAVET-700.)*(.4)
      IREAD=1
      GO TO 2060
C     SINGLE MESH READ IN ***********************************
 2004 IBOSI=1
      IWAVE1=7000
      IWAVE2=7025
      IREAD=2
      GO TO 2006
 2005 IREAD=IREAD-1
      ITT=ITT+1
      IF(ISB) 2001,1870,2003
 2001 SLUMB=1861.
      GO TO 2006
 2003 SLUMB=0.
 2006 LUMB=0
      NUMB=0
      CALL REWI
      IF(ITEMP)2007,2008,2010
 2007 XLUMB=LUMB
      LUMB=XLUMB+7444.+SLUMB
      GO TO 2028
 2008 XLUMB=LUMB
      LUMB=XLUMB+3722.+SLUMB
      GO TO 2028
 2010 XLUMB=LUMB
      LUMB=XLUMB+SLUMB
 2028 IF(LUMB) 1870,2032,2030
 2030 CALL RTAW
      NUMB=NUMB+1
      IF(NUMB-LUMB) 2030,2032,1870
 2032 I=1
      EP=0.
 2034 CALL RTAW
      DO 2036 J=1,5
      H20(I)=A(J)
      I=I+1
 2036 CONTINUE
      EP=EP+2.
      IF(EP-3720.) 2034,2038,2038
 2038 ISEC=-1
      GO TO 1310
C     PARTIAL READ IN OF TWO MESHES ************************
 2060 IF(EPDN-EMAX)2062,2062,2090
C     START READ IN FROM BEG OF TAPE************************
 2062 IF(ITEMP)2064,2066,2068
 2064 LUMB=7444
      GO TO 2070
 2066 LUMB=3722
      GO TO 2070
 2068 LUMB=0
```

```
 2070 IWAVE1=7000
      IWAVE2=7025
      NUMB=0
      CALL REWI
      IF(LUMB) 1870,2074,2072
 2072 CALL RTAW
      NUMB=NUMB+1
      IF(NUMB-LUMB) 2072,2074,1870
 2074 I=1
      EP=0.
 2076 CALL RTAW
      DO 2078 J=1,5
      H2O(I)=A(J)
      I=I+1
 2078 CONTINUE
      EP=EP+2.
      IF(2400.-EP) 2080,2080,2076
 2080 LOWU1=IWAVE1
      LUPU1=60000+LOWU1
      ITEMP1=ITEMP
      CALL REWI
      LUMB=LUMB+1861
      NUMB=0
 2082 CALL RTAW
      NUMB=NUMB+1
      IF(NUMB-LUMB) 2082,2084,1870
 2084 EP=0
 2085 CALL RTAW
      DO 2086 J=1,5
      H2O(I)=A(J)
      I=I+1
 2086 CONTINUE
      EP=EP+2.
      IF(2400.-EP) 2088,2088,2085
 2088 LOWS1=IWAVE2
      LUPS1=60000+LOWS1
      ISEC=+1
      GO TO 1310
C     START READ IN NOT FROM BEG OF TAPE**********************
 2090 IF(ITEMP) 2092,2094,2096
 2092 LUMB=(WAVET-700.-2.5*EMAX)/5.+7444.
      GO TO 2097
 2094 LUMB=(WAVET-700.-2.5*EMAX)/5.+3722.
      GO TO 2097
 2096 LUMB=(WAVET-700.-2.5*EMAX)/5.
 2097 IWAVE1=(WAVET-2.5*EMAX)*10.
      IWAVE2=IWAVE1+25
      NUMB=0
      CALL REWI
 2098 CALL RTAW
      NUMB=NUMB+1
      IF(NUMB-LUMB) 2098,2100,1870
 2100 EP1=EPUP+600.
      I=1
      EP=0
 2102 CALL RTAW
      DO 2104 J=1,5
      H2O(I)=A(J)
      I=I+1
 2104 CONTINUE
      EP=EP+2.
 2106 IF(2400.-EP) 1870,2108,2102
 2108 LOWU1=IWAVE1
      LUPU1=LOWU1+60000
      ITEMP1=ITEMP
```

```
      LUMB=LUMB+1861
      NUMB=0
      CALL REWI
 2110 CALL RTAW
      NUMB=NUMB+1
      IF(NUMB-LUMB)2110,2112,1870
 2112 EP=0
 2114 CALL RTAW
      DO 2116 J=1,5
      H2O(I)=A(J)
      I=I+1
 2116 CONTINUE
      EP=EP+2.
 2118 IF(2400.-EP) 1870,2120,2114
 2120 LOWS1=IWAVE2
      LUPS1=IWAVE2+60000
      ISEC=+1
      GO TO 1310
C     FOR EACH NEW ANGLE OF VIEW REPROCESS TAPE6 TO  MAKE NEW TABLE OF
C     HEIGHT VS TRANSMISSIONS FOR EACH WAVE NUMBER,AND WRITE ON TAPE6
 2128 LAST= 1
 2130 IGAS=1
      ICASE=ICASE+1
      FREQ=WAVEO+DWAVE
      MT=IXB1
      K1=0
      K=1
      K1=K1+INTER
      REWIND 6
C     HEIGHT VS TRANSMISSIONS FOR EACH WAVE NUMBER
C     READ ENTIRE TRANSMISSION VALUES FOR A GIVEN ANGLE INTO H2O(I)
      DO 2140 J=1,MT
      READ(6,1062) (H2O(I),I=K,K1)

      K=K1+1
      K1=K1+INTER
 2140 CONTINUE
C     PRINT OUT OF HEIGHT VS TRANSMITTANCE MATRIX **********************
      WRITE(3,1066)
      WRITE(3,1029)ICASE
      WRITE(3,1010) (WORDS(I),I=1,11)
      IF(IDOP)4220,4220,4225
 4220 WRITE(3,1004)
      GO TO 4230
 4225 WRITE(3,1005)
 4230 CONTINUE
      WRITE(3,1000)
      WRITE(3,1002) PR,TEMP,PATH,HET,WAVEI,WAVEF,DNU,DWAVE,PRNOT,TEMPO,
     1HWIDTH,EMAX,CAIJ
      WRITE(3,1007)CXI,ZETA,ZETA2
      WRITE(3,1041) (CLA(J),CLB(J),J=1,7),(CPA(J),CPX(J),J=1,4)
      WRITE(3,1042) (CLA1(J),CLB1(J),J=1,7),(CPA(J),CPX(J),J=1,4)
      NN11=0
      NNN11=0
      IINTER=INTER-1
      DO 2330 J=1,IINTER
      IADD=J*5
      ADD=FLOAT(IADD)
      TRAND(J)=WAVEI+ADD
 2330 CONTINUE
 2335 XW1=TRAND(NN11+1)
      XW2=TRAND(NN11+2)
      XW3=TRAND(NN11+3)
      XW4=TRAND(NN11+4)
```

```
      XW5=TRAND(NN11+5)
      XW6=TRAND(NN11+6)
      XW7=TRAND(NN11+7)
      XW8=TRAND(NN11+8)
      XW9=TRAND(NN11+9)
      XW10=TRAND(NN11+10)
      XW11=TRAND(NN11+11)
      XW12=TRAND(NN11+12)
      XW13=TRAND(NN11+13)
      XW14=TRAND(NN11+14)
      XW15=TRAND(NN11+15)
      WRITE(3,1008)
      WRITE(3,2340) XW1,XW2,XW3,XW4,XW5,XW6,XW7,XW8,XW9,XW10,XW11,XW12,X
     1W13,XW14,XW15
 2340 FORMAT(1H ,10X,15(2X,F6.1))
 2310 DO 2320 J=1,MT
      TRAN(J)=GEOM(1,J,1)
      NN1=(MT-J)*INTER+NN11
      H201=H20(NN1+2)
      H202=H20(NN1+3)
      H203=H20(NN1+4)
      H204=H20(NN1+5)
      H205=H20(NN1+6)
      H206=H20(NN1+7)
      H207=H20(NN1+8)
      H208=H20(NN1+9)
      H209=H20(NN1+10)
      H2010=H20(NN1+11)
      H2011=H20(NN1+12)
      H2012=H20(NN1+13)
      H2013=H20(NN1+14)
      H2014=H20(NN1+15)
      H2015=H20(NN1+16)
      WRITE(3,2312) TRAN(J),H201,H202,H203,H204,H205,H206,H207,H208,H209
     1,H2010,H2011,H2012,H2013,H2014,H2015
 2312 FORMAT(1H ,3X,F7.2,15(2X,F6.4))
 2320 CONTINUE
      NNN11=NNN11+1
      NN11=NNN11*15
      IF(NN11-INTER)2335,2142,2142
 2142 REWIND 6
      KK=2
      WWAVEI=WAVEI+5.
 2144 CALL RITE1(IXA)
 2145 K=KK
C     REARRANGE DATA IN H20(I),AND CONSTRUCT TABLE OF HEIGHT VS
C     TRANSMISSION***RECORD SEQUENCE FOR EACH SPECTRAL INTERVAL IS  WAVE
C     NUMBER,HEIGHT,TRAN,HEIGHT,TRAN**********
      MT=IXB1
      TRAN(1)=FREQ
      J=2
      DO 2150 I=1,IXB1
      TRAN(J)=GEOM(1,MT,1)
      J=J+1
      TRAN(J)=H20(K)
      MT=MT-1
      K=K+INTER
      J=J+1
 2150 CONTINUE
C     READ TABLE,THUS CONSTRUCTED, INTO TAPE B7 FOR EACH WAVE NUMBER.
      II=IXB+1
      CALL RITEB7(II)
```

```
      KK=KK+1
      FREQ=FREQ+DWAVE
      IF(KK-INTER) 2145,2145,2155
 2155 IF(LAST) 1090,1090,2160
 2160 IF(NUM-1)1864,1864,1080
      END
```

830 CARDS

```
$IBMAP RITEB7  100,LIST,XR7,M94,NODECK
*  RITEB7 WRITES BUFFER TRAN(II) ON TAPE B7, THIS INCLUDES TABLES OF
* TRANSMISSIONS AND OTHER PARAMETERS FOR INPUT TO ATMOS3.
 OUT    FILE    ,B(3),B(3),BLK=300,BIN,HOLD,MOUNT,OUTPUT
RITEB7 SAVE    (4,2,1,3,5,6,7)I
       CLA*    3,4
       ALS     18
       STD     II
       TSX     .OPEN,4
       PZE     OUT
       TSX     .WRITE,4
       PZE     OUT
 II    IOCD    TRAN,,300
       RETURN  RITEB7
 TT    CONTRL  TT
       USE     TT
 TRAN  BSS     300             ALL PARAMETERS FOR OUTPUT
       USE     PREVIOUS
 RITE1 SAVE    1,2,3,4,5,6,7,I
       CLA*    3,4
       ADD     =1              ADD 1 FOR IXA ITSELF
       ALS     18
       STD     JJ
       TSX     .OPEN,4
       PZE     OUT
       TSX     .WRITE,4
       PZE     OUT
       IOCP    BUF1,,20
 JJ    IOCD    BUF2,,200
       RETURN  RITE1
 AA    CONTRL  AA
       USE     AA
 BUF1  BSS     20              WORDS(11),WWAVEI,WAVEF,INTER,IGAS,LA,
       USE     PREVIOUS        HT3,ANGLE,NUM,JTAN
 ZA    CONTRL  ZA
       USE     ZA
 BUF2  BSS     200             IXA,DATA(200)
       USE     PREVIOUS
 READ2 SAVE    1,2,3,4,5,6,7,I
       TSX     .CLOSE,4
       PZE     OUT
       RETURN  READ2
       END
```

43 CARDS

```
$IBFTC KNUMIX  M94,XR7,LIST,REF,NODECK
      SUBROUTINE KNUMIX(XIN,YIN,OUT,I1)
      DIMENSION A(42),HH(10),XX(10)
      DIMENSION RA(32),CA(32),RB(32),CB(32),B(44),AK(5),AM(5),DY(4)
      GO TO (400,401),I1
  400 READ (2,710)          (HH(I),I=1,10),(XX(I),I=1,10),(A(I),I=1,42)
  710 FORMAT (5E14.8/5E14.8/5F14.8/5F14.8/(5E14.8))
      RETURN
  401 X=XIN
      Y = YIN
```

```
      X2 = X*X
      Y2 = Y*Y
      IF (X-10.) 200,201,201
  200 IF (Y-1.) 202,202,203
  203 RA(1) = 0.
      CA(1) = 0.
      RB(1) = 1.
      CB(1) = 0.
      RA(2) = X
      CA(2) = Y
      RB(2) = .5-X2+Y2
      CB(2) = -2.*X*Y
      CB1 = CB(2)
      UV1=0.
      DO 250 J=2,31
      JMINUS = J-1
      JPLUS = J+1
      FLOATJ = JMINUS
      RB1 = 2.*FLOATJ+RB(2)
      RA1 = -FLOATJ*(2.*FLOATJ-1.)/2.
      RA(JPLUS)=RB1*RA(J)-CB1*CA(J)+RA1*RA(JMINUS)
      CA(JPLUS)=RB1*CA(J)+CB1*RA(J)+RA1*CA(JMINUS)
      RB(JPLUS)=RB1*RB(J)-CB1*CB(J)+RA1*RB(JMINUS)
      CB(JPLUS)=RB1*CB(J)+CB1*RB(J)+RA1*CB(JMINUS)
      UV=(CA(JPLUS)*RB(JPLUS)-RA(JPLUS)*CB(JPLUS))/(RB(JPLUS)*RB(JPLUS)+
     1CB(JPLUS)*CB(JPLUS))
      IF (ABS(UV-UV1)-1.E-6) 251,250,250
  250 UV1=UV
  251 OUT = UV/1.772454
      RETURN
  202 IF (X-2.) 301,301,302
  301 AINT = 1.
      MAX = 12.+5.*X2
      DO 303 L=1,MAX
      AJ = MAX-L+1
  303 AINT = AINT*(-2.*X2)/(2.*AJ+1.)+1.
      U = -2.*X*AINT
      GO TO 304
  302 IF (X-4.5) 305,306,306
  305 B(43)=0.
      B(44) = 0.
      J = 42
      DO 307 K = 1,42
      B(J) = .4*X*B(J+1)-B(J+2)+A(J)
  307 J = J-1
      U = B(3)-B(1)
      GO TO 304
  306 AINT = 1.0
      MAX = 2.+40./X
      AMAX = MAX
      DO 308 K=1,MAX
      AINT = AINT*(2.*AMAX-1.)/(2.*X2)+1.
  308 AMAX = AMAX -1.
      U = -AINT/X
  304  V=1.772454*EXP(-X2)
      H = .02
      JM = Y/H
      IF (JM) 310,311,310
  311 H=Y
  310 Z = 0.
      L = 0
      DY(1) = 0.
  312 DY(2) = H/2.
      DY(3) = DY(2)
      DY(4) = H
```

```
  318 AK(1) = 0.
      AM(1) = 0.
      DO 313 J=1,4
      YY = Z+DY(J)
      UU = U+.5*AK(J)
      VV = V+.5*AM(J)
      AK(J+1) = 2.*(YY*UU+X*VV)*H
      AM(J+1) = -2.*(1.+X*UU-YY*VV)*H
      IF (J-3) 313,314,313
  314 AK(4)=2.*AK(4)
      AM(4) = AM(4)+AM(4)
  313 CONTINUE
      Z=Z+H
      L = L+1
      U = U+.1666667*(AK(2)+2.*AK(3)+AK(4)+AK(5))
      V = V+.1666667*(AM(2)+AM(3)+AM(3)+AM(4)+AM(5))
      IF(JM) 315,320,315
      315 IF (L-JM) 318,317,320
      317 AJM = JM
          H = Y-AJM*H
          GO TO 312
      320 OUT = V/1.772454
          RETURN
      201 F1 = 0.
          DO 330 J=1,10
      330 F1=F1+HH(J)/(Y2+(X-XX(J))*(X-XX(J)))+HH(J)/(Y2+(X+XX(J))*(X+XX(J))
         1)
          OUT = Y*F1/3.1415927
          RETURN
          END
```

105 CARDS

```
$IBMAP RTAW     100,NODECK
 RTAW  SAVE     1,2,3,4,5,6,7,I
 IN    FILE     ,A(4),A(4),MOUNT,BLK=250,BIN,HOLD
       TSX      .OPEN,4
       PZE      IN
       TSX      .READ,4
       PZE      IN
       PZE      EOFA,,*-2
       IOCT     A-5,,5
 EOFA  RETURN   RTAW
 REWI  SAVE     1,2,3,4,5,6,7,I
       TSX      .CLOSE,4
       PTW      IN
       RETURN   REWI
 UNPAK SAVE     1
       AXT      5,1
       CAL      A,1
       ANA      =0377
       SLW      NA,1
       CAL      A,1
       ANA      =0777777777400
       SLW      A,1
       TIX      *-6,1,1
       RETURN   UNPAK
 AZ    CONTRL   AZ
       USE      AZ
 A     BES      5
 NA    BES      5
       USE      PREVIOUS
       END
```

```
  .46224367E 0  .28667551E 0  .10901721E 0  .24810521E-1  .32437733E-2
  .22833864E-3  .78025565E-5  .10860694E-6  .43993410E-9 .22939360E-12
     .24534071     .73747373    1.2340762     1.7385377     2.254974
    2.7888061     3.3478546     3.944764      4.6036824     5.3874809
  .00000000E 0  .19999999E 0  .00000000E 0-0.18400000E 0  .00000000E 0
  .15583999E 0  .00000000E 0-0.12166400E 0  .00000000E 0  .87708159E-1
  .00000000E 0-0.58514124E-1  .00000000E 0  .36215730E-1  .00000000E 0
-0.20849765E-1  .00000000E-0  .11196011E-1  .00000000E 0-0.56231896E-2
  .00000000E 0  .26487634E-2  .00000000E 0-0.11732670E-2  .00000000E 0
  .48995199E-3  .00000000E 0-0.19336308E-3  .00000000E 0  .72287745E-4
  .00000000E00-0.25655512E-4  .00000000E 0  .86620736E-5  .00000000E 0
-0.27876379E-5  .00000000E 0  .85668736E-6  .00000000E00-0.25184337E-6
  .00000000E 0  .70936022E-7
0001136760000006750000007000000013000000006300000
05000100005000100005000100001000050001000050001000050001
3626837831370665222381031012285418343464525532417966664896028986
-100000000-0300-0600-0900-0950-1000010000050000000-0300-0600-0900-0950
0100995030000010005001000300000000010000002000000050-1
00000
70.
```

```
EOF E SY
   52 CARDS
```

Appendix E

Atmos 3 — IBM 7094 Fortran IV Program for Computing the Solution to the Radiative Transfer Equation

```
$ID J01T        V KUNDE  OUTGOING ATMOS RADIATION  SECT 3-RAD TRANS EQN
$PAUSE
$DATE           020866
$EXECUTE        IBJOB
$IBJOB          GO,NOLOGIC,NOMAP
$IBFTC ATMOS3   M94,XR7,NOLIST,NOREF,NODECK
      COMMON/AA/GO,XMINH,PO,RAD,CAPK,C1,C2,DELR,DELHO,HT,XMAXH,HC,TO
      COMMON/BB/WORDS(11), WAVEI,WAVEF,INTER,HT2 ,HT3,ANGLE,NUM,IG,IXB
     1,IWAVE,WAVE0,IBC
      COMMON/CC/HEIGHT,DTAUDH,OLIVER,TRANU,XXLOG
      COMMON/PP/NOPE,NOPP,SF
      COMMON/RR/PLOT(300),IZERO(125)
      COMMON/SS/RAD1(1200),RAD2(1200),RAD3(1200),RAD4(1200),RAD5(1200),
     1TWAVE(15)
     2,          STO1(350),STO2(350),STO3(350),STO4(350),STO5(350),
     3STO6(350),STO7(350),STO8(350),STO9(350),STO10(350),STO11(350),
     5TBW(350),TBWO(350),TRANG(350),RATIO(350),ISTO1(350),ISTO2(350),IST
     603(350)
      COMMON/TT/SUMRAT(100),ALTI(100),KMAXIM,SPWORD(11),HH(100),TEMP(100
     1),IIXA
      COMMON/ZA/IXA,DATA(200)
      COMMON/ZB1/WAV01,DATB(200),IXE,A7M,FTSW,IATM1
      COMMON/ZB2/WAV02,DATBB(200),IXF,A8M,GSW,IATM2
      COMMON/ZC1/W1(11), WAV1,WAVF1,INT1,HT21 ,HT31,ANGL1,NUM1,JTAN1,LA1
      COMMON/ZC2/W2(11), WAV2,WAVF2,INT2,HT22 ,HT32,ANGL2,NUM2,JTAN2,LA2
      COMMON/ZC3/IVGK,IATM
      INTEGER A7M,A8M,FTSW,GSW
      COMMON/DATAC/TAB15(100)/DATAD/TABLE(100)
       DATA CA,CB/1.1909000E-12,1.43879/
      DIMENSION ALTIT(100),SUMLA(100),          SUML(100)
      DIMENSION SUMLAY(1200),XH1(1200)
    4 FORMAT(1H ,04X,35HATMOS CONTRIB, FRACTION OF TOTAL = F8.4)
    5 FORMAT(1H0,05X,14HWAVE NUMBER = F8.3)
    6 FORMAT(10X,11A6)
    7 FORMAT(1H0,4X,24HGROUND RADIATION WITH = E15.6,13X,29HATMOSPHERIC
     1RADIATION WITH = E15.6)
    8 FORMAT(1H1,7X,4HWAVE,5X,6HLAMBDA,2X,8HGRD TRAN)
    9 FORMAT(5X,27HTOTAL RADIATION WITH-OUT = E15.6,10X,23HTOTAL RADIATI
     1ON WITH = E15.6)
   10  FORMAT(2F6.0)
   11  FORMAT(1HO, 5(26H     WAVE NO.         PHI   ))
   12  FORMAT(1H ,10F13.4)
   13  FORMAT(3I3,4F6.2)
   14  FORMAT(1HO///5(26H     WAVE NO.       EPSILON))
   15  FORMAT(5F6.1)
   16  FORMAT(I2)
   17  FORMAT(4I4)
   26  FORMAT(1H ,0PF5.2,F8.5,1PE10.2,0PF8.5,1PE10.3,2X,
     1          0PF5.2,F8.5,1PE10.2,0PF8.5,1PE10.3,2X,
     2          0PF5.2,F8.5,1PE10.2,0PF8.5,1PE10.3,2X)
   27  FORMAT(1H ,3(43HHEIGHT DTAU-DH   RADW    TRANSU   XXLOG     ))
   28  FORMAT(1H1,F7.2)
```

```
 29   FORMAT(1H ,5X47H(WITHOUT WEIGHTING FUNCTION) TOTAL RADIATION = E12
     1.5,5X28HRADIATION FROM ATMOSPHERE = E12.5/6X47H(WITH WEIGHTING FUN
     2CTION)    TOTAL RADIATION = E12.5,5X28HRADIATION FROM ATMOSPHERE =
     3 E12.5)
 32   FORMAT(1H1)
 34   FORMAT(1H ,120I1)
 46   FORMAT(1H1,7H       ,12X,42HOUTGOING ATMOSPHERIC RADIATION---SECTI
     1ON 3/20X,47HOUTGOING INFRARED RADIANCE,SPHERICAL ATMOSPHERE//)
 48   FORMAT(1HO,19X,8HANGLE = F6.2,8H DEGREES,3X,8HXMINH = F6.2,12HKM
     1        /20X,19HUPPER INT. LIMIT = F6.2,12HKM          ,3X,19HLOWE
     2R INT. LIMIT = F6.2,12HKM          )
 52   FORMAT(1H ,19X,46HRADIANCE = WATT/((CM**2)*STER*5(WAVE NUMBERS))//
     1)
 54   FORMAT(1H ,34X97HW / O  W E I G H T I N G  F U N C T I O N * * *
     1 W I T H  W E I G H T I N G  F U N C T I O N * *//2X4HWAVE,5X5HLAM
     2DA,4X3HPHI,5X4HEPSI,7X3HGRD,10X5HATMOS,9X5HTOTAL,7X2HTB,9X3HGRD,10
     3X5HATMOS,9X5HTOTAL,7X2HTB)
 56   FORMAT(1H ,0PF7.1,F8.3,F8.3,F8.3,1PE14.4,E14.4,E14.4,0PF8.2,
     1                                1PE14.4,E14.4,E14.4,0PF8.2)
 57   FORMAT(1H ,F10.1,F10.3,F10.6)
 60   FORMAT(6E12.5)
   61 FORMAT(1H ,10X,F10.3,3X,E12.6,3X,F10.5)
   62 FORMAT(1H ,10X,F10.3,3X,E12.6)
C    NOPP NUMBER OF PAIRS OF POINTS IN PHI VS. WAVE NUMBER TABLE (I3)
C    NOPE=NUMBER OF PAIRS OF POINTS IN EPSILON VS. WAVE NUMBER TABLE (I3)
C   SF = PHI, AND IS FOUND IN SUBROUTINE PLANK
C   A7M IS TAPE A7 MULTIPLICITY SWITCH
C   A8M IS TAPE A8 MULTIPLICITY SWIT@H
C   FTSW IS FIRST TIME SWITCH FOR SUBROUTINE READT
C   GSW IS GAS MULTIPLICITY SWITCH
C       INTER--NUMBER OF INTERVAL
C       IXB--NUMBER OF PAIRS OF DATA MULTIPLIED BY TWO FOR HEIGHT VS TRANS
C       MISSION TABLE
C       IG--NUMBER OF ANGLES OF VIEW
C       NUM--NUMBER OF ATMOSPHERIC MODELS
       IBC=1
       FTSW = 0
       XMINH=0.
       IVGK=-1
       READ(2,17) NOPP,NOPE,A7M,A8M
C   READ IN OF SPECTRAL RESPONSE*****************************
       READ(2,6) (SPWORD(I),I=1,11)
       IA = 2*NOPP
       READ(2,10)(TAB15(I),I=1,IA)
       WRITE(3,32)
       WRITE(3,11)
       WRITE(3,12)(TAB15(I),I=1,IA)
C   READ IN OF SPECTRAL EMISSIVITY***************************
       IA =2*NOPE
       READ(2,10) (TABLE(I),I=1,IA)
       WRITE(3,14)
       WRITE(3,12) (TABLE(I), I=1,IA)
C    GSW=GAS SWITCH (0,1 =A7 ONLY , 2,+ = A7 AND A8)**********************
       READ(2,13)IATM1,IATM2,GSW,TMIN1,TMAX1,TMIN2,TMAX2
C   TWAVE(I)--WAVE NUMBER FOR PRINT OUT OF VERTICAL PARAMETERS***
       READ(2,15) (TWAVE(I), I=1,15)
       NNUM=0
       DELR=.1
 19    IANG=0
 21    JTA=0
       DO 50 I=1,125
       IZERO(I)=0
 50    CONTINUE
       DO 1003 I=1,1200
```

```
 1003 SUMLAY(I)=0.0
      IA=1
      IWAVET=TWAVE(IA)*10.
      WRITE(3,32)
C    MODEL ATMOSPHERE TABLE FROM TAPE(S)*********************************
      CALL READF
      GO TO 39
 22   CALL READT
 39   IF(IWAVE-IWAVET) 42,40,42
 40   IWP=1
      IA=IA+1
      IWAVET=TWAVE(IA)*10.
      GO TO 44
 42   IWP=-1
 44   J=1
C   TOP LAYER*************************************************************
      RUPW=0.
      RUPWO=0.
      DTAUDH = 0.0
      DWAVE=5.
      H=HT3
      DELR1=DELR/2.0
      TRANU=1.
      IAA=1
C    ATMOSPHERIC LAYERS*****************************************************
 626  H1=H-DELR1
      XH1(IAA)=H1
      H=H-DELR
      CALL INTB(H,TRAN)
      IF(TRAN) 627,628,628
  627 TRAN=0.0
  628 TRANL=TRAN
      CALL INTA(H1,TH1)
      CALL PLANK(WAVE0,DWAVE,TH1,RADW,RADWO)
      HEIGHT=H1
C   TRANSFER EQUATION*****************************************
      OLIVER=(TRANU-TRANL)*RADW
      RUPW=RUPW + OLIVER
      RUPWO=RUPWO+(TRANU-TRANL)*RADWO
      DTAUDH = (TRANU-TRANL)/DELR
      XXLOG=7.7
      IF(IWP) 665,722,649
 649  CALL STORAD(IAA)
C    SUMMATION OF RADIANCE FOR EACH LAYER FOR ENTIRE SPECTRUM************
 665  OLIVER=(TRANU-TRANL)*RADW
      SUMLAY(IAA)=SUMLAY(IAA) + OLIVER
      TRANU=TRANL
      LAYTOT=IAA
      IAA=IAA+1
      IF(H-HT2)708,708,626
 708  JTA=JTA+1
C   GROUND RADIATION******************************************************
      CALL INTA(H,TH1)
      CALL PLANK(WAVE0,DWAVE,TH1,RADW,RADWO)
      RW=RUPW
      RWO=RUPWO
      CALL INTRPD(WAVE0,EPSI,NOPE)
      RADGW=TRANU*EPSI*RADW
      RADGWO=TRANU*EPSI*RADWO
      TRANG(JTA)=TRANU
C    TOTAL UPWARD RADIATION************************************************
      RUPW=RUPW+RADGW
      RUPWO=RUPWO+RADGWO
      IF(IWP) 709,722,800
```

```
  709  PLOT(JTA)=RUPWO
       STO1(JTA)=WAVE0
       STO2(JTA)=10000./STO1(JTA)
       STO3(JTA) = SF
       STO4(JTA) = EPSI
       STO6(JTA)=RADGWO
       STO7(JTA)=RWO
       STO8(JTA)=RUPWO
       STO9(JTA)=RADGW
       STO10(JTA)=RW
       STO11(JTA)=RUPW
       TBW(JTA)=CB*WAVE0/ALOG(5.0*CA*WAVE0**3/RUPW  +1.0)
       TBWO(JTA)=CB*WAVE0/ALOG(5.0*CA*WAVE0**3/RUPWO +1.0)
C    TEST FOR ANOTHER WAVE NUMBER*****************************************
       WRITE(3,63) WAVE0
    63 FORMAT(1H ,F15.2)
       IF(JTA-INTER)   22,710,710
C    PLOT OF UPWARD RADIATION*********************************************
  710  PLOT1=PLOT(1)
       DO 715 I=1,JTA
       PLOT(I)=PLOT(I)/PLOT1
       PLOT(I)=PLOT(I)*100.
  715  CONTINUE
       WRITE(3,32)
       CALL PWD(4)
       DO 720 I=1,JTA
       IPLOT=PLOT(I)
       IPLOT=IPLOT+1
       IF(IPLOT-120) 718,718,716
  716  IPLOT=120
  718  WRITE(3,34) (IZERO(J),J=1,IPLOT)
  720  CONTINUE
       GO TO 850
C    TEST FOR ANOTHER ANGLE***********************************************
  721  IANG=IANG+1
       IF(IANG-IG) 21,724,724
C    TEST FOR ANOTHER ATMOSPHERIC MODEL************************************
  724  NNUM=NNUM+1
       IVGK=-1
       IF(NNUM-NUM) 19,722,722
   722 CALL READ2
       CALL MESAGE(9)
C   PRINT OUT OF VERTICAL PARAMETERS FOR GIVEN WAVE NUMBER***************
  800  IAB1=0
       IAB2=0
       IAB=IAA
   810 WRITE(3,28)WAVE0
       WRITE(3,27)
       IF(IAB-180) 830,820,820
  820  IAB1=IAB2+1
       IAB2=IAB2+60
       WRITE(3,26) (RAD1(IB),RAD2(IB),RAD3(IB),RAD4(IB),RAD5(IB),RAD1(IB+
      160),RAD2(IB+60),RAD3(IB+60),RAD4(IB+60),RAD5(IB+60),RAD1(IB+120),
      2RAD2(IB+120),RAD3(IB+120),RAD4(IB+120),RAD5(IB+120),IB=IAB1,IAB2)
       IAB2=IAB2+120
       IAB=IAB-180
       GO TO 810
  830  II=FLOAT(IAB)/3.+1.
       IAA1=II
       IAA2=II+II
       IAB1=IAB2+1
       IB=IAB1
       IB1=IB+IAA1
       IB2=IB+IAA2
```

```
      DO 840 I=1,II
      WRITE(3,26) RAD1(IB),RAD2(IB),RAD3(IB),RAD4(IB),RAD5(IB),
     1RAD1(IB1),RAD2(IB1),RAD3(IB1),RAD4(IB1),RAD5(IB1),
     2RAD1(IB2),RAD2(IB2),RAD3(IB2),RAD4(IB2),RAD5(IB2)
      IB=IB+1
      IB1=IB1+1
      IB2=IB2+1
  840 CONTINUE
      K=1
      II=LAYTOT-9
      III=LAYTOT
  841 SUMLA1=0.0
      DO 842 I=II,III
  842 SUMLA1=SUMLA1 + RAD3(I)
      ALTITU=XH1(II+5) + DELR1
      ALTIT(K)=ALTITU
      SUMLA(K)=SUMLA1
      K=K+1
      II=II-10
      III=III-10
      IF(II) 843,843,841
  843 WRITE(3,32)
      KMAXIM=K-1
      DO 845 I=1,KMAXIM
      JJJJJJ=KMAXIM-I+1
      ALTI(I)=ALTIT(JJJJJJ)
      SUML(I)=SUMLA(JJJJJJ)
      SUMRAT(I)=SUML(I)/RUPW
  845 WRITE(3,61) ALTI(I),SUML(I),SUMRAT(I)
      WTMAX=0.05
      WTMIN=0.0
      CALL OCPLOT(WTMAX,WTMIN,SUMRAT,3)
      WRITE(3,5) WAVE0
      GO TO 709
C  PRINT OUT OF ALL SPECTRAL INTERVALS***********************************
  850 WRITE(3,46)
      CALL PWD(4)
      WRITE(3, 6) (SPWORD(I),I=1,11)
      WRITE(3,48) ANGLE,XMINH,HT3,HT2
      WRITE(3,17)INTER
      WRITE(3,52)
      IAB1=0
      IAB2=0
      IAB=INTER
  860 WRITE(3,54)
      IF(IAB-47) 880,870,870
  870 IAB1=IAB2+1
      IAB2 = IAB2 + 47
      WRITE(3,56) (STO1(IB),STO2(IB),STO3(IB),STO4(IB),STO6(IB),STO7(IB)
     1,STO8(IB),TBWO(IB),STO9(IB),STO10(IB),STO11(IB),TBW(IB),IB=IAB1,
     2IAB2)
      IAB = IAB - 47
  872 WRITE(3,32)
      WRITE(3,54)
      IF(IAB-55) 880,874,874
  874 IAB1=IAB2+1
      IAB2=IAB2+55
      WRITE(3,56) (STO1(IB),STO2(IB),STO3(IB),STO4(IB),STO6(IB),STO7(IB)
     1,STO8(IB),TBWO(IB),STO9(IB),STO10(IB),STO11(IB),TBW(IB),IB=IAB1,
     2IAB2)
      IAB=IAB-55
      GO TO 872
  880 IAB1=IAB2+1
      IB=IAB1
```

```
      DO 890 I=1,IAB
      WRITE(3,56) (STO1(IB),STO2(IB),STO3(IB),STO4(IB),STO6(IB),STO7(IB)
     1,STO8(IB),TBWO(IB),STO9(IB),STO10(IB),STO11(IB),TBW(IB))
      IB=IB+1
  890 CONTINUE
      SSUMW=0.0
      SSUMWO=0.0
      SUMATM=0.0
      SUMGRD=0.0
      DO 925 I=1,INTER
      SUMATM=SUMATM+STO10(I)
      SUMGRD=SUMGRD+STO9(I)
      SSUMWO=SSUMWO + STO8(I)
  925 SSUMW=SSUMW + STO11(I)
      ATMCON=SUMATM/SSUMW
      WRITE(3,7) SUMGRD,SUMATM
      WRITE(3,9)SSUMWO,SSUMW
      WRITE(3,4) ATMCON
      WRITE(3,8)
      WRITE(3,57) (STO1(I),STO2(I),TRANG(I),I=1,INTER)
      K=1
      II=LAYTOT-9
      III=LAYTOT
 1009 SUMLA1=0.0
      DO 1010 I=II,III
 1010 SUMLA1=SUMLA1 + SUMLAY(I)
      ALTITU=XH1(II+5) + DELR1
      ALTIT(K)=ALTITU
      SUMLA(K)=SUMLA1
      K=K+1
      II=II-10
      III=III-10
      IF(II) 1021,1021,1009
 1021 WRITE(3,32)
      KMAXIM=K-1
      DO 1033 I=1,KMAXIM
      JJJJJJ=KMAXIM-I+1
      ALTI(I)=ALTIT(JJJJJJ)
      SUML(I)=SUMLA(JJJJJJ)
      SUMRAT(I)=SUML(I)/SSUMW
 1033 WRITE(3,61) ALTI(I),SUML(I),SUMRAT(I)
      CALL EOFA3
C    PLOT WAVE NUMBER VS TBW*************************************************
      CALL OCPLOT(TMAX1,TMIN1,TBWO,1)
      TRMAX = 1.0
      TRMIN = 0.0
C    PLOT WAVE NUMBER VS TRANG***********************************************
      CALL OCPLOT(TRMAX,TRMIN,TRANG,2)
C    PLOT WEIGHTING FUNCTIONS************************************************
      WTMAX=0.05
      WTMIN=0.0
      CALL OCPLOT(WTMAX,WTMIN,SUMRAT,3)
      WRITE(3,7) SUMGRD,SUMATM
      WRITE(3,9) SSUMWO,SSUMW
      WRITE(3,4) ATMCON
C    PLOT TEMPERATURE VS HEIGHT**********************************************
      TMAX3=330.
      TMIN3=130.
      IIXA=IXA/2
      DO 1041 N=1,IIXA
      JIJ=IXA-N*2+2
      JIJI=IXA-N*2+1
      TEMP(N)=DATA(JIJ)
      HH(N)=DATA(JIJI)
```

```
 1041 CONTINUE
      CALL OCPLOT(TMAX3,TMIN3,TEMP,4)
C    PROGRAM IS FINISHED AT 722*********************************************
      GO TO 721
      END
```

377 CARDS

```
$IBFTC OCPLOT  M94,XR7,NOLIST,NODECK,NOREF
      SUBROUTINE OCPLOT(XMAX,XMIN,VS,NAME)
CONSTANT NAME =1(IS WAVE NO. VS TBB),=2(IS WAVE NO. VS TRANG)***********
      DIMENSION NSCALE(5)
      COMMON/BB/WORDS(11), WAVEI,WAVEF,INTER,HT2 ,HT3,ANGLE,NUM,IG,IXB
     1,IWAVE,WAVE0,IBC
      COMMON/OP/TMAX,TMIN
      COMMON/RR/PLOT(300),IZERO(125)
      COMMON/SS/A(6000),
     1TWAVE(15)
     2,          STO1(350),STO2(350),STO3(350),STO4(350),STO5(350),
     3STO6(350),STO7(350),STO8(350),STO9(350),STO10(350),STO11(350),
     5TBW(350),TBWO(350),TRANG(350),RATIO(350),ISTO1(350),ISTO2(350),IST
     603(350)
      COMMON/TT/SUMRAT(100),ALTI(100),KMAXIM,SPWORD(11),HH(100),TEMP(100
     1),IIXA
      COMMON/ZB2/WAV02,DATBB(200),IXF,A8M,GSW,IATM2
      COMMON/ZC1/W1(11), WAV1,WAVF1,INT1,HT21 ,HT31,ANGL1,NUM1,JTAN1,LA1
      COMMON/ZC2/W2(11), WAV2,WAVF2,INT2,HT22 ,HT32,ANGL2,NUM2,JTAN2,LA2
      INTEGER A7M,A8M,FTSW,GSW
      DATA BCD/0546060606060/,(NSCALE(I),I=1,5)/32767,0,2,0,3/
      DATA HMIN,HMAX/0.0,70.0/
      DATA WOMIN,WOMAX/500.0,2000.0/
      WRITE (3,30)
  30  FORMAT(1H1)
      GO TO (50,55), GSW
   50 WRITE(3,10) (W1(I),I=1,11)
      WRITE(3,10) (SPWORD(I),I=1,11)
   10 FORMAT(30X,11A6)
      GO TO 60
   55 WRITE(3,10) (W1(I),I=1,11)
      WRITE(3,10) (W2(I),I=1,11)
      WRITE(3,10) (SPWORD(I),I=1,11)
   60 CONTINUE
      GO TO (200,200,210,220,205),NAME
  200 CALL PLOT1(NSCALE,12,25,10,10)
C THE 2ND ARG IS NO. OF BLOCKS DESIRED ALONG Y
C THE 3RD ARG IS NO. OF POINTS DESIRED IN EACH BLOCK ALONG Y
C THE 4TH ARG IS NO. OF BLOCKS DESIRED ALONG X
C THE 5TH ARG IS NO. OF SUB-INTERVALS DESIRED IN EACH BLOCK ALONG X
      CALL PLOT2(A,XMAX,XMIN,WOMAX,WOMIN)
      CALL PLOT3(BCD,VS,STO1,INTER)
C THE 1ST ARG IS THE BCD CHARACTER DESIRED TO REPRESENT THE POINTS
      CALL FPLOT4(52,52HW    A    V    E         N    U    M    B    E
     1  R )
      GO TO (201,202,203,204,205),NAME
 201  WRITE(3,21)
  21  FORMAT(//  42X,52HT    E    M    P    E    R    A    T    U    R
     1  E )
      RETURN
 202  WRITE(3,22)
  22  FORMAT(//  42X,52HG R O U N D   T R A N S M I S S I O N   V A L U
     2E S )
 203  RETURN
  210 CALL PLOT1(NSCALE,14,10,10,10)
      CALL PLOT2(A,XMAX,XMIN,HMAX,HMIN)
```

```
      CALL PLOT3(BCD,VS,ALTI,KMAXIM)
      CALL FPLOT4(52,52H                    H  E  I  G  H  T  *  K  M
     1     )
      WRITE(3,26)
   26 FORMAT(//  42X,52HFRACTIONAL OUTGOING EFFECTIVE RADIANCE / KM
     1     )
      RETURN
  220 CALL PLOT1(NSCALE,14,10,10,10)
      CALL PLOT2(A,XMAX,XMIN,HMAX,HMIN)
      CALL PLOT3(BCD,VS,HH   ,IIXA)
      CALL FPLOT4(52,52H                    H  E  I  G  H  T  *  K  M
     1     )
      WRITE(3,21)
  204 RETURN
  205 RETURN
      END
```

72 CARDS

```
$IBFTC PLANK   M94,XR7,NOLIST,NODECK,NOREF
      SUBROUTINE PLANK(WAVE0,DWAVE,TH1,RADW,RADWO)
      DIMENSION PLK(5)
      COMMON/PP/NOPE,NOPP,SF
C   SF = PHI, AND IS FOUND IN SUBROUTINE PLANK
       DATA CA,CB/1.1909000E-12,1.43879/
      RADW=0.
      RADWO=0.
      DW=WAVE0-2.0*DWAVE/5.0
      DO 21 I=1,5
      PLK(I) = CA*DW**3/(EXP(CB*DW/TH1)-1.0)
   17 CALL INTRPC(DW,SF,NOPP)
      RADW=RADW+PLK(I)*SF
   18 RADWO=RADWO+PLK(I)
      DW=DW+DWAVE/5.
   21 CONTINUE
      RETURN
      END
$IBFTC STORAD  M94,XR7,NOLIST,NODECK,NOREF
      SUBROUTINE STORAD(IAA)
C    THIS SUBROUTINE STORES HEIGHT,DTAUDH,R1PW,TRANU,RUPWO IN RADX(IAA),
C WHERE X=1---5 .
      COMMON/CC/HEIGHT,DTAUDH,OLIVER,TRANU,XXLOG
      COMMON/SS/RAD1(1200),RAD2(1200),RAD3(1200),RAD4(1200),RAD5(1200),
     1TWAVE(15)
     2,          STO1(350),STO2(350),STO3(350),STO4(350),STO5(350),
     3STO6(350),STO7(350),STO8(350),STO9(350),STO10(350),STO11(350),
     5TBW(350),TBWO(350),TRANG(350),RATIO(350),ISTO1(350),ISTO2(350),IST
     603(350)
      RAD1(IAA)=HEIGHT
      RAD2(IAA) = DTAUDH
      RAD3(IAA)=OLIVER
      RAD4(IAA)=TRANU
      RAD5(IAA)=XXLOG
      RETURN
      END
```

36 CARDS

```
$IBFTC MATMUL  M94,XR7,NOLIST,NODECK,NOREF
      SUBROUTINE MATMUL(NOOM)
C    SUBROUTINE MATMUL MULTIPLIES MATRICES DATB AND DATBB, OR EXCHANGES
C   DATBB FOR DATB ACCORDING TO WHETHER NOOM IS .EQ. 1 OR 2 .
C   ALL ARGUMENTS(EXCEPT NOOM) ARE TRANSMITTED THROUGH COMMON STO-AGE
```

```
C  AREAS. SUBROUTINE READT CALLS MATMUL AND DIRECTS ITS USAGE.
      COMMON/BB/WORDS(11), WAVEI,WAVEF,INTER,HT2 ,HT3,ANGLE,NUM,IG,IXB
     1,IWAVE,WAVE0,IBC
      COMMON/ZA/IXA,DATA(200)
      COMMON/ZB1/WAV01,DATB(200),IXE,A7M,FTSW,IATM1
      COMMON/ZB2/WAV02,DATBB(200),IXF,A8M,GSW,IATM2
      COMMON/ZC1/W1(11), WAV1,WAVF1,INT1,HT21 ,HT31,ANGL1,NUM1,JTAN1,LA1
      COMMON/ZC2/W2(11), WAV2,WAVF2,INT2,HT22 ,HT32,ANGL2,NUM2,JTAN2,LA2
      COMMON/ZC3/IVGK,IATM
      COMMON/TS/TRAM(300)
      INTEGER A7M,A8M,FTSW,GSW
      DATA C1/6HMUTAPE/
C  A7M IS TAPE A7 MULTIPLICITY SWITCH
C  A8M IS TAPE A8 MULTIPLICITY SWITCH
C  FTSW IS FIRST TIME SWITCH FOR SUBROUTINE READT
C  GSW IS GAS MULTIPLICITY SWITCH
C  NOOM IS THE NO. OF OPERATING MODE (1=MULTIPLICATION OF DATB*DATBB
C  AND 2=EXCHANGE DATBB FOR DATB)
      GO TO(90,250),IBC
   90 GO TO (100,200),GSW
  100 ANGLE=ANGL1
      WAVEI=WAV1
      WAVEF=WAVF1
      HT2=HT21
      HT3=HT31
      INTER=INT1-1
      NUM=NUM1
      IG=JTAN1
      IBC=2
      WRITE(3,500) WAV1,WAVF1,INT1,HT21,HT31,ANGL1,NUM1,JTAN1,LA1
      WRITE(3,500) WAVEI,WAVEF,INTER,HT2,HT3,ANGLE,NUM,IG,IVGK
  500 FORMAT(1H0,10X,2F10.1,I5,3F10.2,3I5)
      GO TO 250
  200 INT78 = (WAVF2-WAV1)/5. + 1.
      IF(INT1-1-INT78) 11,12,12
   11 INTER=INT78
      WAVEI=WAV1
      WAVEF=WAVF2
      GO TO 13
   12 INTER=INT1-1
      WAVEI = WAV1
      WAVEF = WAVF1
   13 NUM=NUM1
      IG = JTAN1
      ANGLE = ANGL1
      HT3 = HT31
      HT2=HT21
      IBC=2
      WRITE(3,500) WAV1,WAVF1,INT1,HT21,HT31,ANGL1,NUM1,JTAN1,LA1
      WRITE(3,500) WAV2,WAVF2,INT2,HT22,HT32,ANGL2,NUM2,JTAN2,LA2
      WRITE(3,500) WAVEI,WAVEF,INTER,HT2,HT3,ANGLE,NUM,IG,IVGK
  250 CONTINUE
      IXB = LA1*2
      IX = IXB/2
      J = 2
      GO TO (1,2,3),NOOM
C    TWO GASES*************************************************************
    1  DO 10 I=1,IX
      DATB(J)=DATB(J)*DATBB(J)
   10 J=J+2
C    ONE GAS,A7************************************************************
     3 IWAVE=WAV01*10.0
      IATM=ATM1
      WAVE0 = WAV01
      GO TO 4
```

```
C    ONE GAS,A8*****************************************************************
     2  DO 20 I=1,IX
        DATB(J)=DATBB(J)
    20  J = J+2
        IWAVE=WAV02*10.0
        IATM=ATM2
        WAVE0 = WAV02
      4 GO TO (60,30),GSW
     30 IF(IVGK) 31,31,35
     31 IVGK=+1
        W1(11)=C1
        INTER=INTER+1
        CALL RITE1(IXA)
        INTER=INTER-1
        WRITE(3,6280) WAVE0
   6280 FORMAT(F10.3)
        WRITE(3,6281) (DATB(J),J=1,IXB)
   6281 FORMAT(10F10.5)
     35 TRAM(1)=WAVE0
        IFB=IXB+1
        DO 37 I=2,IFB
     37 TRAM(I)=DATB(I-1)
        CALL RITEB7(IFB)
     60 RETURN
        END
```

95 CARDS

```
$IBFTC MESAGE  M94,XR7,NOLIST,NODECK,NOREF
       SUBROUTINE MESAGE(NOM)
       COMMON/ZB1/WAV01,DATB(200),IXE,A7M,FTSW,IATM1
       COMMON/ZB2/WAV02,DATBB(200),IXF,A8M,GSW,IATM2
       INTEGER A7M,A8M,FTSW,GSW
C   A7M IS TAPE A7 MULTIPLICITY SWITCH
C   A8M IS TAPE A8 MULTIPLICITY SWITCH
C   FTSW IS FIRST TIME SWITCH FOR SUBROUTINE READT
C   GSW IS GAS MULTIPLICITY SWITCH
C    SUBROUTINE MESAGE PRINTS ON LINE ERRORS,TAPE HANDLING AND SNAFUES
C THAT OCCURS DURING THE READING OF TAPES A7 AND A8. MOST OF THE
C MESSAGES ORIGINATE IN SUBROUTINE READT
C   NOM IS THE NUMBER OF THE MESSAGE THAT IS TO BE PRINTED
C
       GO TO (1,2,3,4,5,6,7,8,9),NOM
    1  PRINT 10
   10  FORMAT(1H0,30X50HSWITCH TAPES A7 AND A8---PRESS START(AC HAS HPR 1
      1)//////////)
       PAUSE 1
       RETURN
    2  REWIND 8
   21  REWIND 7
   22  PRINT 20
   20  FORMAT(1H0,30X89HTHIS MESS IS IMPOSSIBLE, DATA IS OUT OF FOCUS----
      1STOP--(AC HAS HPR 2),PRESS START TO EXIT//////////)
       PAUSE 2
       CALL EXIT
    3  PRINT 30
   30  FORMAT(1H0, 30X53HWAVE01 IS .GT. WAVE02,NO MORE CORRELATION IS POS
      1SIBLE)
       GO TO 2
    4  REWIND 7
       PRINT 40
   40  FORMAT(1H0,30X48HMOUNT NEXT A7 TAPE ON TAPE UNIT A7(AC HAS HPR 4)/
      1//////////)
       PAUSE 4
```

```
      RETURN
    5 REWIND 8
      PRINT 50
   50 FORMAT(1H0,30X48HMOUNT NEXT A8 TAPE ON TAPE UNIT A8(AC HAS HPR 5)/
     1/////////)
      PAUSE 5
      RETURN
    6 PRINT 60
   60 FORMAT(1H0,30X38HTAPE A7 HAS EOF INITIALLY,STOP PROGRAM)
      GO TO 21
    7 PRINT 70
   70 FORMAT(1H0,30X54HTAPES (A7,A8) ARE  OUT OF DATA TABLES AT THE SAME
     1 TIME)
      GO TO 2
    8 PRINT 80
   80 FORMAT(1H0,30X38HTAPE B7 HAS EOF INITIALLY,STOP PROGRAM)
      GO TO 2
    9 PRINT 90
   90 FORMAT(1H0,30X48HTHIS RUN IS FINISHED, NOTE NEXT INSTRUCTION     )
      GO TO (21,2),GSW
      END
```

57 CARDS

```
$IBFTC PWD     M94,XR7,NOLIST,NODECK,NOREF
       SUBROUTINE PWD(LL)
       COMMON/ZA/IXA,DATA(200)
       COMMON/ZB1/WAV01,DATB(200),IXE,A7M,FTSW,IATM1
       COMMON/ZB2/WAV02,DATBB(200),IXF,A8M,GSW,IATM2
       COMMON/ZC1/W1(11), WAV1,WAVF1,INT1,HT21 ,HT31,ANGL1,NUM1,JTAN1,LA1
       COMMON/ZC2/W2(11), WAV2,WAVF2,INT2,HT22 ,HT32,ANGL2,NUM2,JTAN2,LA2
       COMMON/ZC3/IVGK,IATM
  6    FORMAT(1H0,3X,11HHT BOTLAY= F9.5,3X,20HATMOSPHERE NUMBER = I2,3X,2
      11HHEIGHT OF TOP LAYER =F6.2,12HKM           /4X,15HANGLE OF VIEW =F
      25.2,8H DEGREES,3X,20HWAVE NUMBER RANGE =(F6.1,3H TOF6.1,6H) CM-1)
   10  FORMAT(9X,11A6)
   11  FORMAT(5(3X,F6.2,2X,F8.2))
       GO TO (100,200,100,400),LL
  100  WRITE(3,10) (W1(I),I=1,11)
       WRITE(3,11) (DATA(I),I=1,IXA)
       WRITE(3,6) HT21 ,IATM1,HT31,ANGL1,WAV1,WAVF1
       GO TO (300,300,200),LL
  200  WRITE(3,10) (W2(I),I =1,11)
       WRITE(3,11) (DATBB(I),I =1,IXA)
       WRITE(3,6) HT22 ,IATM2,HT32,ANGL2,WAV2,WAVF2
  300  RETURN
  400  WRITE(3,10) (W1(I), I=1,11)
       RETURN
       END
```

25 CARDS

```
$IBMAP EOFA3    10,NODECK,M94,NOLIST,NOREF
 OUTPT FILE     ,OU1,OU2,READY,OUTPUT,BLK=25
 EOFA3 SAVE     (4,2,1,3,5,6,7)I
       TSX      .OPEN,4
       MZE      OUTPT
       TSX      .CLOSE,4
       MZE      OUTPT
 RET   RETURN   EOFA3
       END
```

9 CARDS

```
$IBMAP READT   200,NOLIST,XR7,M94,NODECK,NOREF
*   READT SUBROUTINE READS TAPE A7, AND TAPE A8 IF REQUIRED
* CHECKS FOR INITIAL WAVE NUMBER CORRELATION BETWEEN A7 AND
* A8,APPROPIATELY CALLS FOR MATMUL (MATRIX MULTIPLICATION)
* OF DATB X DATBB AND DIRECTS THE PROPER MAINTENANCE OF
* DATB AT ALL TIMES. ALL PARAMETERS ARE TRANSMITTED
* THROUGH COMMON //. DATB IS UPDATED ONCE DURING EACH
* CALL READT
 INP1  FILE    ,A(3),A(3),BLK=300,BIN,HOLD,MOUNT
 INP2  FILE    ,A(4),A(4),BLK=300,BIN,HOLD,DEFER
 READT SAVE    (4,2,1,3,5,6,7)I
       CLA     GSW             ARE THERE TWO GASES
       CAS     =2              OR MORE
       TRA     READ3           GSW GREATER THAN 2
       TRA     READ3           GSW EQUAL TO 2
       TRA     READ1           GSW LESS THAN 2
* THIS PART IS FOR SINGLE TAPE (A7) ONLY.........
 READ1 TSX     READA,4         READ TAPE A7
       CALL    MATMUL(=3)      SET FOR DATB ONLY
       RETURN  READT
* THIS PART IS FOR NTH TIME OF DOUBLE TAPE (A7,A8) READ...................
 READ3 CLA     BUF1            WAVE01
       FSB     BUF4+12         WAV1
       TNZ     *+3             TEST A8 STATUS
       CLA     =1
       STO     FSW1            TURN A7 FILL SWITCH TO ON
       CLA     BUF2            WAVE02
       FSB     BUF5+12
       TNZ     *+3             CONTINUE
       CLA     =1
       STO     FSW2            TURN A8 FILL SWITCH TO ON
       NZT     FSW1            IS A7 BEING FILLED
       TRA     READ31          NO
       NZT     FSW2            IS A8 BEING FILLED
       TRA     READ41          NO
       CALL    MESAGE(=3)
READ31 NZT     FSW2            IS A8 BEING FILLED
       TRA     READ42          NO
 READ4 TSX     READA,4         READ A7 ONLY
       CLA     BUF1            WAVE01
       CAS     BUF2            COMPARE WAVE02
       TRA     TRUBL           WAVE01.GT.WAVE02
       TRA     ALINE           WAVE01.EQ.WAVE02
       TRA     BNETH           WAVE01.LT.WAVE02
READ41 TSX     READB,4         READ A8 ONLY
       CALL    MATMUL(=2)      SET FOR DATBB ONLY
       RETURN  READT
READ42 TSX     READA,4         READ A7 AND A8
       TSX     READB,4
       CLA     BUF1            WAVE01
       CAS     BUF2            COMPARE WAVE02
       TRA     EOFA            WAVE01.GT.WAVE02
       TRA     READ43          WAVE01.EQ.WAVE02
       TRA     EOFA+2          WAVE01.LT.WAVE02
READ43 CALL    MATMUL(=1)      MULTIPLY DATB AND DATBB MATRICES
       RETURN  READT
 ALINE STZ     FSW2            SET A8 FILL SWITCH TO OFF=1
       TRA     READ43
 BNETH CALL    MATMUL(=3)      SET FOR DATB ONLY
       RETURN  READT
* THIS SUBROUTINE READS NTH RECORD FROM TAPE A7.....................
 READA SXA     KEEPA,4
       TSX     .READ,4         READ TABLES FROM
       PZE     INP1            TAPE A7
```

```
        PZE     EOFA,,*-2
        IORT    BUF1,,**
 KEEPA  AXT     **,4
        TRA     1,4
* THIS SUBROUTINE READS NTH RECORD FROM TAPE A8.........................
 READB  SXA     KEEPB,4
        TSX     .READ,4         READ TABLES FROM
        PZE     INP2            TAPE B7
        PZE     EOFB,,*-2
        IORT    BUF2,,**
 KEEPB  AXT     **,4
        TRA     1,4
 EOFA   ZET     FSW2            IS A8 BEING FILLED
        TRA     EOFC            YES
        CLA     =1              NO
        STO     FSW1            TURN A7 FILL SWITCH TO ON =1
        TRA     READ41+1
 EOFB   ZET     FSW1            IS A7 BEING FILLED
        TRA     EOFC            YES
        CLA     =1              NO
        STO     FSW2            TURN A8 FILL SWITCH TO ON =1
        TRA     BNETH
 EOFC   CALL    MESAGE(=2)      OUT OF FOCUS-STOP
* THIS SUBROUTINE READS,DIRECTS TAPE HANDLING OF A7........
* THIS SUBROUTINE READS,DIRECTS TAPE HANDLING OF A8.....................
 READF  SAVE    1,2,3,4,5,6,7,I
        CLA     GSW
        CAS     =2              IS THERE MORE THAN 1 GAS
        TRA     *+3             YES
        TRA     *+2             YES
        TRA     READM           NO
* THIS PART IS FOR FIRST TIME OF DOUBLE TAPE (A7,A8) READ..............
        ZET     FTSW            IS THIS FIRST TIME
        TRA     READG
        TSX     .OPEN,4
        PZE     INP1
        TSX     .OPEN,4
        PZE     INP2
        STZ     FSW1            SET FILL SWITCHES
        STZ     FSW2            TO = 0
        CLA     =1
        STO     FTSW            SET FIRST TIME SWITCH TO OFF=1
 READR  TSX     .READ,4
        PZE     INP1
        PZE     EOF1,,*-2
        IOCP    BUF4,,20        READ(W1(11),ETC...)    FOR GAS1
        IORT    BUF3,,**        READ(IXA,DATA(200)) FOR GAS 1
        TSX     .READ,4
        PZE     INP2
        PZE     EOF2,,*-2
        IOCP    BUF5,,20        READ(W2(11), ETC...)   FOR GAS2
        IORT    BUF2,,**        READ(IXA,DATA(200)) FOR GAS 2
        CALL    PWD(=3)
        TSX     READA,4
        TSX     READB,4
        CLA     BUF1            WAVE 01
        CAS     BUF2            COMPARE WAVE 02
        TRA     MES1            WAVE01.GT.WAVE02
        TRA     MULT1           WAVE01.EQ.WAVE02
        NOP                     WAVE01.LT.WAVE02
        CLA     =1              LEAVE DATB AS IS
        STO     FSW2            SET FILL SWITCH FOR A8 TO ON = 1 ............
        CALL    MATMUL(=3)      SET FOR DATB ONLY
        RETURN  READF
```

```
 MULT1 CALL    MATMUL(=1)      MULTIPLY MATRICES DATB AND DATBB
       RETURN  READF
* THIS PART HANDLES THE SWITCHING OF TAPES WHEN A7 STARTS WITH WAVE01...
* GREATER THAN WAVE02  FROM A8.....................................
 MES1  TSX     .REW,4          REWIND TAPE A7
       PZE     INP1
       TSX     .REW,4          REWIND TAPE A8
       PZE     INP2
       CALL    MESAGE(=1)      WRONG TAPE ON A7
       TRA     READR
 READG NZT     FSW1           IS A7 BEING FILLED
       TRA     READH           NO
       NZT     FSW2            IS A8 BEING FILLED
       TRA     READJ           NO
       CALL    MESAGE(=3)
* THIS PART IS FOR A7 READ WHILE A8 IS BEING FILLED.................
 READH NZT     FSW2            IS A8 BEING FILLED
       TRA     READK           NO
 READI TSX     .READ,4         READ TAPE A7 ONLY
       PZE     INP1
       PZE     EOF3,,*-2
       IOCP    BUF4,,20        W1 ETC...
       IORT    BUF3,,**        READ(IXA,DATA(200)) FOR GAS 1
       CALL    PWD(=3)
       TSX     READA,4
       CLA     BUF1            WAVE01
       CAS     BUF2            COMPARE WAVE02
       TRA     TRUBL           WAVE01.GT. WAVE02
       TRA     ALIGN           WAVE01.EQ.WAVE02
       TRA     BELOW           WAVE01.LT.WAVE02
* THIS PART IS FOR TAPE A8 READ ONLY IF A7 IS BEING FILLED..........
 READJ TSX     .READ,4         READ TAPE A8 ONLY
       PZE     INP2
       PZE     EOF4,,*-2
       IOCP    BUF5,,20        W2 ETC...
       IORT    BUF2,,**        READ(IXA,DATA(200)) FOR GAS 2
       CALL    PWD(=3)
       TSX     READB,4
       CALL    MATMUL(=2)      SET FOR DATBB ONLY
       RETURN  READF
* THIS PART READS A8 AFTER A7 READS IN STEP(CORRELATED).............
 READK TSX     .READ,4         TAPE A7
       PZE     INP1
       PZE     EOF5,,*-2
       IOCP    BUF4,,20        W1,ETC...
       IORT    BUF3,,**        READ(IXA,DATA(200)) FOR GAS 1
 READL TSX     .READ,4         TAPE A8
       PZE     INP2
       PZE     EOF6,,*-2
       IOCP    BUF5,,20        W2, ETC...
       IORT    BUF2,,**        READ(IXA,DATA(200)) FOR GAS 2
       CALL    PWD(=3)
       TSX     READA,4
       TSX     READB,4
       CLA     BUF1            WAVE01
       CAS     BUF2            COMPARE WAVE02
       TRA     TRUBL           WAVE01.GT.WAVE02
       TRA     ALIGN+1         .EQ.
       TRA     TRUBL           .LT.
* THIS PART IS USED WHEN A7 READ FIRST MATCHES A8...................
 ALIGN STZ     FSW2            SET A8 FILL SWITCH TO OFF = 0
       CALL    MATMUL(=1)      MULTIPLY MATRICES DATB AND DATBB
       RETURN  READF
 BELOW CALL    MATMUL(=3)      SET FOR DATB ONLY
       RETURN  READF
```

```
 TRUBL CALL    MESAGE(=2)      OUT OF FOCUS - - STOP
 EOF1  CALL    MESAGE(=6)      EXIT (FIRST TIME)
 EOF2  CALL    MESAGE(=8)      EXIT (FIRST TIME)
 EOF3  TRA     TRUBL
 EOF4  TRA     TRUBL
 EOF5  CLA     =1
       STO     FSW1            SET A7 FILL SWITCH TO ON =1
       TRA     READJ
 EOF6  CLA     =1              NO
       STO     FSW2            SET A8 FILL SWITCH TO ON =1
       CALL    PWD(=3)
       TSX     READA,4
       TRA     BELOW
* THIS PART IS FOR THE NTH TIME OF SINGLE TAPE READ (A7)..............
 READM ZET     FTSW
       TRA     READN
       CLA     =1
       STO     FTSW            SET FIRST TIME SWITCH TO OFF = 1
       TSX     .OPEN,4
       PZE     INP1
 READN TSX     .READ,4
       PZE     INP1
       PZE     EOF1,,*-2
       IOCP    BUF4,,20        W1,ETC...
       IORT    BUF3,,**        READ(IXA,DATA(200)) FOR GAS 1
       CALL    PWD(=1)         PRINT WORDS (11) AND DATA (200)
       TSX     READA,4
       TRA     BELOW
 FSW1  BSS     1               FILL SWITCH FOR GAS 1
 FSW2  BSS     1               FILL SWITCH FOR GAS 2
 ZA    CONTRL  ZA
       USE     ZA
 BUF3  BSS     202             WAVE0,DATA(200),IATM
       USE     PREVIOUS
 ZB1   CONTRL  ZB1
       USE     ZB1             TABLE FOR WAV01
 BUF1  BSS     201             AND DATB(200)
 IXE   BSS     1
 A7M   BSS     1               TAPE A7 MULTIPLICITY SWITCH
 FTSW  BSS     1               FIRST TIME SWITCH (INITIALLY=0)
       USE     PREVIOUS
 ZB2   CONTRL  ZB2
       USE     ZB2             TABLE FOR WAV02
 BUF2  BSS     201             AND DATBB (200)
 IXF   BSS     1
 A8M   BSS     1               TAPE A8 MULTIPLICITY SWITCH
 GSW   BSS     1               GAS MULTIPLICITY SWITCH
       USE     PREVIOUS
 ZC1   CONTRL  ZC1
       USE     ZC1             (W1(11),WAV1,WAVF1,INT1,IGAS1,
 BUF4  BSS     20              (HT31,ANGL1,NUM1,JTAN1,LA1
       USE     PREVIOUS
 ZC2   CONTRL  ZC2
       USE     ZC2             W2(11),WAV2,WAVF2,INT2,IGAS2,
 BUF5  BSS     20              HT32,ANGL2,NUM2,JTAN2,LA2
       USE     PREVIOUS
       END
                                                        250 CARDS


$IBMAP INTA    100,NODECK,NOLIST,NOREF
 INTA  SAVE
       SXA     SAV4,4
       CLA     IXA
       ALS     17
```

```
        STD     MOD+2
        CLA     4,4
        STA     TEM
        CLA*    3,4
MOD     TSX     TIN1,4
        PZE     DATA
        PZE     3,,**
SAV4    AXT     **,4
        STO*    TEM
        RETURN  INTA
TEM     BSS     1
INTB    SAVE
        SXA     SAV4,4
        CLA     IXB
        ALS     17
        STD     MOD1+2
        CLA     4,4
        STA     TEM1
        CLA*    3,4
MOD1    TSX     TIN1,4
        PZE     DATB
        PZE     1,,**
        LXA     SAV4,4
        STO*    TEM1
        RETURN  INTB
TEM1    BSS     1
BB      CONTRL  BB
        USE     BB
BUF6    BSS     19
IXB     BSS     1
IWAVE   BSS     1
WAVE0   BSS     1
        USE     PREVIOUS
ZA      CONTRL  ZA
        USE     ZA
IXA     BSS     1
DATA    BSS     200
IATM    BSS     1
        USE     PREVIOUS
ZB1     CONTRL  ZB1
        USE     ZB1             TABLE FOR WAV01
WAV01   BSS     1
DATB    BSS     200             AND DATB(200)
IXE     BSS     1
A7M     BSS     1               TAPE A7 MULTIPLICITY SWITCH
FTSW    BSS     1               FIRST TIME SWITCH (INITIALLY=0)
        USE     PREVIOUS
        END
```

53 CARDS

```
$IBMAP  INTRPC  50,NODECK,NOLIST,NOREF
INTRPC  SAVE    (1,2,4)I
        CLA     4,4
        STA     CSF
        CLA*    5,4
        ALS     18
        STD     PAIRS
        CLA*    3,4
        STO     CWAVE
        TSX     TIN1,4
        PZE     TAB15
PAIRS   PZE     1,0,**
        STO*    CSF
        RETURN  INTRPC
```

```
 CWAVE PZE      0
 CSF   PZE      0
*      TABLE OF PHI VS. WAVE NUMBER
 DATAC CONTRL   DATAC
       USE      DATAC
 TAB15 BSS      100
       USE      PREVIOUS
INTRPD SAVE     (1,2,4,3,5,7)I
       CLA      4,4
       STA      EPSI
       CLA*     5,4
       ALS      18
       STD      PARES
       CLA*     3,4
       TSX      TIN1,4
       PZE      TABLE
 PARES PZE      1,0,**
       STO*     EPSI
       RETURN   INTRPD
 EPSI  PZE      0
*  TABLE OF EPSILON VS. WAVE NUMBER
 DATAD CONTRL   DATAD
       USE      DATAD
 TABLE BSS      100
       USE      PREVIOUS
       END
```

40 CARDS

```
$IBMAP TIN1     125,M94,NODECK,NOLIST,NOREF
*      INTERPOLATION SUBROUTINE     TIN1
*     CARDS COLUMN
*      FAP
       ENTRY TIN1
 TIN1  STO      TIN1+98
       SXD      TIN1+87,1
       SXD      TIN1+88,2
       SXD      TIN1+89,4
       CLA      2,4
       STO      TIN1+94
       ADD      TIN1+91
       PAX      0,1
       SXD      TIN1+29,1
       ALS      1
       STA      TIN1+95
       CLA      TIN1+94
       ARS      17
       SUB      TIN1+95
       PAX      0,1
       SXD      TIN1+31,1
       ADD      TIN1+95
       PAX      0,1
       ADD      1,4
       STA      TIN1+23
       STA      TIN1+41
       STA      TIN1+43
       CLA      TIN1+98
       CAS      0,1
       TIX      *-1,1,2
       TRA      TIN1+26
       CLA      TIN1+94
       LBT
       TRA      TIN1+41
       TIX      TIN1+31,1,0
```

```
LXD     TIN1+90,1
TXL     TIN1+33,1,0
LXD     TIN1+31,1
PXD     0,1
ARS     18
CHS
ADD     TIN1+23
STA     TIN1+54
ADD     TIN1+91
STA     TIN1+52
TRA     TIN1+50
CLA     0,1
TXI     TIN1+43,1,2
FAD     0,1
LRS     35
FMP     TIN1+92
CAS     TIN1+98
TXI     TIN1+29,1,-1
TXI     TIN1+29,1,-1
TXI     TIN1+29,1,-3
LXD     TIN1+90,2
LXA     TIN1+95,1
CLA     0,1
STO     COM+1,2
CLA     0,1
FSB     TIN1+98
STO     COM,2
TXI     TIN1+58,2,-2
TIX     TIN1+52,1,2
CLA     COM
STO     COM,2
LXA     TIN1+94,4
LXD     TIN1+93,2
TXI     TIN1+64,2,-2
PXD     0,2
PDX     0,1
CLA     COM+2,1
FSB     COM,2
TZE     TIN1+79
STO     TIN1+97
LDQ     COM,2
FMP     COM+3,1
STO     TIN1+96
LDQ     COM+2,1
FMP     COM+1,2
FSB     TIN1+96
FDP     TIN1+97
STQ     COM+3,1
TXI     TIN1+66,1,-2
CLA     COM+2,2
STO     COM+2,1
TIX     TIN1+63,4,1
CLA     COM+1,1
LXD     TIN1+87,1
LXD     TIN1+88,2
LXD     TIN1+89,4
TRA     3,4
HTR
HTR
HTR
HTR
HTR     1,0,0
DEC     .5
HTR     0,0,2
```

```
        HTR
        HTR
        HTR
        HTR
        HTR
        PZE
        PZE
 COM    BSS     40
        END
                                                                    108 CARDS

$IBMAP RITEB7  100,LIST,XR7,M94,NODECK
*  RITEB7 WRITES BUFFER TRAN(II) ON TAPE B7, THIS INCLUDES TABLES OF
* TRANSMISSIONS AND OTHER PARAMETERS FOR INPUT TO ATMOS3.
 OUT    FILE    ,B(3),B(3),BLK=300,BIN,HOLD,MOUNT,OUTPUT
RITEB7  SAVE    (4,2,1,3,5,6,7)I
        CLA*    3,4
        ALS     18
        STD     II
        TSX     .OPEN,4
        PZE     OUT
        TSX     .WRITE,4
        PZE     OUT
 II     IOCD    TRAM,,300
        RETURN  RITEB7
 TS     CONTRL  TS
        USE     TS
 TRAM   BSS     300             ALL PARAMETERS FOR OUTPUT
        USE     PREVIOUS
 RITE1  SAVE    1,2,3,4,5,6,7,I
        CLA*    3,4
        ADD     =1              ADD 1 FOR IXA ITSELF
        ALS     18
        STD     JJ
        TSX     .OPEN,4
        PZE     OUT
        TSX     .WRITE,4
        PZE     OUT
        IOCP    BUF1,,20
 JJ     IOCD    BUF2,,200
        RETURN  RITE1
 ZC1    CONTRL  ZC1
        USE     ZC1
 BUF1   BSS     20              WORDS(11),WWAVEI,WAVEF,INTER,IGAS,LA,
        USE     PREVIOUS        HT3,ANGLE,NUM,JTAN
 ZA     CONTRL  ZA
        USE     ZA
 BUF2   BSS     200             IXA,DATA(200)
        USE     PREVIOUS
 READ2  SAVE    1,2,3,4,5,6,7,I
        TSX     .CLOSE,4
        PZE     OUT
        RETURN  READ2
        END
'
   2    2    1    1
                    SPECTRAL RESPONSE=UNITY
0500.01.0
3000.01.0
500.001.0
3000.01.0
        2205.00305.00105.00305.00
                                                          EOF E SY
                                                                    55 CARDS
```

"The aeronautical and space activities of the United States shall be conducted so as to contribute . . . to the expansion of human knowledge of phenomena in the atmosphere and space. The Administration shall provide for the widest practicable and appropriate dissemination of information concerning its activities and the results thereof."

—NATIONAL AERONAUTICS AND SPACE ACT OF 1958

NASA SCIENTIFIC AND TECHNICAL PUBLICATIONS

TECHNICAL REPORTS: Scientific and technical information considered important, complete, and a lasting contribution to existing knowledge.

TECHNICAL NOTES: Information less broad in scope but nevertheless of importance as a contribution to existing knowledge.

TECHNICAL MEMORANDUMS: Information receiving limited distribution because of preliminary data, security classification, or other reasons.

CONTRACTOR REPORTS: Scientific and technical information generated under a NASA contract or grant and considered an important contribution to existing knowledge.

TECHNICAL TRANSLATIONS: Information published in a foreign language considered to merit NASA distribution in English.

SPECIAL PUBLICATIONS: Information derived from or of value to NASA activities. Publications include conference proceedings, monographs, data compilations, handbooks, sourcebooks, and special bibliographies.

TECHNOLOGY UTILIZATION PUBLICATIONS: Information on technology used by NASA that may be of particular interest in commercial and other non-aerospace applications. Publications include Tech Briefs, Technology Utilization Reports and Notes, and Technology Surveys.

Details on the availability of these publications may be obtained from:

SCIENTIFIC AND TECHNICAL INFORMATION DIVISION

NATIONAL AERONAUTICS AND SPACE ADMINISTRATION

Washington, D.C. 20546